DATA COMPRESSION WITH PARTICULAR APPLICATIONS TO VIDEO SIGNALS

by

Stephen S.T. Tsui, B. Eng. (Hons. Elect.)

Department of Electrical Engineering

McGill University,
Montreal, Canada.

DATA COMPRESSION WITH PARTICULAR APPLICATIONS TO VIDEO SIGNALS

by

Stephen S.T. Tsui, B. Eng. (Hons. Elect.)

A thesis submitted to the Faculty of Graduate Studies and Research in partial fulfillment of the requirements for the degree of Master of Engineering.

Department of Electrical Engineering,
McGill University,
Montreal, Canada.

December, 1972

© Stephen S.T. Tsui 1974

ABSTRACT

There have been many developments in the area of data compression during the past decade, with particular emphasis on video data because of the rapid increase in the amount of image transmission requirements.

Different schemes of redundancy reduction techniques are considered, especially the run-length encoding and differential pulse-code-modulation (DPCM). They are found to be more sensitive to channel errors than the conventional PCM. However, for channels with a low probability of bit error, bandwidth compression is achieved while the noise performance of these systems can be made as good as that of PCM. The transform method of image coding has the attractive feature that it is relatively immune to channel errors because of its inherent averaging property.

Reduction of the number of quantization levels with a decrease in the bit-rate will introduce false contours. An interpolation scheme has been suggested to combat this effect. The error analysis on the system shows that the method is acceptable in the mean square error sense for particular algorithms. Suggestions for future work are included.

ACKNOWLEDGEMENTS

The author would like to express his indebtedness to Dr. M. Fukada, under whose supervision this project was undertaken.

The author also wishes to thank the National Research Council for its financial assistance.

Thanks are also due to Miss P. Cunningham and Miss L. Lee for the careful typing.

TABLE OF CONTENTS

			Page
ABSTRACT			i
ACKNOWLEDGEMENTS			ii
TABLE OF CONTENTS			iii
CHAPTER	I	INTRODUCTION	1
	1.1	Introduction to Data Compression Systems	1
	1.2	Compression Ratios	6
	1.3	Classification of Data Compression Systems	10
CHAPTER	II	PICTURE CODING	25
	2.1	A Model for the Random Video Process	28
	2.2	Properties of the Human Visual System as an Image Evaluator	32
	2.3	Image Digitization and Coding	38
	2.4	Redundancy Reduction	43
	2.5	Contour Coding	73
	2.6	Transform Picture Coding	75
CHAPTER	III	EFFECTS OF CHANNEL NOISE ON SOME DATA COMPRESSION SYSTEMS	87
	3.1	Effect of Channel Noise on PCM Systems	87
	3.2	Effect of Channel Noise on Run-length Encoded ZOP Systems	92
	3.3	DPCM System: Channel Noise and Bit Compression	101
	3.4	Fourier Transform Coding: Effect of Errors and Bit Compression	116
CHAPTER	IV	IMAGE RECONSTRUCTION BY INTERPOLATION	128
	4.1	Contouring Effect	128
	4.2	Reduction of Contouring Effect	129
	4.3	Analysis of the Interpolation Process	131
	4.4	Sensitivity Weighted Error	140
CHAPTER	V	CONCLUSION	143
REFERENCES			145

CHAPTER I

INTRODUCTION

1.1 Introduction to Data Compression Systems

Communication of information consists basically of three operations: the preprocessing of the signal, the transmission over the channel, and the reconstruction of the signal at the destination. The past several years have seen notable advances in the processing of signals before transmission, especially with the evolution of the digital computer and the reduction in price of integrated circuits. The processing might include, for example, any combination of modulation, data reduction, and insertion of redundancy to combat the channel noise.

Modern communication techniques have made possible the transmission of analog signals in digital form. Transmission in digital form is attractive for several reasons:

(1) A saving in transmission power over conventional analog FM for high accuracy systems;

(2) the ability to regenerate the digital signal accurately;

(3) the ease of handling ON-OFF or YES-NO signals;

(4) the ease of multiplexing digital signals;

(5) the possibility of being applied to some future transmission media such as laser pipes.

Pulse-code-modulation (PCM) is one way to achieve digital transmission of voice, video and telemetry data. Recently, there is a tremendous increase in the amount of video data to be transmitted. This increase results from the recent interest in digital picture transmission in the following areas:

(1) Deep space probes with bandwidth restrictions due to power limitations, hence requiring digital processing;

(2) meteorological satellites requiring automatic data processing before and after transmission;

(3) communication satellites for commercial television and picture-phones;

(4) the convenience of teleconferencing;

(5) military applications where security measures may require the encryption of the information;

(6) applications in which digital memories become practical for space use.

Normally, a large amount of data are required for reasonably accurate digital representation of the video signal, resulting in exceptionally high bit-rate or bandwidth. It becomes apparent that new means of data processing must be found to increase the information transmission capabilities of communication facilities.

To achieve a high communication efficiency, it is necessary to maintain the channel capacity close to the information rate of the signal at all times [1]. This has led to the definition of the channel utilization index which is the ratio of the information rate of a source through a channel to the channel capacity. Many terminologies have arisen: data compression, data compaction, bandwidth compression, redundancy removal, redundancy reduction, adaptive telemetry and adaptive sampling. The following is an attempt to clarify the meaning of these terms.

Data compaction has a broad meaning and embodies both signal conditioning processes (analyzers, frequency discriminators, etc.) and data compression. Data compression is the process of matching the channel capacity of the system to the time-varying information rate of the signal. The desired end result is bandwidth compression. Adaptive sampling and redundancy reduction are subsets of data compression, where redundancy is defined as that fraction of a message or datum which is unnecessary in the sense that if it were omitted the message would still be essentially complete, or could be completed. Redundancy removal implies the complete removal of all redundancy, an objective which cannot be achieved. Adaptive telemetry is the mechanization of adaptive process, adaptive sampling or redundancy reduction.

The sampling theorem states that a bandlimited time function must be sampled at least at twice the highest frequency contained in that signal in order to extract all the information contained in the waveform. Most PCM systems are built

according to this rule. However, in the case of TV data and most telemetry data, there are some periods of low activity, and redundancy occurs during these periods when the signal is grossly oversampled. As an example, consider the fact that a 3 kc voice signal is normally converted to a 64 kc PCM bit stream (8 bit samples or an 8 kc rate) for digital transmission. This has aroused the interest of numerous people who have developed schemes to achieve more efficient communication. Such systems are called data compression systems.

As has been defined before, data compression consists of processing the data prior to transmission so that the received waveform can be reconstructed with a minimum number of samples to any desired accuracy. A buffer is usually required for temporary storage of the compressed data, so that the transmission can be synchronized and be transmitted at a rate lower than the Nyquist rate. A simplified block diagram of a data compression system is shown in Fig. 1.1, [2].

The cost of data transmission grows with the bit rate of the channel, the distance between stations and the complexity of the system. Incorporating data compression will reduce the bit rate but increase the complexity of the system. Hence, the communication engineers are confronted with the tradeoff problem in their design of data compression systems. If the cost for installing data compression is acceptable, data compression can be used in many applications to reduce the cost of data transmission, storage and processing and at the same time improve the data quality. Much work has been done and magnificent results were claimed. In fact, the true achievements are less than what is claimed, but they still are substantial. Whether any of these results

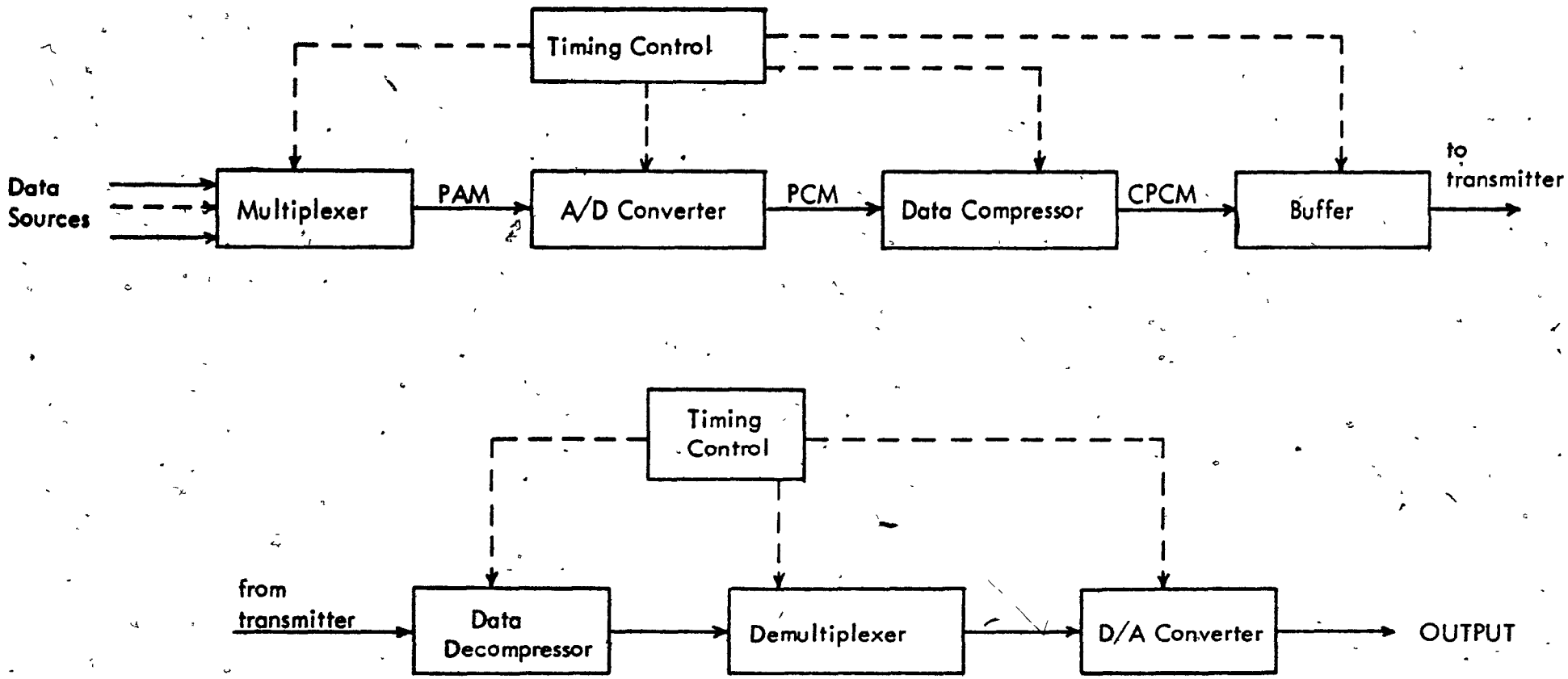

FIGURE 1.1 FUNCTIONAL BLOCK DIAGRAM OF A DATA COMPRESSION SYSTEM

are practical is an economic question which has to be re-evaluated continually in the light of the technological evolution.

To evaluate compression algorithms, some figures of merit must be used to serve as a basis of comparison. All things being equal, a "good" system should exhibit a high compression ratio. However, the compression ratio itself is quite meaningless unless it is relative to a well-defined basic system.

The type of compression technique used depends on (1) the user's requirements; (2) the channel noise; (3) modulation technique; (4) implementation restrictions; (5) the object material. Two aspects of data compression are often neglected. The first one is the interface between the data compressor and the remaining system [3]. The second one is the effect of channel noise on the system performance. Errors in compressed data are less tolerable than errors in uncompressed data because all the samples sent over a compressed system are essential and unprotected by redundancy. Two obvious solutions to combat channel errors are increase of signal power and adding controlled redundancy. However, both schemes will tend to reduce specific compression ratios.

1.2. Compression Ratios

Three compression ratios will be defined, using the fixed rate PCM system as a reference.

(1) Sample Compression Ratio

It is defined by

$$C_S = \frac{\text{total number of samples generated}}{\text{number of compressed samples transmitted}} = \frac{S_T}{S_{NR}} \tag{1.2.1}$$

This formula is useful to determine the amount of redundancy inherent in the message for a specific compression algorithm. But, it does not indicate the efficiency of the overall system which depends also on the timing information, synchronization, the coding procedure and the error correcting code. This leads to the definition of a bit compression ratio.

(2) Bit Compression Ratio

$$C_B = \frac{\text{number of bits to be sent in uncompressed data}}{\text{number of bits to be sent in compressed data}} \tag{1.2.2}$$

The number of bits in a compressed system consists of bits required for level information, timing information, synchronization and also error-correcting codes. Hence C_B can be expressed as

$$C_B = \frac{S_T N + K_1}{S_{NR}(N + W) + K_2 + P} \tag{1.2.3}$$

where

N = number of bits to represent one sample level;

W = number of bits to represent the timing information;

K_1 = bits for sync-word in uncompressed system;

K_2 = bits for sync-word in compressed systems;

P = bits for error-correcting code;

or

$$C_B = \frac{S_T}{S_{NR}} \frac{1 + \frac{K_1}{NS_T}}{1 + \frac{W}{N} + \frac{K_2 + P}{NS_{NR}}} \tag{1.2.4}$$

The sync-words and error-correcting codewords are usually short compared with the total number of bits in a line, therefore,

$$C_B \simeq \frac{\frac{S_T}{S_{NR}}}{1 + \frac{W}{N}} = \frac{C_S}{1 + \frac{W}{N}} \tag{1.2.5}$$

It can be seen that C_S, the sample compression ratio, is an upper bound for the compression ratio of any system.

It is important to note that in defining the above ratios, the two systems should exhibit the same signal-to-noise power ratios for a meaningful comparison, since higher bit compression ratios are obtained by relaxing the fidelity requirement for the compressed data.

As an example, let us consider the bit compression ratio for the run-length encoding scheme. Run-length encoding consists of transmitting the levels of all non-redundant samples together with words expressing the number of redundant samples following each non-redundant sample. A run is defined as a

sequence of consecutive redundant samples and the run length is the number of redundant samples in a given run. Assume that T is the maximum run length, then the number of bits required to represent the timing information is

$$W = \log_2 T \tag{1.2.6}$$

Hence,

$$C_B = \frac{C_S}{1 + \frac{\log_2 T}{N}} \tag{1.2.7}$$

Because it is easy to implement, run-length encoding is used very often, especially in digital TV signal encoding.

3. Energy Compression Ratio

Since bit errors are inevitable in transmission over noisy channels, it is sometimes necessary to increase the transmitter power to remedy the situation. But, the bit compression ratio does not take into account this extra energy spent. This leads to a new basis of comparison, defined by the system energy compression ratio, the ratio of the average energy required to send a sample in an uncompressed communication system to that required in a compressed system for the same data quality [4], [5]. This ratio is a function of the probability of bit error in the compressed system. The fidelity criterion for data quality can be chosen as the average of any cost function suited to the particular application. Usually the mean square error or probability of bit error is chosen.

The energy compression ratio may be expressed as

$$C_E = C_B \frac{E_u}{E_c} \tag{1.2.9}$$

where

E_u = energy per bit for the uncompressed system;

E_c = energy per bit for the compressed system,

both systems having the same data quality. It turns out that this ratio is very difficult to compute.

1.3 Classification of Data Compression Systems [6] - [13]

There are basically two types of data compression: Entropy Reducing (ER) and Information Preserving (IP) transformations. These two main transformations are described briefly in the following and more detailed description of some specific applications to picture coding will be given in Chapter II. A schematic classification of data compression models by category of their effects on the signal is given in Fig. 1.3.1.

(1) Entropy Reducing Transformations

Entropy is defined as the average value of the self-information and is given by

$$H(x) = \sum_{k=1}^{k} P_x(a_k) \log_2 \frac{1}{P_x(a_k)} \tag{1.3.1}$$

$$= -\sum_{x} P(x) \log_2 P(x) \tag{1.3.2}$$

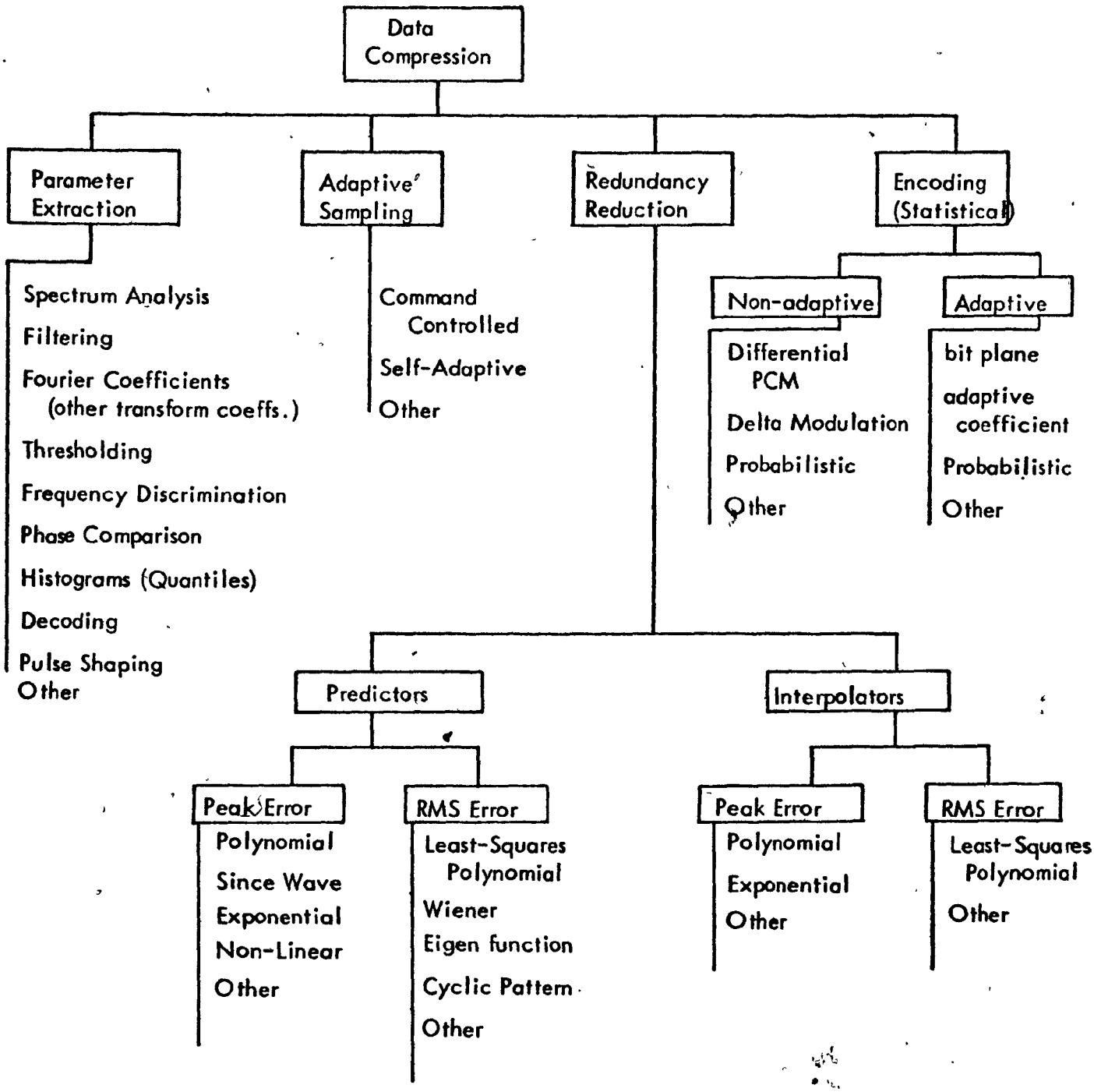

FIGURE 1.3.1 CLASSIFICATION OF DATA COMPRESSION MODELS, [6]

An entropy-reducing (ER) data compression operation is an irreversible operation on the data source which results in an "acceptable" reduction in data quality. Generally, a special ER device must be designed for each application and no interchange is possible. An ER compressor usually operates directly on the data source, before sampling and quantization. Typical examples of ER devices are filters and frequency discriminators.

It is relevant at this point to show that ER transformations always reduce the entropy of the source. Assume that the data source at the input of the ER device has a basic limitation in measurement precision due to source noise and measurement hardware design, then the input to the ER compressor may be expressed as a discrete source of K levels. If $\{X_i\}$ is the input and $\{Y_i\}$ the output of the device, then

$$H(X, Y) = H(X) + H(Y|X) = H(Y) + H(X|Y) \tag{1.3.3}$$

Since $Y_i = f(X_i)$, we have

$$H(Y|X) = 0 \tag{1.3.4}$$

Also, ER transformation is irreversible, thus

$$H(X|Y) > 0 \tag{1.3.5}$$

Hence,

$$H(Y) = H(X) - H(X|Y) < H(X) \tag{1.3.6}$$

which proves that ER compression results in a reduction in entropy. However, the probability distributions are appreciably affected in some cases.

It is well know that if the events are equally probable, i.e.,

$$P(X_i) = \frac{1}{K} \tag{1.3.7}$$

then

$$H = H_{max} = \log_2 K = L \log_2 N \tag{1.3.8}$$

where

L = dimensionality of the signal space,

N = number of quantization levels used for each co-ordinate.

We, therefore, conclude that the maximum entropy of a source is proportional to the dimensionality of the signal space and only logarithmically proportional to the number of quantum levels per co-ordinate. A narrow band low-pass filter reduces the dimensionality of the signal space and hence is an ER device.

The compression ratio defined in terms of entropies is given by

$$C_R = \frac{H_{max}}{H} = \frac{L \log_2 N}{-\sum_{i=1}^{K} P(X_i) \log_2 P(X_i)} \geq 1 \tag{1.3.9}$$

This ratio can be regarded as the ideal compression ratio. The relative redundancy is given by

$$R = \frac{H_{max} - H}{H_{max}} = 1 - \frac{1}{C_R} \tag{1.3.10}$$

or

$$C_R = \frac{1}{1-R} \tag{1.3.11}$$

The implementation of an ER system will be described below.

Non-Adaptive Encoder for Statistical Phenomena:

Let $\{P_i\}$ represent the probability distribution of an observed sequence. The resulting sequence must be transmitted only when the expected statistical low is violated. Let S be the number of observations and $\{\lambda_i\}$ be the empirical probabilities of the quantum states. The following equations result:

$$\Delta H(S) = S \sum_{i=1}^{K} \lambda_i \log \frac{\lambda_i}{P_i} \tag{1.3.12}$$

$$\sum_{i=1}^{K} P_i = 1 \tag{1.2.13}$$

$$\sum_{i=1}^{K} \lambda_i = 1 \tag{1.3.14}$$

The statistical law is that

$\Delta H(S) \leq \Delta H_o \rightarrow$ expected law is confirmed

$\Delta H(S) > \Delta H_o \rightarrow$ expected law is violated

A block diagram realization of this system is given in Fig. 1.3.2.

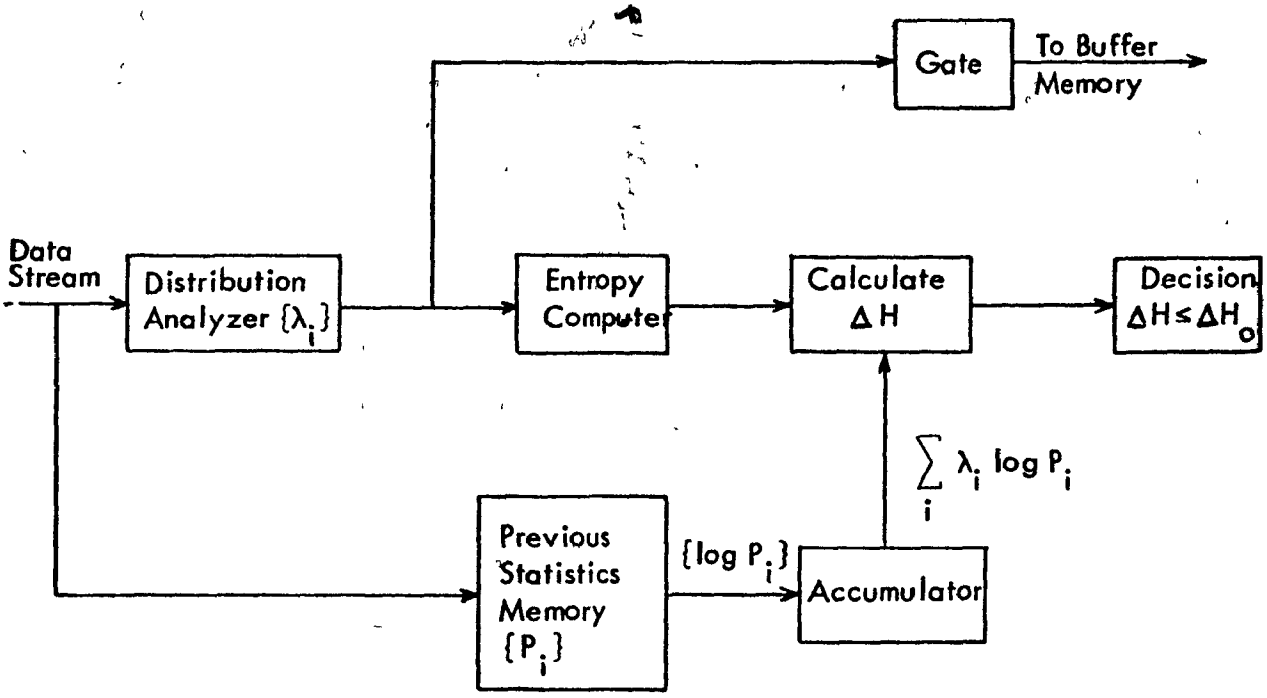

FIGURE 1.3.2 STATISTICAL DATA COMPRESSOR.

(2) Information - Preserving (IP) Transformations (Exact Coding)

An Information - Preserving data compression operation reduces the number of samples that need to be transmitted in order to reconstruct the original waveform. Hence, the transformation is reversible.

To realize the transformation, the source statistics must be known. Consider a sampled, quantized data stream $\{x\}$,

$$\{x\} = \{x_o(t_o), x_1(t_o + \Delta t), \ldots, x_i(t_o + i\,\Delta t) \ldots\} \qquad (1.3.15)$$

where x is quantized. Another way of expressing this sequence is,

$$\{x\} = \{x_o, t_o; x_1, t_1; x_2, t_2; \ldots; x_i, t_i; \ldots\} \qquad (1.3.16)$$

When these samples are fed into an IP device, some of these do not appear at the output. The missing data can later be re-inserted at the receiver according to a reconstruction algorithm. Both the timing information and the amplitude information must be sent in an IP data compressor.

Fig. 1.3.3 is a block diagram representation of operations on message source at transmitter and receiver.

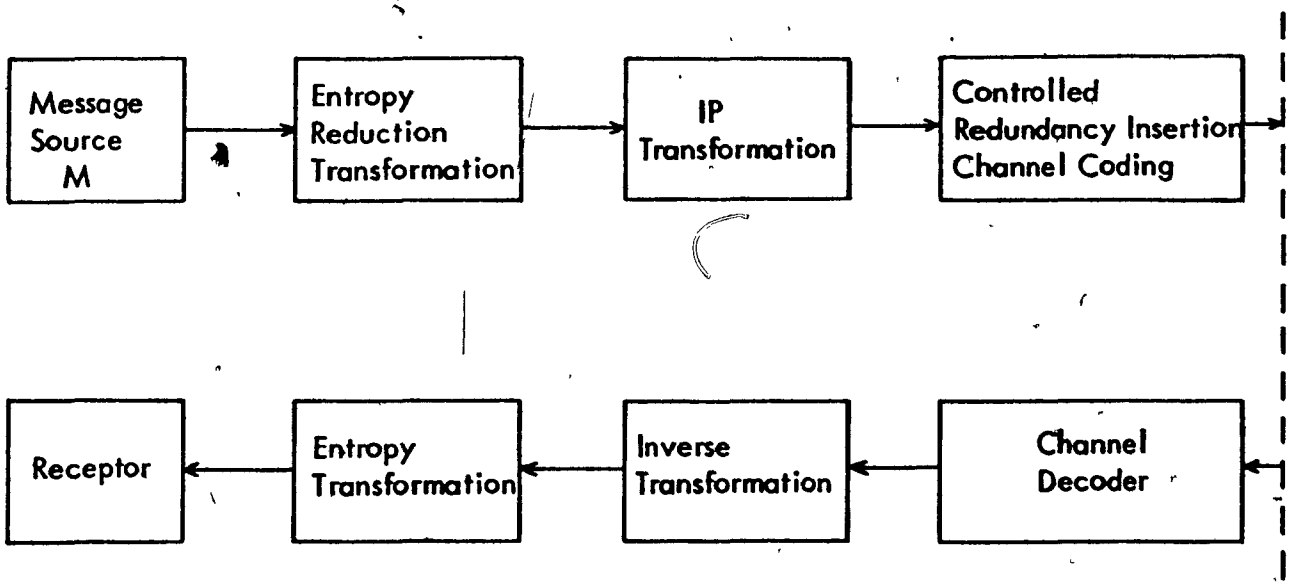

FIGURE 1.3.3 OPERATIONS ON MESSAGE SOURCE AT TRANSMITTER AND RECEIVER.

In may cases, predictive mapping which is an IP transformation to reduce redundancy is cascaded with another IP transformation called run-length coding to achieve compression [14]. The output of the run-length coder is a compressed version of the input message. This technique can be easily implemented and is of practical interest, most often applied to TV data. A detailed description

is given in Chapter II.

It is important to note that IP compressors can be cascaded without loss of information. Since compressors require memory, it is possible to save memory by using simple compression techniques and then cascading the simple operations with more complex ones which require less memory. An example of this technique is shown in Fig. 1.3.4 , where a simple cascaded predictor removes sample-to sample correlations by previous value prediction and then uses previous line prediction on the remainder for TV.

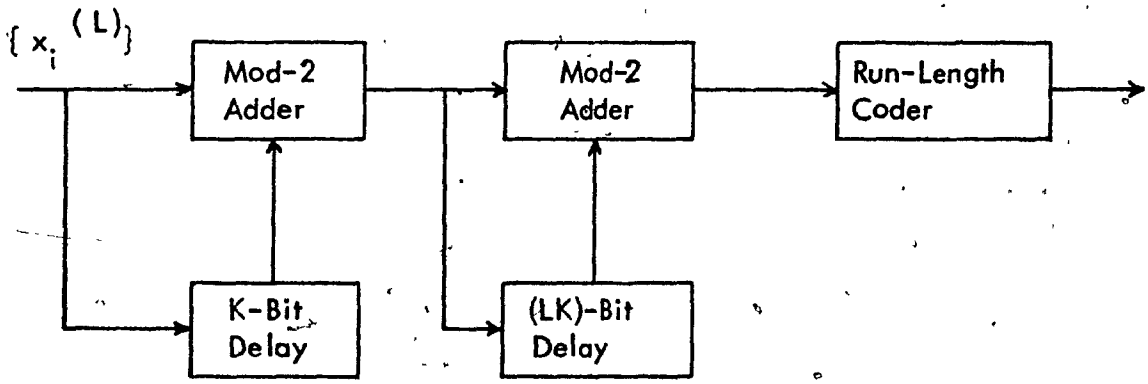

FIGURE 1.3.4. CASCADED PREVIOUS SEQUENCE AND PREVIOUS LINE COMPRESSOR FOR TV.

Typical examples of IP transformations are polynomial predictors, interpolators, differential PCM, transform coding, run-length encoders and bit-plane encoders [15].

In many literature, information - preserving transformation is referenced as redundancy removing data compression. This leads to the following view point. For M quantization levels, the redundancy is

$$R = 1 - \frac{H}{\log_2 M} \tag{1.3.17}$$

Thus, before compression

$$R_X = 1 - \frac{H_X}{\log_2 M} \tag{1.3.18}$$

and after compression,

$$R_Y = 1 - \frac{H_Y}{\log_2 M} \tag{1.3.19}$$

But, $R_Y \leq R_X$ since it is a redundancy reduction procedure.

Therefore,

$$H_Y \geq H_X \tag{1.3.20}$$

This increase in entropy is due to the reduction of dependence between successive samples when prediction is successful. The ideal compression ratio is again given by

$$C_R = \frac{1}{1 - R_X} \tag{1.3.21}$$

Fig. 1.3.5 is a block diagram of redundancy type data compressor, and the operation is as follows: The reference memory stores all data which will serve to perform the compression; they are previous samples, tolerance limits, slope limits, selection of a particular algorithm, etc. The comparator determines whether each new sample is redundant or non-redundant, and the reference memory is updated accordingly. The

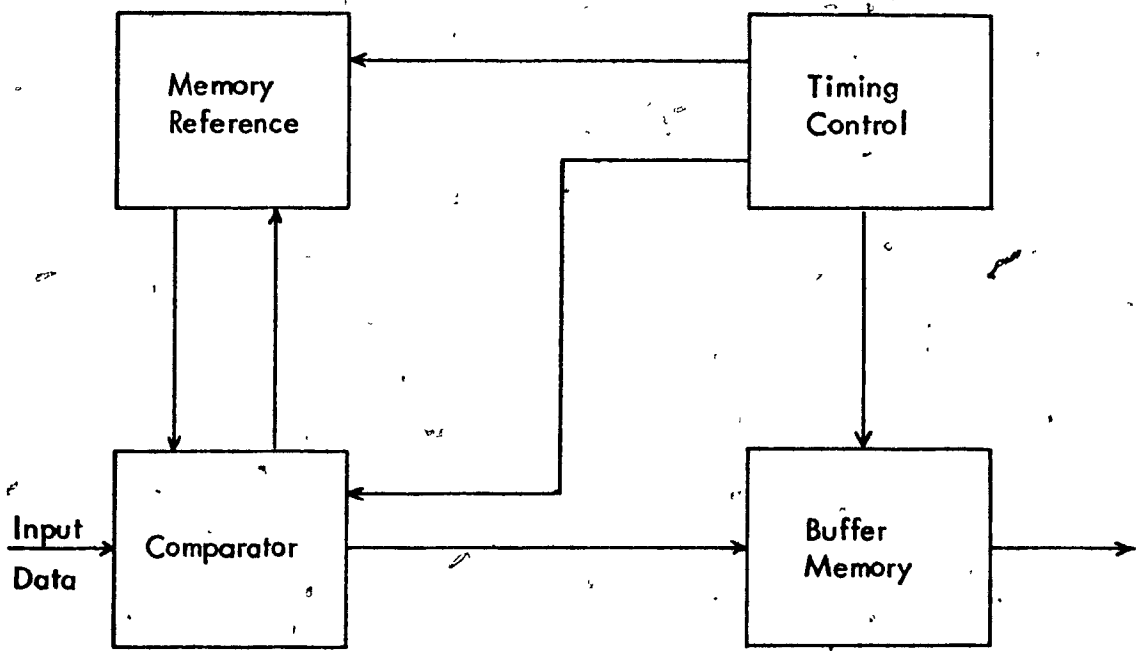

FIGURE 1.3.5 SIMPLIFIED BLOCK DIAGRAM OF REDUNDANCY REDUCTION TYPE COMPRESSOR.

non-redundant samples are sent to the buffer memory which permits synchronous transmission. Buffer design is always a difficult task and overflow is the most serious problem because non-redundant samples will be lost, [16], [17]. The "timing and control" provides the necessary signals to control the sequence of operations which the data compression system must perform. A more elaborate block diagram of a telemetry data compressor is shown in Figure 1.3.6.

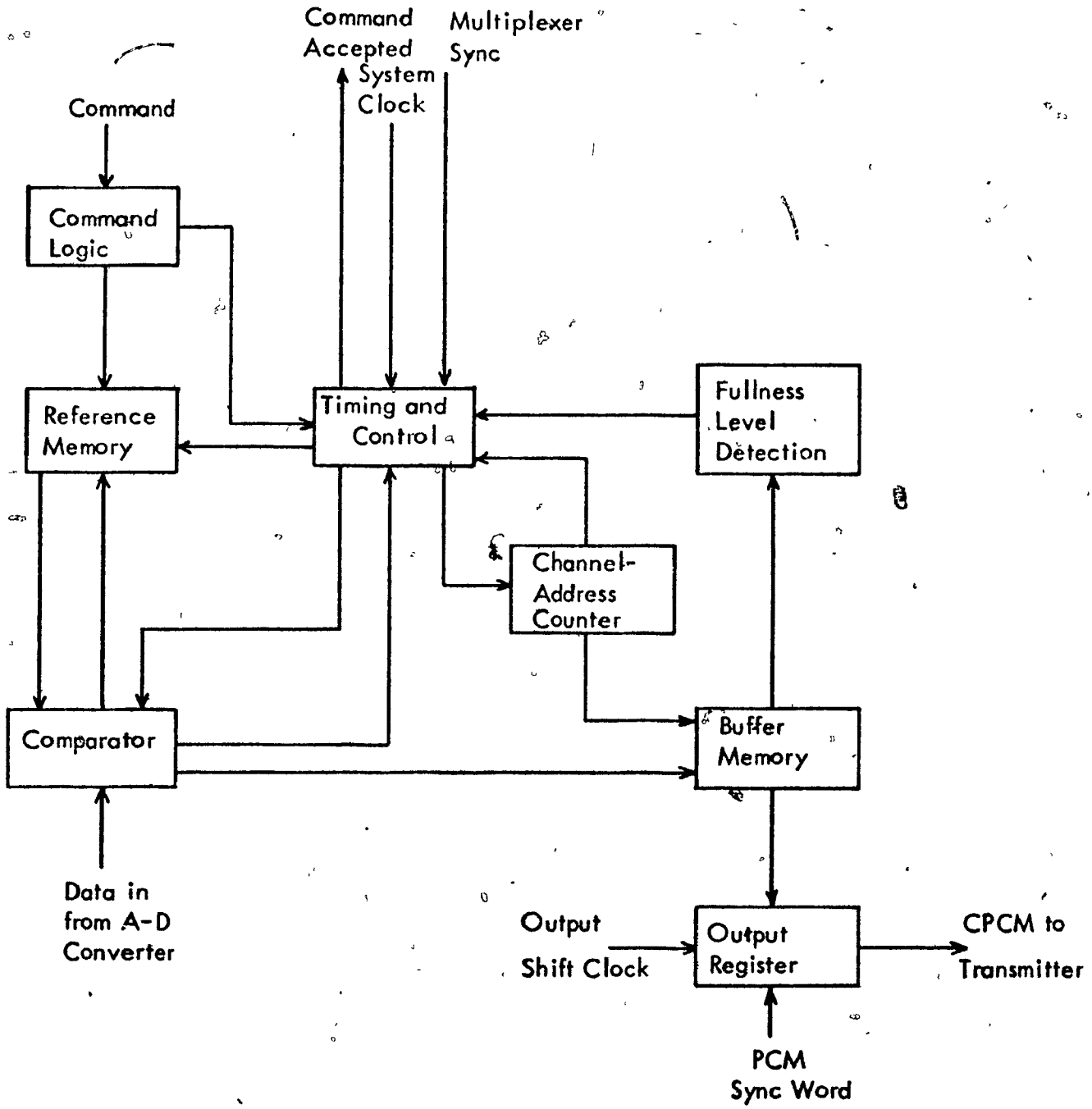

FIGURE 1.3.6 FUNCTIONAL BLOCK DIAGRAM OF A TELEMETRY DATA COMPRESSOR.

An example of adaptive coding will be considered next. For TV signals, the probability of obtaining long consecutive runs of the same sequence is high. The output of the mod-2 adder will contain long strings of zeros. Fig. 1.3.7 represents a predictive transformation which includes a decision device which gives a "one" if the prediction is correct and a "zero" otherwise. This is the Shannon-Fano compressor

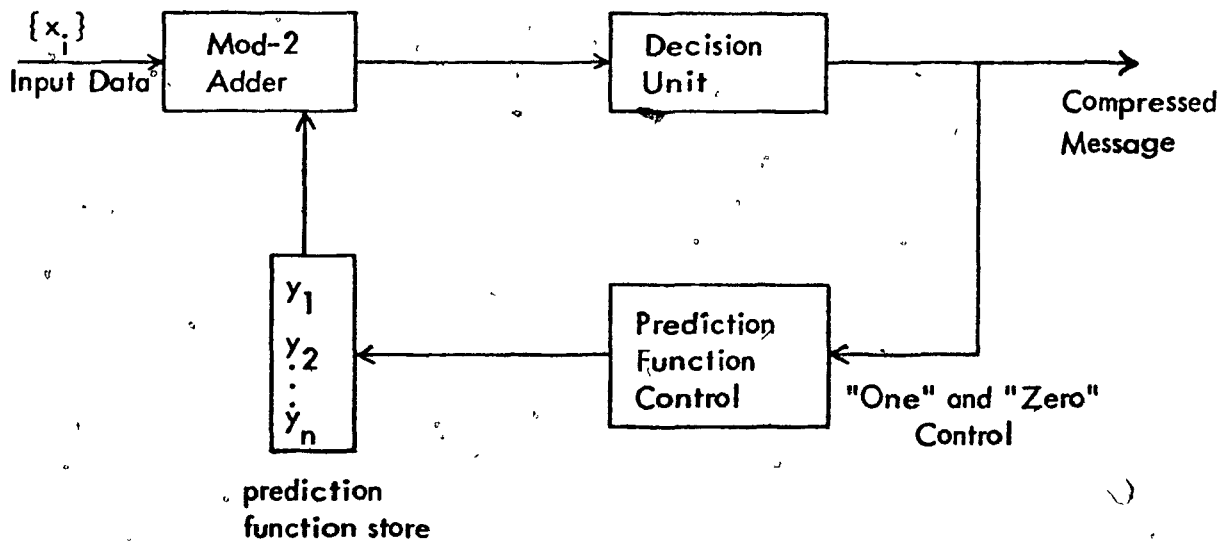

FIGURE 1.3.7. SHANNON-FANO COMPRESSOR.

By combining the non-adaptive encoder described before in Fig. 1.3.2 with this Shannon-Fano compressor, the optimum adaptive compressor is obtained. It is represented in Fig. 1.3.8. A control line has been added to adjust the source

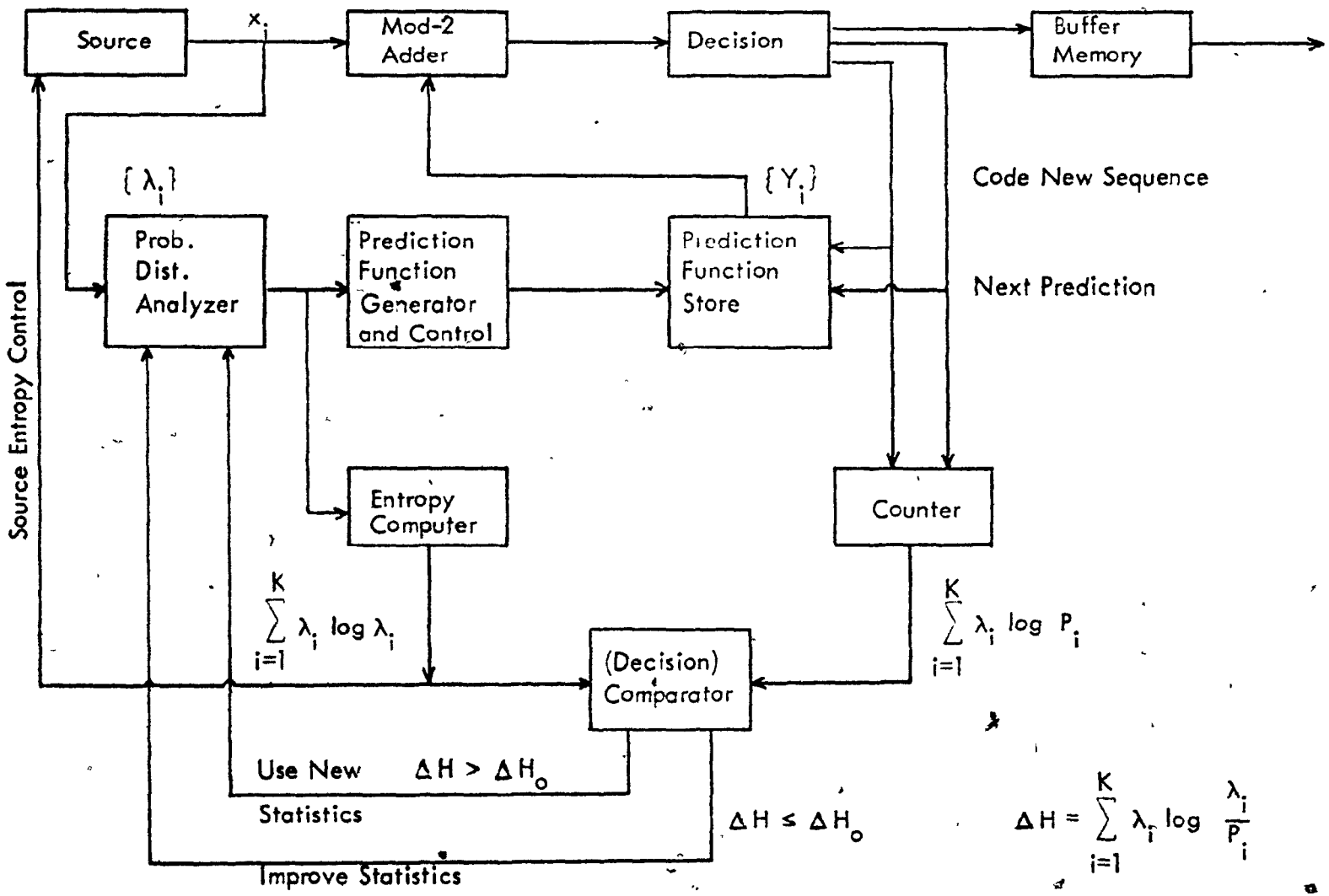

FIGURE 1.3.8 FUNCTIONAL BLOCK DIAGRAM OF AN ADAPTIVE CODER

entropy in accordance with the channel status, hence avoiding excessive degradation of the data during channel overload.

For a prediction process in which we wish to predict the K th sample S_K, having observed the m preceding samples, the best nonlinear estimate for S_K is

$$\hat{S}_K = E(S_K | S_{K_1}, S_{K_2}, \ldots, S_{K_m}) \tag{1.3.22}$$

$$= \sum_{i=1}^{m} i \Pr(S_K = i | S_{K_1}, S_{K_2}, \ldots, S_{K_m}) \tag{1.3.23}$$

where i denotes the i th quantum level [18].

For the system described above, it can be shown [25] that the upper bound of the bit compression ratio is

$$C_B \leq \frac{\log_2 K}{p \log_2 (\frac{1}{p}) + (1-p) \log_2 \frac{K}{(1-p)}} \tag{1.3.24}$$

where p is the probability of making an accurate prediction.

In this chapter, the basic philosophy of data compression systems has been discussed. Their importance, the economic factors which govern their design and the criteria for comparing their performance have been presented. An attempt has been made to classify them into categories. In the next chapter, the description of some of their applications to video signal compression will be given. Chapter III will discuss

in detail their performance under noisy channel condition. A new technique in picture compression by interpolation will be described in Chapter IV.

CHAPTER II

PICTURE CODING

Nowadays most video information is transmitted over digital channels. Basically the method consists of line scanning the two-dimensional picture transforming it into 1 - dimensional data which is sampled uniformly and quantized to one of the 2^k levels and is transmitted using the k bits [19]. The function of an image transmission system is to convey to the observer a "best" reproduction of the original picture. But, what gives the "best" representation varies according to the application. A 6 - 8 bits per sample PCM is used mostly as a standard for comparison. It has been shown that most pictorial data indicated an entropy of two to three bits per sample [20] - [22]. Hence, a reduction in the number of bits representing a picture is possible by using some coding schemes. The reason that this reduction is possible is twofold. Firstly, there is statistical redundancy in images. High correlation exists between spatially close samples. The lower-bound redundancy is approximately given by

$$R \simeq -\frac{1}{2} \log_2 (1-A) \text{ bits/sample}$$

where A is the correlation between neighbouring pels. Secondly, there is psychovisual redundancy in images. By intentionally altering the original image in such a way so as not to cause a loss in its subjective quality, a saving is possible. Fig. 2.1 gives a general block diagram representation of a transmission system.

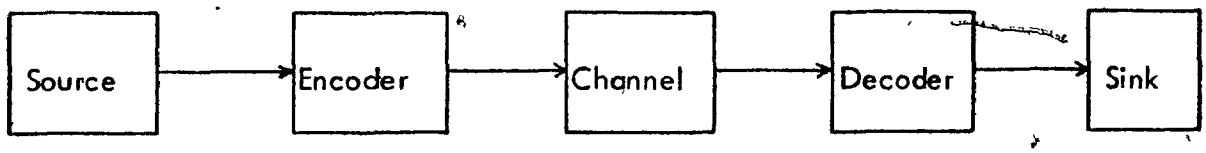

FIGURE 2.1. A GENERAL BLOCK DIAGRAM FOR A TRANSMISSION SYSTEM.

In our case, the input is an image and the sink is a human observer. The signals are encoded to suit the channel and the decoder transforms the channel output into an image suitable for the human observer. A more detailed layout of a practical system is given in Fig. 2.2. The filters, the sampler, the quantizer, and the psychovisual and statistical encoders are designed according to the source properties: hence called source encoding. The channel coding includes the operation of the error-detection and correction coding and the modem which are designed to suit the channel properties. Due to the interaction between the blocks, optimization of the overall system is almost impossible. Hence, "good" systems are usually designed instead of optimal ones, based on particular applications and individual judgement. The properties of the source, which is the random video process in this case, will be presented in the following section.

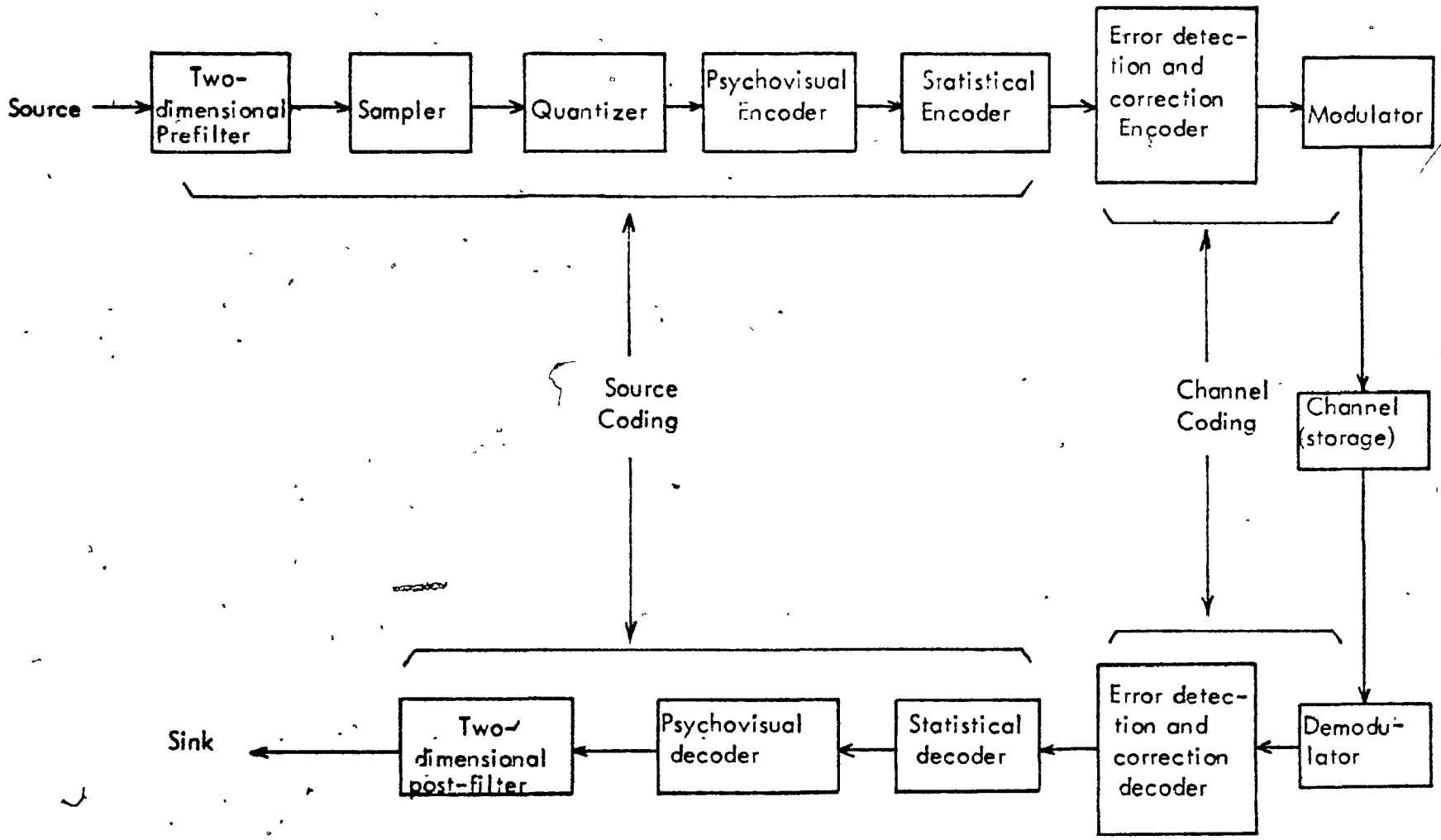

FIGURE 2.2 A PRACTICAL BLOCK DIAGRAM FOR AN IMAGE TRANSMISSION (STORAGE) SYSTEM

2.1 A Model for the Random Video Process

The statistical characteristics of the video signal have been measured by many workers and the following results are based mostly on the work by Franks [23], Kretzmer [21], Estournet [24] [25], Seyler and Budrikis [26] and Deriugin [27].

Any picture can be modelled by a luminance function of three variables $I(x,y,t)$ where x and y are the spatial co-ordinates and t the time co-ordinate. It can be expressed in the form of a discrete representation $I(m\Delta x, n\Delta y, kT)$ which also indicates the sampling procedure of TV signals. An optical scanner moving at constant velocity across the picture transforms a two-dimensional process into a stationary function of time. Franks [23] proposed a model for the luminance process which has the following characteristics:

(1) The probability of occurrences of a particular number of level changes is not dependent on the position on the time axis;

(2) For a small interval, the probability of a jump in level is proportional to the length of the interval, while probability of more than one jump in a very short interval is zero;

(3) The amplitudes are statistically independent with a rectangular probability distribution.

Hence, it has the characteristics of the random step function [28] as shown in Fig. 2.1.1.

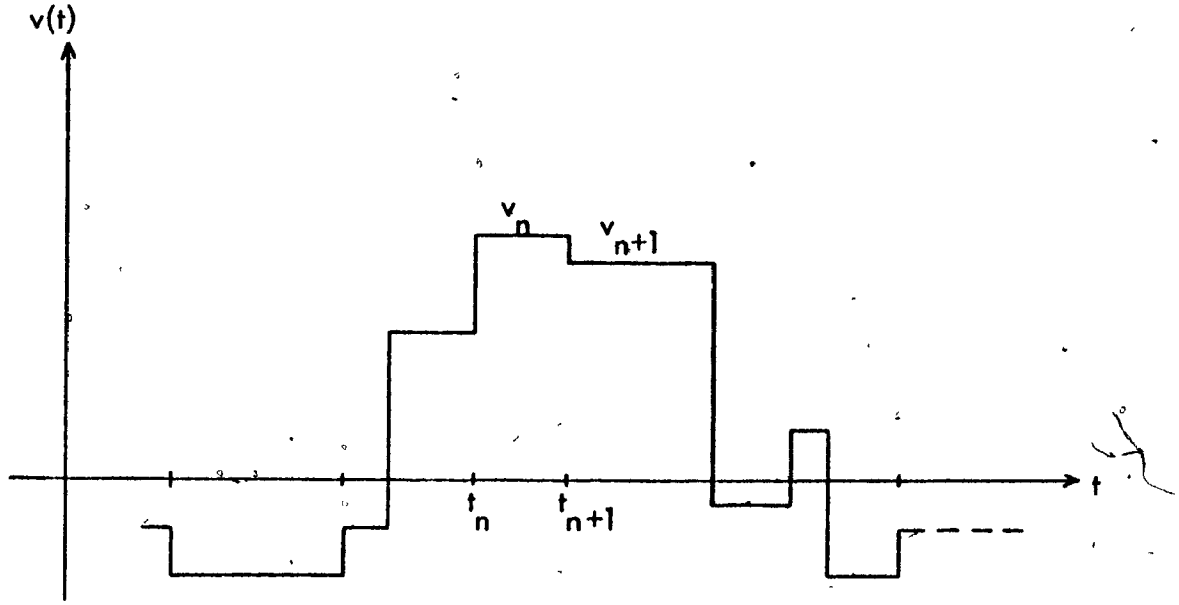

FIGURE 2.1.1 RANDOM VIDEO SIGNAL

Now the probability of n jumps in interval of $t + \Delta t$ is given by

$$P_n(t+\Delta t) = [(\text{probability of } n \text{ jumps in } t) \cdot (\text{probability of no jump in } \Delta t)] + [(\text{probability of } (n-1) \text{ jumps in } t) \cdot (\text{probability of 1 jump in } \Delta t)] \tag{2.1.1}$$

Thus,

$$P_n(t+\Delta t) = P_n(t)\,P_o(\Delta t) + P_{n-1}(t)\,P_1(\Delta t) \tag{2.1.2}$$

From the characteristics in (2) the probability of a jump in Δt is $\lambda \Delta t$.

$$P_n(t+\Delta t) = P_n(t)(1-\lambda\Delta t) + P_{n-1}(t)\lambda\Delta t \tag{2.1.3}$$

or

$$\frac{P_n(t+\Delta t) - P_n(t)}{\Delta t} = -\lambda P_n(t) + \lambda P_{n-1}(t) \tag{2.1.4}$$

Hence,

$$\frac{d}{dt} P_n(t) = -\lambda P_n(t) + \lambda P_{n-1}(t) \text{ as } \Delta t \to 0 \tag{2.1.5}$$

Since $P_n(0) = 0$, i.e., $n = 1,2,\ldots$ jumps in zero time is impossible,

$$P_n(t) = \lambda \int_0^t e^{-\lambda(t-\tau)} P_{n-1}(\tau)\, d\tau \text{ for } n \geq 1 \tag{2.1.6}$$

and since $P_o(0) = 1 - P_n(0) = 1$,

$$P_o(t) = e^{-\lambda t} \text{ for } t \geq 0 \tag{2.1.7}$$

Hence, by induction using (2.1.6) and (2.1.7),

$$P_n(t) = \frac{(\lambda t)^n}{n!} e^{-\lambda t}, \quad t \geq 0 \tag{2.1.8}$$

Equation (2.1.8) shows that the $\{t_i\}$ are Poisson distributed.

If we assume that the random step function is a stationary, wide-sense Markov sequence, it can be shown that the correlation function is

$$\phi(\Delta x, \Delta y, T) = A \exp[-\alpha|\Delta x| - \beta|\Delta y| - \lambda T] \tag{2.1.9}$$

which has a separable property giving rise to three factors characterizing the element-to-element, line-to-line and frame-to-frame correlation. In (2.1.9), $A = \phi(0,0,0)$ and α, β, λ are constants. Other authors [21] expressed (2.1.9) as

$$\phi(\Delta x, \Delta y) = \exp\left[-\sqrt{(\Delta x)^2 + (\Delta y)^2}\right] \tag{2.1.10}$$

by considering only spatial correlation, and has been born out by measurements with $\alpha = 0.0256$ and $\beta = 0.0289$.

The average number of jumps occurred in an interval of t can be derived. From previous discussions,

$$P_n(t) = \frac{(\lambda t)^n}{n!} e^{-\lambda t}$$

Thus,

$$E[n] = \sum_{n=0}^{\infty} n \left(\frac{\lambda t}{n!}\right)^n e^{-\lambda t}$$

$$= \lambda t e^{-\lambda t} \sum_{m=0}^{\infty} \left(\frac{\lambda t}{m!}\right)^m$$

$$= \lambda t \tag{2.1.11}$$

Hence, λ is a rate parameter equal to the probability of a jump at any instance.

With the above proposed model, Franks and others have reached at conclusions which are summarised below:

(1) The amplitude distribution is uniformly distributed and upper bounded;

(2) The three-dimensional TV process has a separable autocorrelation function representing the element-to-element, line-to-line, and frame-to-frame correlation in exponential form;

(3) The time of occurrences of jumps are Poisson distributed while the distribution of level differences between runs is exponential;

(4) Probability of zero difference between two picture elements is large;

(5) Successive jumps tend to be equal in magnitude if the first jump is not too large;

(6) If the first jump is large, the next jump will more likely be small;

(7) From power spectral density measurements, it has been shown [23] [24] that large concentrations of power occur at multiples of frame rate, line rate and sampling rate for PCM or DPCM coded pictures.

The properties of the sink which is in our case the human visual system will be presented in the next section.

2.2 Properties of the Human Visual System as an Image Evaluator

The results of video transmission schemes are well known to the scientific and engineering community, and even to the public through TV and the availability of picture phones. However, the development of these schemes usually

has not taken into account of the response of the human observers to the pictorial errors. The error criteria used to optimize the parameters of video transmission systems have been chosen primarily for their mathematical tractability. The most commonly used one is mean-square error. On the other hand, it has been demonstrated experimentally that pictures of equal amounts of mean-square error are substantially different in quality. In the following, a brief review of the properties of the human visual system is given [30] - [38]. The conclusions here will have a large bearing on the design of most pictorial data compression schemes.

(1) Resolution

(a) Spatial Resolution: The spatial frequency response of the human visual system has been studied by De Palma and Lowry [30]. They concluded that the modulation transfer function of the visual system has a bell-shaped structure as shown in Fig. 2.2.1. It has a maximum sensitivity at 20 lines/mm. and falls off at both higher and lower frequencies. This is intuitively justified; for some objects are too small to see and the eye cannot distinguish easily a gradual change in brightness from one side of a scene to the other. The above is in contrary to the previous theories that the sensitivity function is a monotonic decreasing response with frequency. Hence, the eye acts more like a differentiator than an integrator which is implied by the monotonic decreasing assumption [39].

(b) Temporal Resolution: There is a strong link between temporal and spatial resolution which show similar responses. Both low frequency and high frequency

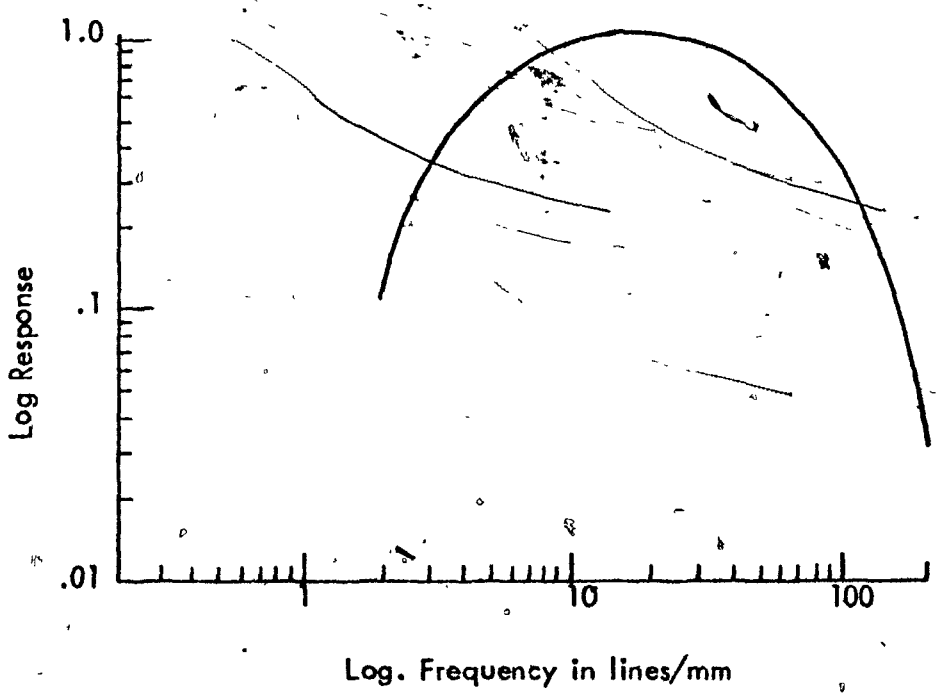

FIGURE 2.2.1 SPATIAL MODULATION TRANSFER FUNCTION OF THE EYE AT THE RETINA

variations are insensitive to the human eye. This fact is being exploited in psycho-visual coding.

(2) Spatial Acuity

This is a subjective effect of the sharpness present at the boundaries of images. The rendition of line structure and boundary regions is of principal importance in visual perception. It has been demonstrated that the width of the boundary transition varies directly with subjective acuity, and that the subjective visual unsharpness is inversely related to the maximum first derivative of the boundary transition. The Mach phenomenon has been postulated. The effect is best illustrated in the diagram shown in Fig. 2.2.2, which shows that the eye tends to minimize the unsharpness psychovisually.

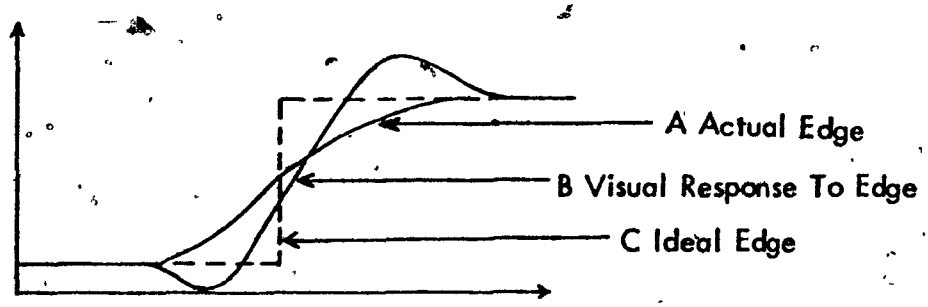

FIGURE 2.2.2 EDGE RENDITION

(3) Image Contrast

A lot of experiments have been conducted to test the contrast sensitivity of the eye [34]. It is found that contrast sensitivity is interrelated to resolution and, to a lesser extend, acuity. The observer is exposed to a uniform field of brightness B_o with a sharp-edged region in the centre as shown in Fig. 2.2.3.

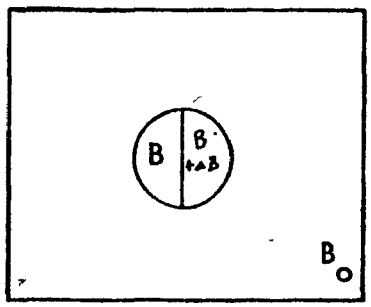

FIGURE 2.2.3 TEST PATTERN FOR CONTRAST SENSITIVITY

The just noticeable difference ΔB is measured as a function of B, with the background brightness B_o as a parameter. It is found that the eye has a dynamic range which is quite similar to that of electronic imaging systems. It has also been found that the minimum contrast ratio necessary for perception is less for large areas than for small ones.

(4) Noise Visibility

Since noise has a tremendous effect on the visual response, the important facts known about it are summarised below. Additive Gaussian noise interference is assumed.

a. The visual perception is dependent upon the noise contrast present and also upon the spatial frequency response of the visual system upon the scene;

b. Schreiber [39] concludes that noise is less visible in a complicated picture;

c. Its presence reduces picture contrast and edge sharpness;

d. Roberts [40] states that noise is more visible if it is correlated with the picture than if it is random. Quantization noise results when the image is quantized into too few levels, resulting in false contours. It is more annoying than random noise of the same r.m.s. value;

e. The eye is more sensitive to noise with local structures (in bursts) than scattered noise.

Although a large amount of work has been done, the way in which the spectrum of the image affects the noise visibility is still unknown.

2.3 Image Digitization and Coding

(1) Sampling:

Consider the sampling process shown in Fig. 2.3.1, [41]

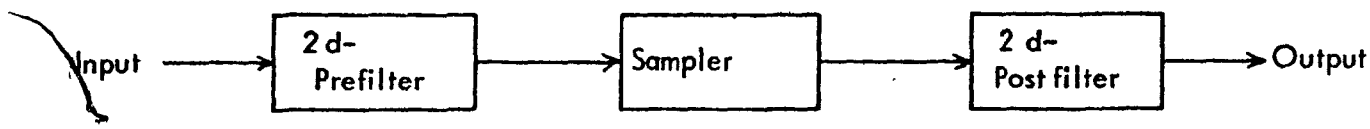

FIGURE 2.3.1 SAMPLING PROCESS

Suppose that each picture is sampled into an $L \times L$ square array of points, and each sample is quantized into 2^k levels. In order to obtain a received image with resolution comparable to that of present-day commercial television pictures, about 500×500 samples per frame are required, and 64 to 128 levels are used. Therefore, $L = 500$ and $k = 6$ or 7. A smaller L results in poorer resolution or spurious patterns generally called moiré patterns. Small k will introduce false contours. One bit per sample can be saved by logarithmic quantization which matches more closely with the response of the human vision.

Peterson and Middleton [42] have shown that, for a fixed number of samples per frame, prefiltering and postfiltering with ideal low-pass filters gives

minimum difference between the input and the output in the mean-square sense. Huang and Tretiak [43] indicated that these same filters also yield reconstructed pictures of the best subjective quality in the case of low resolution (L=64). For high resolution systems (L=256), high spatial frequency accentuation at the post-filter will probably improve the output image.

(2) Quantization

The output from the sampler consists of samples with a continuous brightness range. These samples have to be digitized before they can be transmitted. The quantizer assigns a discrete level to each sample and by doing so introduces the so called quantization noise. The quantizer can be uniform or non-uniform, but enough levels must be used to avoid obvious discontinuity. If a discontinuity is visible in an area where the subject has no detail, such as a sky or a face area, a false contour is produced. 6 bits are usually required for contour-free PCM transmission. D.N. Graham [44] has shown that by placing a prefilter and a postfilter around the quantizer, quantization noise can be reduced and a contour-free picture can be reproduced using only 3 bits per sample. The fact that quantization noise is more visible than additive noise of the same r.m.s. value has been pointed out by Roberts [40] who proposed a pseudo-random noise modulation scheme. It essentially consists of adding a noise of flat amplitude distribution, with peak-to-peak value equal to one quantum step, to the analog signal before quantization and an identical noise being subtracted at the receiver. Good contour-free pictures are produced with 4 bits per sample. Since

then, a fair amount of work has been devoted to the study of ordered dither [45] - [47]. The idea of the dither design is to concentrate the error in the high frequency parts of the picture to which the eye is less sensitive. It has been pointed out [45] that dither can do more than hiding quantization effects behind a mask of noise or change the pattern of quantization errors to reduce their visual annoyance; it is capable of restoring some of the information which the coarse quantizer without dither would remove. The effect of dither is best illustrated in Fig. 2.3.2. The dither provides rapid switching between the quantizer levels on either side of the time input signal, hence it has the effect of breaking up the contours.

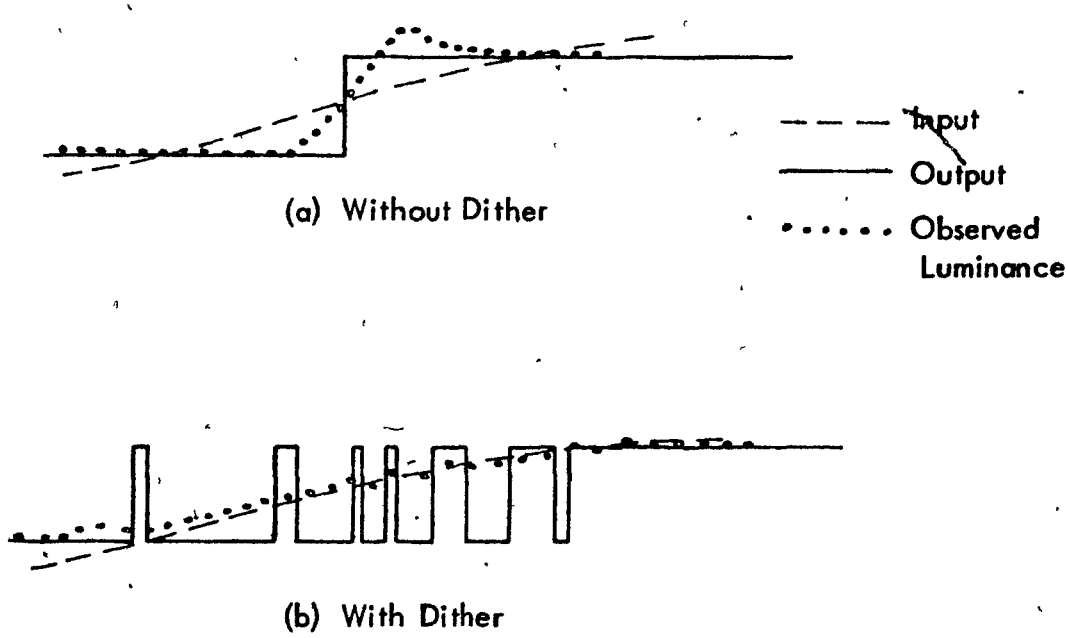

FIGURE 2.3.2 EFFECT OF DITHER

In the following, we shall consider the effect of quantization noise on a constant rate, time sampling PCM system with 2^k levels in the quantizer.

Assume that the amplitude of the source is uniformly distributed between 0 and 1, and that each sample is quantized into q levels where $q = 2^k$. Thus, k is the length of the PCM word. The mean square quantization error is given by

$$\epsilon_q^2 = \int_{-\frac{1}{2q}}^{\frac{1}{2q}} f(x)\, x^2\, dx \tag{2.3.1}$$

where $f(x)$ is the distribution of the samples.

Assuming uniform distribution, i.e. $f(x) = q$ for $-\frac{1}{2q} \le x \le \frac{1}{2q}$, we have

$$\epsilon_q^2 \doteq \int_{-\frac{1}{2q}}^{\frac{1}{2q}} q x^2\, dx$$

$$= q \left. \frac{x^3}{3} \right|_{-\frac{1}{2q}}^{\frac{1}{2q}}$$

$$= \frac{1}{3(2q)^2} \tag{2.3.2}$$

But

$$q = 2^k. \tag{2.3.3}$$

Hence,

$$\epsilon_q^2 = \frac{1}{12 \cdot 2^{2k}} \tag{2.3.4}$$

Note that ϵ_q^2 depends on k which is the number of bits per word. Since data compression is usually applied after the quantizer, this quantity is common for both compressed and uncompressed systems.

(3) Coding and Channel Noise:

For a noiseless channel, the received picture quality is independent of the particular code word. For noisy channels, however, coding has a definite effect on the amount of noise in the picture. It will be shown in Chapter III that for k-bit straight binary code, the mean-square error due to channel noise is

$$\epsilon_c^2 = \frac{P_B}{3} \left(1 - \frac{1}{2^{2k}}\right) \tag{2.3.5}$$

where P_B is the probability of bit error in the channel.

In general, the effect of channel noise is different for different transmission and coding systems. This will be studied in some detail in Chapter III. In the following, we shall present some methods which lead to compression in picture transmission. These include redundancy reduction (run-length encoding, differential pulse-code modulation and psychovisual coding), contour coding and transform coding.

2.4 Redundancy Reduction

As have been pointed out before, high redundancy is found in video data. Long runs of the same brightness levels are present quite often. This suggests the use of run-length encoding and the zero-order prediction.

2.4.1 Zero-Order Predictor (ZOP) and Run-Length Encoding [7] [48]

Zero-order prediction is the simplest case of polynomial prediction. If we let $\hat{x}_t$ represent the predicted value of a sample at time t, it is given by

$$\hat{x}_t = x_{t-1} \tag{2.4.1}$$

where x_{t-1} is the value of the previous sample, the sample occurring at time $t-1$. Practically an aperture (tolerance) is set usually equal to a multiple of the quantum step. If the value of the sample at time t exceeds the ZOP by the tolerance, this sample is considered non-redundant and is sent. The next prediction will be based on this non-redundant sample. If the tolerance limit is not exceeded, that particular sample is considered redundant and hence discarded. Note that the timing information must be supplied in order to reconstruct the waveform at the receiver. A flag is required to distinguish between level information and time information. Figs. 2.4.1 and 2.4.2 illustrate how this can be done.

Before transmission, the level information must be quantized and coded. Hence, it is subjected to both quantization error and transmission error. The transmission error is dependent on the coding scheme used and the quantization error is

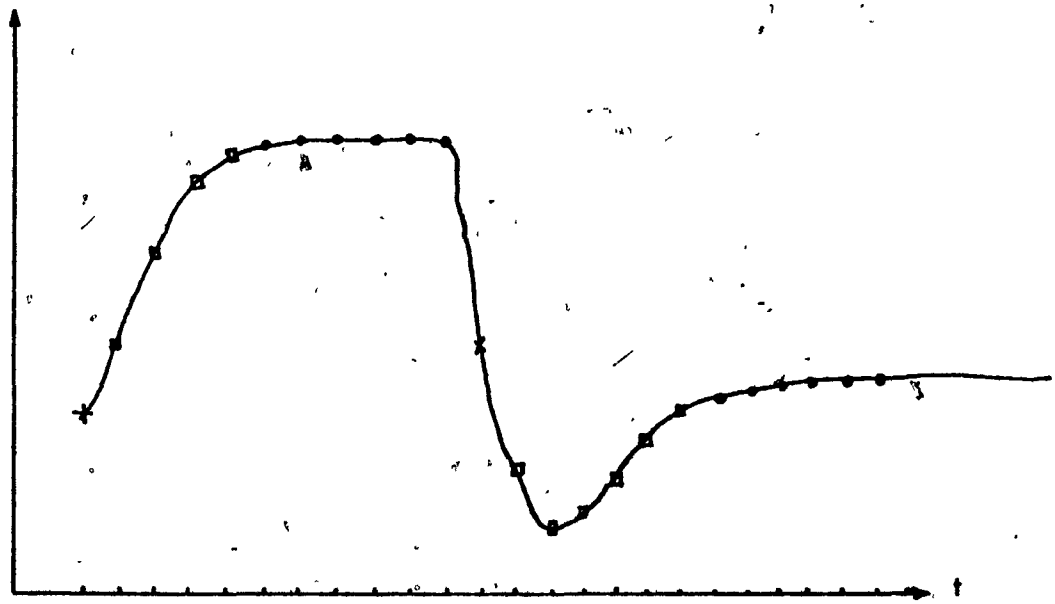

x -- level and timing information sent

□ -- level information sent

• -- nothing sent

FIGURE 2.4.1 ZERO-ORDER PREDICTOR

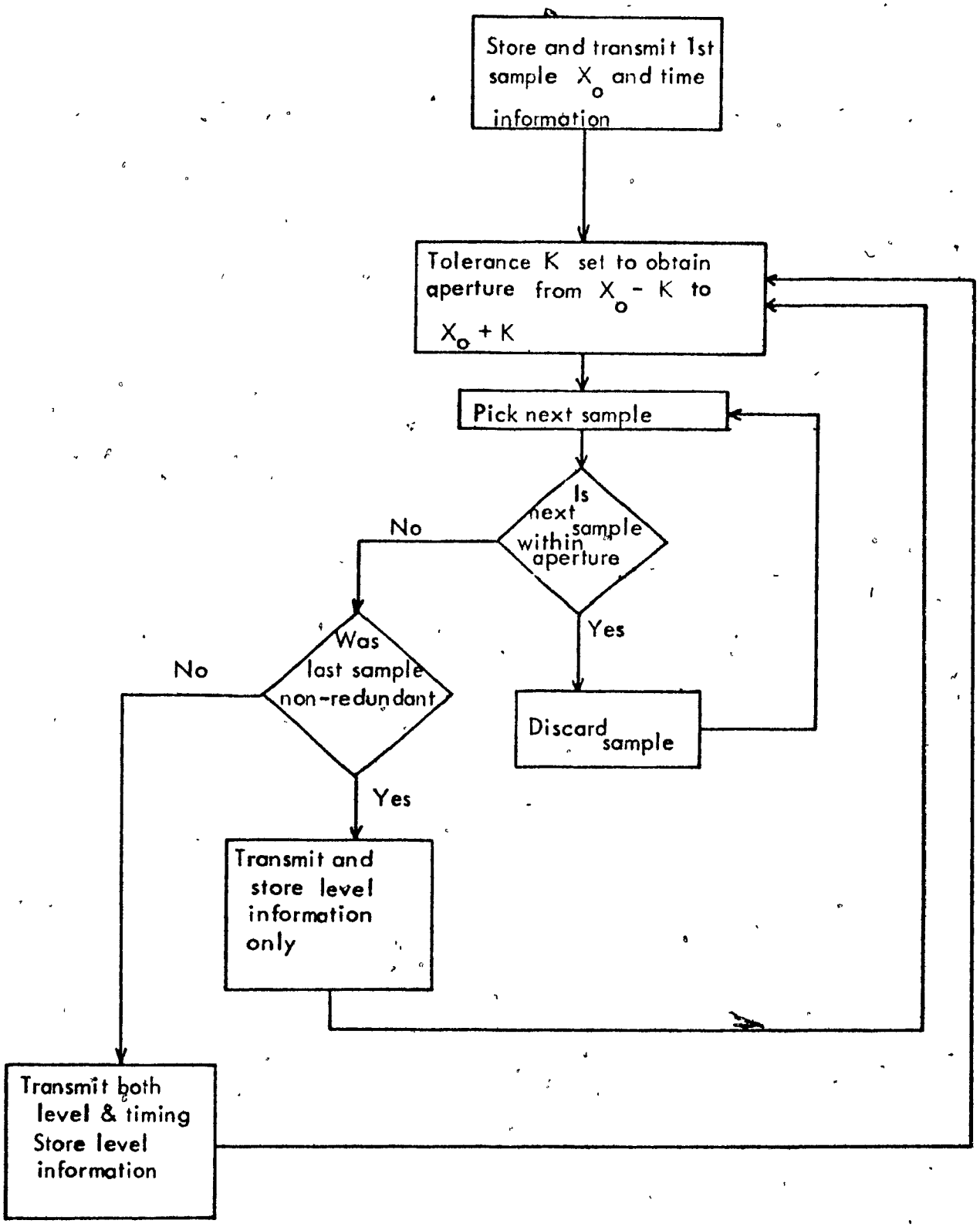

FIGURE 2.4.2 OPERATION OF ZOP

the same as that in PCM system. However, an additional error called "aperture error" results from the aperture used to compare samples in the prediction process.

Let us suppose that K is the aperture magnitude. Hence, S_{i+1} is non-redundant if $|S_{i+1} - S_i| > K$. Let q be the magnitude of a quantum step, and let

$$K = mq \quad , \quad m = 0, 1, 2, \ldots \tag{2.4.2}$$

Note that if $m = 0$, we have no aperture error. We shall assume that the error is uniformly distributed in the whole interval of $-mq$ to $+mq$. Hence,

$$P(K) = \frac{1}{2m+1} \tag{2.4.3}$$

and

$$E[K^2] = \sum_{i=-m}^{m} P(K)K^2 = \frac{1}{2m+1} \sum_{i=-m}^{m} q^2 i^2$$

$$= \frac{2q^2}{2m+1} \sum_{i=1}^{m} i^2 = \frac{2q^2}{2m+1} \frac{m(m+1)(2m+1)}{6}$$

$$= \frac{q^2}{3} m(m+1) \tag{2.4.4}$$

Since $q = \frac{1}{2^k}$, we have

$$E[K^2] = \frac{m(m+1)}{3 \cdot 2^{2k}} \tag{2.4.5}$$

which gives the m.s.e due to aperture error.

A most commonly used coding scheme for ZOP is run-length encoding where the levels of all non-redundant samples together with binary words expressing the run-lengths are transmitted. It is also known as differential co-ordinate encoding. A run is defined as a series of consecutive redundant samples. The statistics of runs will be studied below.

The autocorrelation function of a video process is

$$\phi(\tau) = \lambda e^{-\lambda\tau} \tag{2.4.6}$$

Let ω_i ($i = 1, 2, \ldots$) be a random variable denoting the run-length and $p(\omega_i)$ be the probability density of the run-length. Let us assume that the distance from an arbitrary point t_o to the next random point t_i is a r.v. independent of what happened outside the interval (t_o, t_i), then

$$p(\omega | \omega \geq t_o) = p(\omega - t_o) \tag{2.4.7}$$

which together with (2.4.6) will give

$$p(\omega) = \lambda e^{-\lambda\omega} \tag{2.4.8}$$

The probability distribution can easily be derived.

$$P(\omega) = \int_0^{\omega} \lambda e^{-\lambda x}\, dx = 1 - e^{-\lambda\omega} \tag{2.4.9}$$

For a discrete process, the probability density is derived as

$$p(n) = P(\omega \le n) - P(\omega \le n-1)$$

$$= (1-e^{-\lambda n}) - (1-e^{-\lambda(n-1)})$$

$$= (e^{\lambda}-1)\,e^{-\lambda n} \qquad 1 \le n < \infty \tag{2.4.10}$$

Therefore, the discrete probability distribution for the run length is

$$P(n) = \sum_{i=1}^{n} (e^{\lambda}-1)\,e^{-\lambda i}$$

$$= (e^{\lambda}-1)\,e^{-\lambda}\left[\frac{1-e^{-\lambda n}}{1-e^{-\lambda}}\right]$$

$$= 1 - e^{-\lambda n} \tag{2.4.11}$$

The expected value of the run-length is given by

$$E[n] = \sum_{n=1}^{\infty} n\,p(n) = \sum_{n=1}^{\infty} n\,(e^{\lambda}-1)\,e^{-\lambda n}$$

$$= (e^{\lambda}-1)\left[\frac{e^{-\lambda}}{(1-e^{-\lambda})^2}\right]$$

Hence, the expected value of run-length is

$$E[n] = \frac{1}{1-e^{-\lambda}} \tag{2.4.12}$$

The compression ratio offered by run-length encoding is given by the average length of the run, E [n]. A relationship between the compression ratio C_S and the probability p that a sample will have a different brightness level from the previous one can be derived.

$$\text{Probability of a run of length } n = p(n) = p(1-p)^{n-1} \tag{2.4.13}$$

$$\begin{aligned} \text{Average length of run} &= \sum_n n\, p(n) \\ &= \sum_n n\, p(1-p)^{n-1} \\ &= \frac{1}{p} \end{aligned} \tag{2.4.14}$$

Hence,

$$C_S = \frac{1}{p} = E[n] \tag{2.4.15}$$

or,

$$p = \frac{1}{C_S} \tag{2.4.16}$$

This value of p is approximate and implies that it does not depend on the size of the initial jump. Also p (n) can be written as

$$\frac{1}{E[n]}\left(1 - \frac{1}{E[n]}\right)^{n-1} = \left[\frac{E[n]-1}{E[n]}\right]^{n} \frac{1}{E[n]-1} \tag{2.4.17}$$

which agrees with the result derived by Cherry [49].

Also,

$$p(1) = p = \frac{1}{E[n]} \tag{2.4.18}$$

Hence,

$$p(n) = \frac{p(1)}{1-p(1)} \; (1 - p(1))^n \tag{2.4.19}$$

where $p(1)$ is the probability of a run consisting of a single element. This result is in agreement with that derived by Estournet [24]. From (2.4.12)

$$E[n] = C_S = \frac{1}{1-e^{-\lambda}} \tag{2.4.20}$$

By expanding $e^{-\lambda}$ as a series and taking first-order approximations, we can approximate C_S as

$$C_S \simeq \frac{1}{\lambda} \tag{2.4.21}$$

or,

$$\lambda = \frac{1}{C_S} \tag{2.4.22}$$

In general, the analysis of run-length encoding does not take into account all the dependence which exists among the various pels in the picture, thus the results concerning information ratio and savings in channel capacity are only first-order approximations.

It has also been shown that, for Markov processes, run-length encoding systems achieve the lower bound in entropy as the number of bits to code

a picture by non-statistical methods approaches infinity [40].

2.4.2 Psychovisual Coding

The intention of these coding techniques is to alter the signal in such a way that within acceptable degradation of the picture, some advantage in transmission is gained through the exploitation of the properties of the human vision. Statistical encoders can be inserted at the output of the psychovisual coders to further reduce statistical redundancy. Schreiber [39] has referred to such a combination as psychostatistical coding. The main results of psychovisual coding are summarised below.

(1) Many experiments have been performed to improve picture quality by high frequency accentuation [51] and snow removal [41]. It is found that most people prefer the band above 350 k Hz to be emphasized in commercial television.

(2) Spatial and contrast resolutions are exchanged in vision so that a smaller number of brightness levels can be distinguished in small objects than in large or uniform areas. Hence, in run-length encoding, the levels of short runs could be quantized more coarsely than those of long runs, yielding bit reduction.

(3) The resolution of spatial details in moving objects also deteriorates. Therefore, the number of samples per frame can be reduced.

(4) If some of the wasted channel capacity is used for the colour information of the scene, substantial improvement in quality is possible.

(5) Seyler and Budrikis [26] showed that the human observer would not perceive a temporary reduction of spatial detail for an average of 750 milliseconds after a scene change. This part of wasted channel capacity can then be applied to some aspects of the original scene, resulting in an overall improvement of quality. Alternatively, a large reduction in bandwidth can be achieved by disregarding the spatial details during the scene changes. This enables TV transmission at around 30 frames per second.

This result also justifies the use of frame-difference coding [52], where a new frame is transmitted if a sufficient number of different picture elements exists between consecutive frames. Other frame-to-frame coding methods also exist where only the difference between frames are transmitted, by taking advantage of the frame-to-frame correlation.

2.4.3 Differential PCM

Redundancy reduction is also achieved by a technique known as differential pulse-code-modulation (DPCM) [53], [54], which offers bit rate reduction over straight PCM as shown in Fig. 2.4.3. It aims at removing the inherent signal redundancy through a feedback prediction around the quantizer. It will be shown later that this feedback feature is essential for improvement over

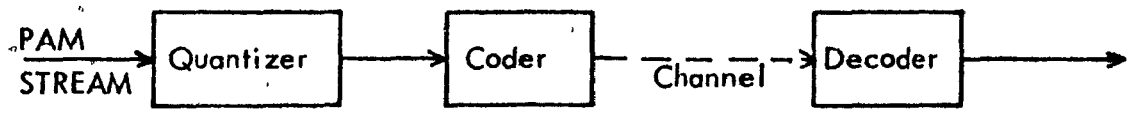

FIGURE 2.4.3 BASIC PCM SYSTEM

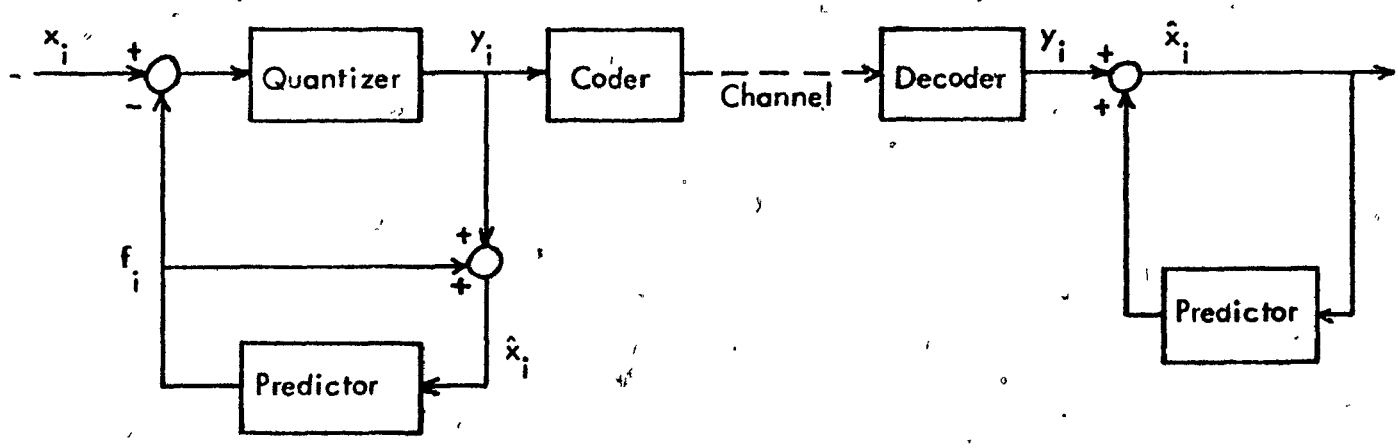

FIGURE 2.4.4 BASIC DPCM SYSTEM

straight PCM. If the quantizer is placed outside the feedback loop, no improvement is possible. It should be noted as well that the quantizer must be an instantaneous device. The following is an analysis of the operation of the system, based on various papers on the same topic [55] - [63].

In DPCM shown in Fig. 2.4.9, the difference between the actual signal and an estimate of the signal, based on its past, is transmitted. The receiver adds the estimate to the received difference yielding the true signal. It is hence obvious that highly redundant signals such as TV, are well suited for DPCM systems due to the possibility of accurate prediction. We shall first review the prediction process and we shall restrict ourselves to linear prediction.

(1) Optimum Linear Prediction [61] , [64]

Assume that $S(t)$ be a stationary random signal with zero mean and variance σ^2, sampled at times $t_1, t_2, \ldots, t_n, \ldots$ yielding samples of $S_1, S_2, \ldots, S_n, \ldots$, respectively. A linear estimate of the next sample S_o can be made from the knowledge of the n previous samples.

$$\hat{S}_o = a_1 S_1 + a_2 S_2 + \ldots + a_n S_n \tag{2.4.23}$$

where $\hat{S}_o$ is the linear estimate of S_o and a_i's and S_i's are real

The error generated is given by

$$e_o = S_o - \hat{S}_o \tag{2.4.24}$$

We wish to find the set of ai's such that $\hat{S}_o$ is the best estimate of S_o in the mean square sense, i.e. $E[(S_o - \hat{S}_o)^2]$ is to be a minimum. Now

$$E[(S_o - \hat{S}_o)^2] = E[(S - (a_1 S_1 + a_2 S_2 + \ldots + a_i S_i + \ldots + a_n S_n))^2] \quad (2.4.25)$$

Partial differentiating the above with respect to the a_i's and setting the result to zero for minimum gives

$$E[(S_o - (a_1 S_1 + \ldots + a_n S_n)) S_i] = 0, \quad i = 1, 2, \ldots n \quad (2.4.26)$$

or

$$E[(S_o - \hat{S}_o) S_i] = 0, \quad i = 1, 2, \ldots, n \quad (2.4.27)$$

Hence,

$$E[S_o S_i] = E[\hat{S}_o S_i], \quad i = 1, 2, \ldots n \quad (2.4.28)$$

If we write R_{ij} as the covariance of S_i and S_j, then (2.4.28) becomes

$$R_{oi} = a_1 R_{1i} + a_2 R_{2i} + \ldots + a_n R_{ni} \quad i = 1, 2, \ldots n \quad (2.4.29)$$

yielding a set of n simultaneous linear equations in the n unknowns a_i's, provided of course that the covariances R_{ij}'s are known. With the best linear estimate of S_o, the error resulted is

$$\sigma_e^2 = E[(S_o - \hat{S}_o)^2] = E[(S_o - \hat{S}_o) S_o]$$

$$= R_{oo} - (a_1 R_{o1} + a_2 R_{o2} + \ldots + a_n R_{on}) \quad (2.4.30)$$

where R_{oo} is the variance σ^2 of the original sequence. From (2.4.30), it is obvious that the error sequence is less correlated and has a smaller variance than the sequence $\{S_i\}$.

For an nth order Markov process, only n samples are required for the best prediction. Television signals are very close to first-order Markov process and have an autocorrelation of $e^{-\lambda\tau}$. Hence, the best estimate is from the previous sample given by

$$\hat{S}_o = \frac{R_{o1}}{\sigma^2} S_1 \tag{2.4.31}$$

However, if access to samples on adjacent lines and frames are possible, it has been shown that the prediction can be improved.

(2) Operation of the DPCM System

Let us refer back to Fig. 2.4.4 which shows a block diagram representation of the DPCM system, where x_i is a random signal of zero mean. The primed quantities differ from the unprimed ones only from channel noise.

From the diagram we have the following relations

$$e_i = z_i - y_i \tag{2.4.32}$$

which is the quantization error,

$$z_i = x_i - f_i \tag{2.4.33}$$

$$\hat{x}_i = f_i + y_i \tag{2.4.34}$$

$$f_i = \sum_{j=1}^{\infty} h_j \hat{x}_{i-j} \tag{2.4.35}$$

The h_j's are characteristic of the predictor. Note that the predictor introduces delay around the loop. From (2.4.32) - (2.4.34), we get

$$e_i = (x_i - f_i) - (\hat{x}_i - f_i) = x_i - \hat{x}_i \tag{2.4.36}$$

A very important conclusion results, the quantization error samples are identical to the error samples for the overall system, assuming error-free channel transmission.

The input to the quantizer is z_i

$$\begin{aligned} z_i &= x_i - f_i \\ &= x_i - \sum_{j=1}^{\infty} h_j \hat{x}_{i-j} \\ &= x_i - \sum_{j=1}^{\infty} h_j (x_{i-j} - e_{i-j}) \end{aligned}$$

or

$$z_i = x_i - \sum_{j=1}^{\infty} h_j x_{i-j} + \sum_{j=1}^{\infty} h_j e_{i-j} \tag{2.4.37}$$

The output from the quantizer, which is the sequence sent over the digital channel is

$$y_i = z_i - e_i$$

$$= x_i - e_i - \sum_{j=1}^{\infty} h_j x_{i-j} + \sum_{j=1}^{\infty} h_j e_{i-j} \tag{2.4.38}$$

Now, let us construct a simple table giving the data streams. This will enable us to see more clearly the operation of the DPCM. Assume that we shall use a simple, non-optimal system where,

$$h_1 = 1$$

$$h_j = 0, \quad j \neq 1 \tag{2.4.39}$$

x_i	x_1	x_2	x_3	x_4	x_i
z_i	x_1	$x_2-(x_1-e_1)$	$x_3-(x_2-e_2)$	$x_4-(x_3-e_3)$	$x_i-(x_{i-1}-e_{i-1})$
$\hat{x}_i$	x_1-e_1	x_2-e_2	x_3-e_3	x_4-e_4	x_i-e_{i-1}
y_i	x_1-e_1	(x_2-e_2) $-(x_1-e_1)$	(x_3-e_3) $-(x_2-e_2)$	(x_4-e_4) $-(x_3-e_3)$	(x_i-e_i) $-(x_{i-1}-e_{i-1})$

(2) Quantization Noise and Signal-to-Noise Ratio Improvement Over PCM

It has been shown [65] for PCM that the variance of the quantization error of an L step quantizer of step sizes Δ_i is given by

$$E[e_i^2]|_{PCM} = \sum_{i=1}^{L} p_{xi} \frac{\Delta_i^2}{12} \tag{2.4.40}$$

where p_{xi} is the probability of the ith step. A similar expression for DPCM is

$$E[e_i^2]|_{DPCM} = \sum_{i=1}^{L} p_{zi} \frac{\Delta'^2_i}{12} \tag{2.4.41}$$

We shall assume for comparison purposes that $p_{xi} = p_{zi}$ and the step sizes Δ_i and Δ'_i are chosen at a ratio equal to the ratio of the r.m.s values of the two inputs.

$$\frac{E[e_i^2]|_{PCM}}{E[e_i^2]|_{DPCM}} = \frac{E[x_i^2]}{E[z_i^2]} \tag{2.4.42}$$

This ratio is defined as the SNR IMPROVEMENT RATIO.

It can be seen from (2.4.37) that the statistical properties of z_i depend on the joint statistics of the input and past samples of the input, which is still unknown up to date. However, we shall assume that the spectrum of x_i and that of z_i are very similar for simplified analysis (this holds very well for both voice and TV signals). We further assume that the error samples are uncorrelated. Then,

$$E[z_i^2] = E[(x_i - \sum_{j=1}^{\infty} h_j x_{i-j})^2] + E[e_i^2] \sum_{j=1}^{\infty} h_j^2 \tag{2.4.43}$$

At this point, it is worth pointing out that the optimal linear predictor derived earlier is optimal only for a set of statistics and does not necessarily perform well for other signals. Hence, we shall first consider a simple case.

(A) Simple Delayed Feedback (single integrator feedback)

In this simple case,

$$h_1 = 1,$$

$$h_i = 0, \qquad i \neq 0 \tag{2.4.44}$$

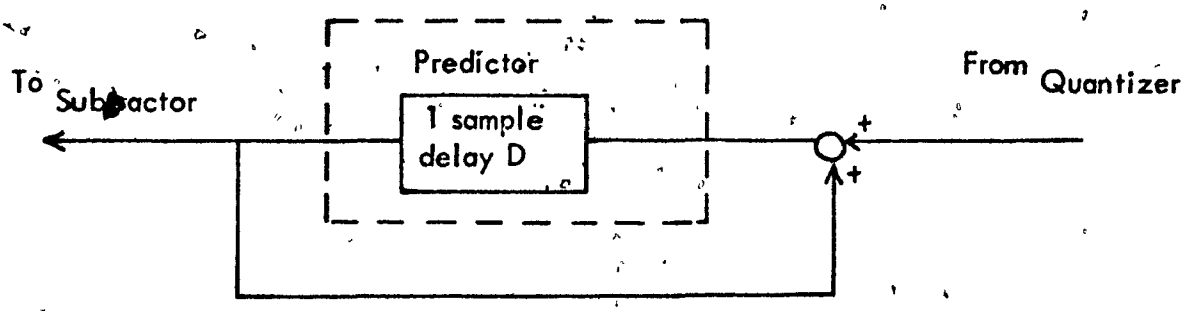

FIGURE 2.4.5 PREVIOUS SAMPLE PREDICTOR

Then,

$$z_i = x_i - x_{i-1} + e_{i-1}$$

and

$$E[z_i^2] = E[x_i^2][2(1-\rho_1)] + E[e_{i-1}^2] \tag{2.4.45}$$

where

$$\rho_1 = \frac{E[x_i \, x_{i-1}]}{E[x_i^2]} \tag{2.4.46}$$

Neglecting the last term in (2.4.45), we get

$$\frac{E[x_i^2]}{E[z_i^2]} \simeq \frac{1}{2(1-\rho_1)} \tag{2.4.47}$$

Hence, the SNR improvement is greater than unity if the normalized adjacent sample correlation of the input signal is greater than 0.5.

The above system, though non-optimal, is simple to implement. The predictor parameters are independent of signal statistics. Note that if $\rho_1 < 0.5$, the system performance is worse than PCM.

(B) Optimal Linear Feedback

The result of the previous discussion on optimal linear prediction is not directly applicable here because the input to the predictor is $x_i - e_i$ instead of x_i. Note that the SNR improvement is defined by the ratio of the variance of x_i to that of z_i, hence we could optimize this figure of merit by minimizing the variance of z_i, Now,

$$E[z_i^2] = E[(x_i - \sum_{j=1}^{\infty} h_j x_{i-j})^2] + E[e_i^2] \sum_{j=1}^{\infty} h_j^2$$

from (2.4.43). For a minimum,

$$\frac{\partial E[z_i^2]}{\partial h_i} = -2E[(x_i - \sum_{l=1}^{\infty} h_l x_{i-l}) x_{i-i}] + 2h_i E[e_i^2] \tag{2.4.48}$$

$$= 0$$

or

$$E[x_i x_{i-i}] = h_i E[e_i^2] + E[(\sum_{l=1}^{\infty} h_l x_{i-l}) x_{i-i}] \tag{2.4.49}$$

Defining

$$\rho_i = \frac{E[x_i x_{i-i}]}{E[x_i^2]} \tag{2.4.50}$$

and

$$R = SNR = \frac{E[x_i^2]}{E[e_i^2]} \tag{2.4.51}$$

We can rewrite (2.4.49) as a set of linear algebraic equations:

$$\begin{aligned} \rho_1 &= (1+\tfrac{1}{R})h_1 + h_2\rho_1 + h_3\rho_2 + \ldots + h_n\rho_{n-1} \\ \rho_2 &= h_1\rho_1 + (1+\tfrac{1}{R})\rho_2 + h_3\rho_1 + \ldots + h_n\rho_{n-2} \\ &\vdots \\ \rho_n &= h_1\rho_{n-1} + h_2\rho_{n-2} + h_3\rho_{n-3} + \ldots + (1+\tfrac{1}{R})h_n \end{aligned} \tag{2.4.52}$$

This set of equations has the same form as (2.4.29) except for the coefficients in the diagonal terms. Divide through by $1 + \frac{1}{R}$ to normalise the set of equations. Hence the error in the prediction, by analogy with (2.4.30), is given by

$$E[z_i^2]_{min} = E[x_i^2][1 - \sum_{i=1}^{n} h_i(\rho_i/(1+\tfrac{1}{R}))] \tag{2.4.53}$$

Therefore,

$$\text{SNR Improvement}\Big|_{\text{optimal}} = \frac{1}{1 - \sum_{i=1}^{n} h_i \left(\rho_i / \left(1+\frac{1}{R}\right)\right)} . \tag{2.4.54}$$

It can be seen that the SNR improvement $\Big|_{\text{opt.}}$ increases for larger n since each past sample can only add information to a better prediction. However, both speech and video processes are not totally predictable from past samples and a limit will reach when the figure of merit remains constant. The following is an example which illustrates this situation for voice [56].

Autocorrelation coefficients - ρ_n

n	8.0 k Hz samples
0	1.0000
1	0.8644
2	0.5570
3	0.2274
4	-0.0297
5	-0.1939
6	-0.2788
7	-0.3030
8	-0.2823
9	-0.2208
10	-0.1330

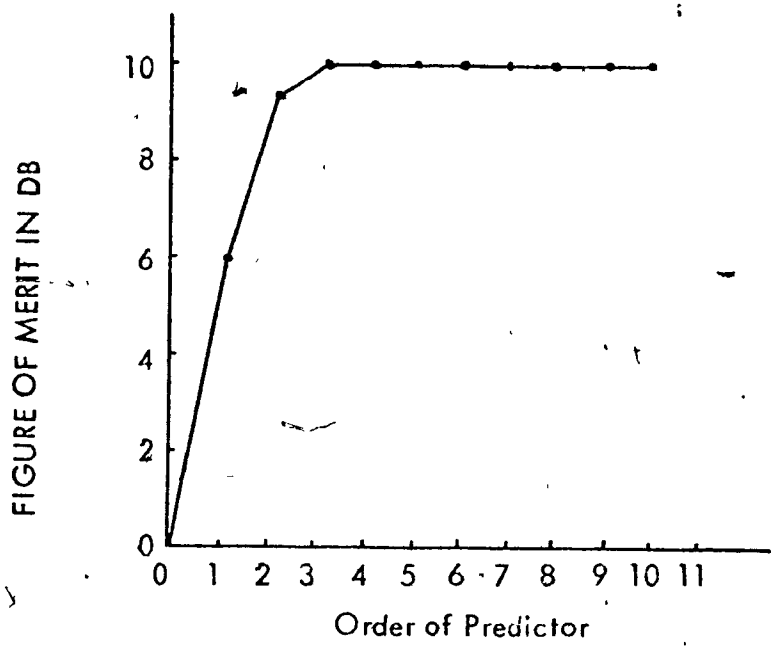

FIGURE 2.4.6 FIGURE OF MERIT VS PREDICTOR COMPLEXITY FOR 8 KHz SAMPLING [56]

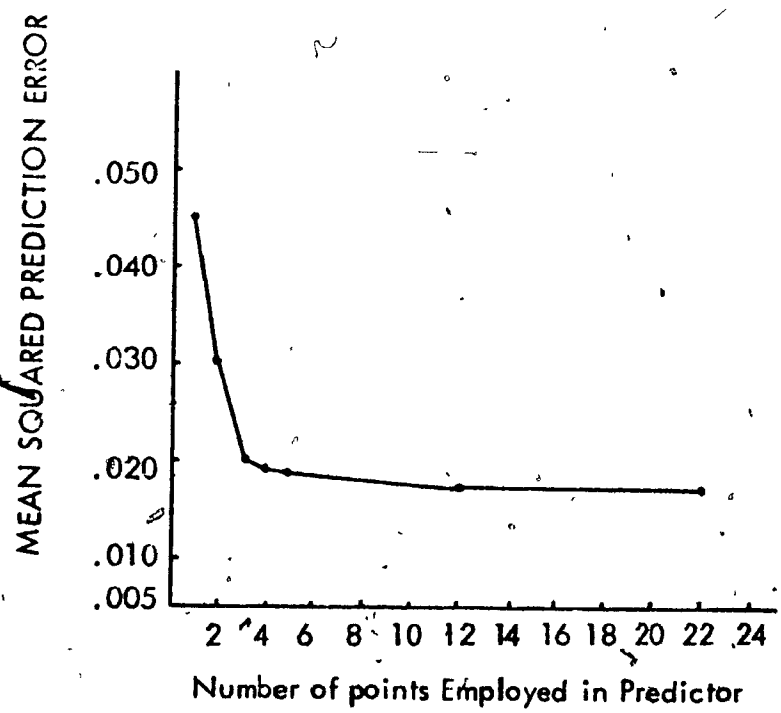

FIGURE 2.4.7 MEAN SQUARED ERROR VS ORDER OF PREDICTOR [66]

Assuming that $R \to \infty$ for high signal-to-noise ratio, the set of h_i's can be found. Using (2.4.54), the SNR inprovement is plotted as a function of n. This is shown in Fig. 2.4.6. Habibi [66] has also shown the similar results for a particular picture, where he used points from previous lines as well, Fig. 2.4.7.

Let us consider the simple case when only 1 delay element is used, i.e. $n = 1$. Then,

$$h_1 = \frac{\rho_1}{1+\frac{1}{R}} \tag{2.4.55}$$

and

$$\text{SNR improvement}\Big|_{N=1} = \frac{1}{1 - [\rho_1 / 1+\frac{1}{R}]^2} \tag{2.4.56}$$

Assuming that $R \to \infty$,

$$\text{SNR improvement}\Big|_{N=1} = \frac{1}{1-\rho_1^2} \tag{2.4.57}$$

From (2.4.57), we may conclude that the optimal system always holds an advantage over PCM whereas the non-optimal cases has advantage over PCM only when $\rho_1 > 0.5$. However, the characteristics of the predictor for the optimal case is dependent on the signal statistics (h_i's are dependent on ρ_i's).

(4) Analysis of System with Quantizer Outside the Feedback Loop

A block diagram representation of the system with the quantizer outside the feedback loop is shown in Fig. 2.4.8.

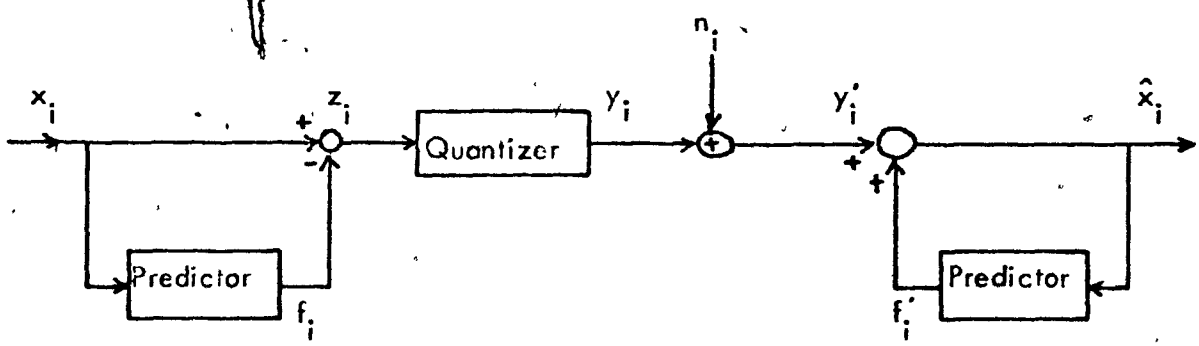

FIGURE 2.4.8 : QUANTIZER OUTSIDE FEEDBACK LOOP

We shall neglect channel noise for the analysis, i.e. $n_i = 0$. The following algebraic relations result

$$z_i = x_i - f_i \tag{2.4.58}$$

$$f_i = \sum_{j=1}^{\infty} h_j \, x_{i-j} \tag{2.4.59}$$

$$y_i = z_i - e_i \tag{2.4.60}$$

$$\hat{x}_i = y_i + f_i' \tag{2.4.61}$$

$$f_i' = \sum_{j=1}^{\infty} h_j \, \hat{x}_{i-j} \tag{2.4.62}$$

Let $h_1 = 1$ and $h_j = 0$ for $j \neq 1$. Then,

$$\hat{x} = x_i - e_i - (x_{i-1} - \hat{x}_{i-1}) \tag{2.4.63}$$

or,

$$\hat{x}_i - \hat{x}_{i-1} = x_i - x_{i-1} - e_i \tag{2.4.64}$$

Hence,

$$E[(\hat{x}_i - \hat{x}_{i-1})^2] = E[(x_i - x_{i-1})^2] + E[e_i^2] \tag{2.4.65}$$

where we have assumed the error samples are uncorrelated.

$$E[\hat{x}_i^2]\, 2(1-\rho_1') = E[x_i^2]\, 2(1-\rho_1) + E[e_i^2] \tag{2.4.66}$$

where,

$$\rho_1 = \frac{E[x_i x_{i-1}]}{E[x_i^2]}, \quad \rho_1'' = \frac{E[\hat{x}_i \hat{x}_{i-1}]}{E[\hat{x}_i^2]} \tag{2.4.67}$$

Further assume that $\rho_1 \simeq \rho_1'$, then

$$E[\hat{x}_i^2] = E[x_i^2] + \frac{E[e_i^2]}{2(1-\rho_1')} \tag{2.4.68}$$

which essentially says that the error signal power is amplified at the decoder by a factor of $\dfrac{1}{2(1-\rho_1')}$

Now, at the transmitter end, we have

$$z_i = x_i - x_{i-1} \tag{2.4.69}$$

and

$$\begin{aligned} E[z_i^2] &= E[(x_i - x_{i-1})^2] \\ &= E[x_i^2]\, 2(1-\rho_1) \end{aligned} \tag{2.4.70}$$

or

$$\frac{E[z_i^2]}{E[x_i^2]} = 2(1-\rho_1) \tag{2.4.71}$$

This factor will exactly cancel the factor introduced at the decoder. Hence, the overall performance is the same as that of PCM. We conclude, therefore, that the quantizer must be placed within the feedback loop in order to attain superior performance over PCM. However, the operation of the subtractor and the feedback at the transmitter may be separated at a very slight increase in complexity. This will be shown below.

(5) Equivalent Systems [67] - [69]

Such a system is shown in Fig. 2.4.9, for the simplest case when $h_1 = 1$ and $h_i = 0$ for $i \neq 1$.

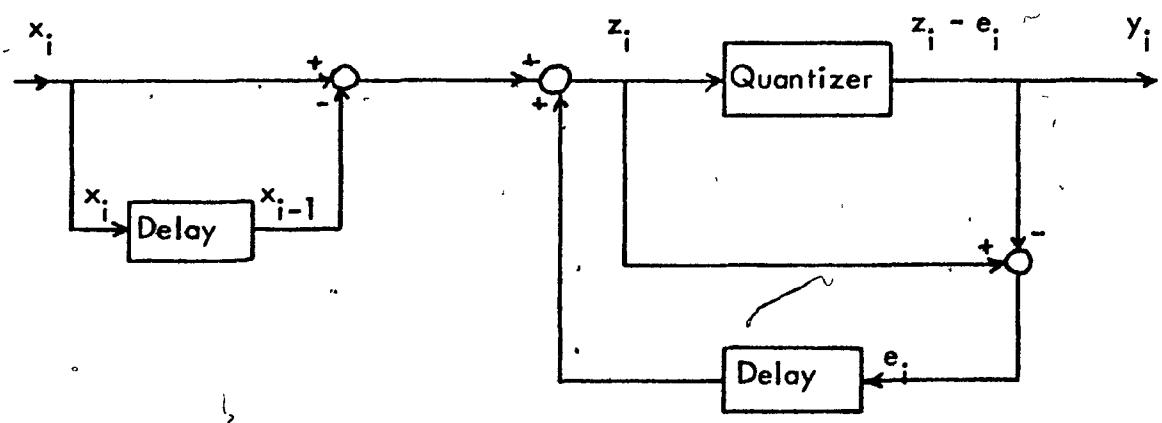

FIGURE 2.4.9 EQUIVALENT SYSTEM

The corresponding relations are

$$z_i = x_i - x_{i-1} + e_{i-1} = x_i - (x_{i-1} - e_{i-1}) \tag{2.4.72}$$

$$y_i = z_i - e_i = (x_i - e_i) - (x_{i-1} - e_{i-1}) \tag{2.4.73}$$

which essentially is the same data stream sent over the digital channel as that in the DPCM case. The present system however, allows the subtraction operation and the feedback quantization be separated.

It has been shown that there is an equivalence between a noise feedback system with pre-distortion and post-distortion filters and a DPCM system with a similar pair of filters.

(6) Design of the Quantizer

In order to design the optimal system a criterion must be set. We shall use the minimum mean-squared-error for such a purpose. It will be noticed that the analysis of the DPCM system is complicated by the non-linear characteristic of the quantizer. To get around this difficulty, we shall seek the optimal solution in the following manner. First, a best predictor is designed ignoring the quantizer, then an optimal quantizer which matches with the statistics of the difference signal is built. This procedure will give a suboptimal system instead of an optimal one.

The best linear predictor has been discussed before and we shall limit ourselves here to the quantizer design for video input. The probability density of the difference signal z_i is a two-sided exponential. Smith [70] showed that the least m.s.e. quantizer is a uniform quantizer with pre- and post- quantization transforms $y(z)$ and $z^*(y^*)$ defined as

$$y(z) = \frac{E_o\,[1-\exp(-mz/E_o)]}{1-\exp(-m)}, \quad y(-z) = -y(z) \tag{2.4.74}$$

and

$$z^*(y^*) = \frac{E_o}{m} \ln\left[1 - \frac{y^*}{E_o}(1-\exp(-m))\right], \quad z^*(-y^*) = z^*(y^*) \tag{2.4.75}$$

where

$$E_o = \text{maximum value of } z$$

$$m = \frac{\sqrt{2 E_o}}{3 \sigma_z}$$

$$y^* = \text{the quantized value of } y$$

and

$$\sigma_z = \text{variance of the difference signal.}$$

Now, the operation of the DPCM has been explained in detail. We shall study some of its applications to TV signal processing. It is found that the amplitude density function of the quantizer input in a well-designed DPCM is approximately Laplacian. The quantization noise has a flat spectrum, highly correlated with the deriviative of the signal.

A DPCM can be modified to include the previous sample plus the adjacent sample on the previous line. This is shown in Fig. 2.4.10 and Fig. 2.4.11. Hence,

$$\hat{S}_o = a_1 S_1 + a_2 S_6 \qquad (2.4.76)$$

Such a system is known as a previous line-and-sample feedback system. Additional improvement of 4.9 db at best in S/N ratio is reported by this additional feature. By analogy, the concept can be extended to include frame feedback where frame-to-frame correlation is made use of. In this case,

s_9 s_8 s_7 s_6 s_5 s_4

s_3 s_2 s_1 s_0

FIGURE 2.4.10 : SAMPLES ON THE TWO LINES

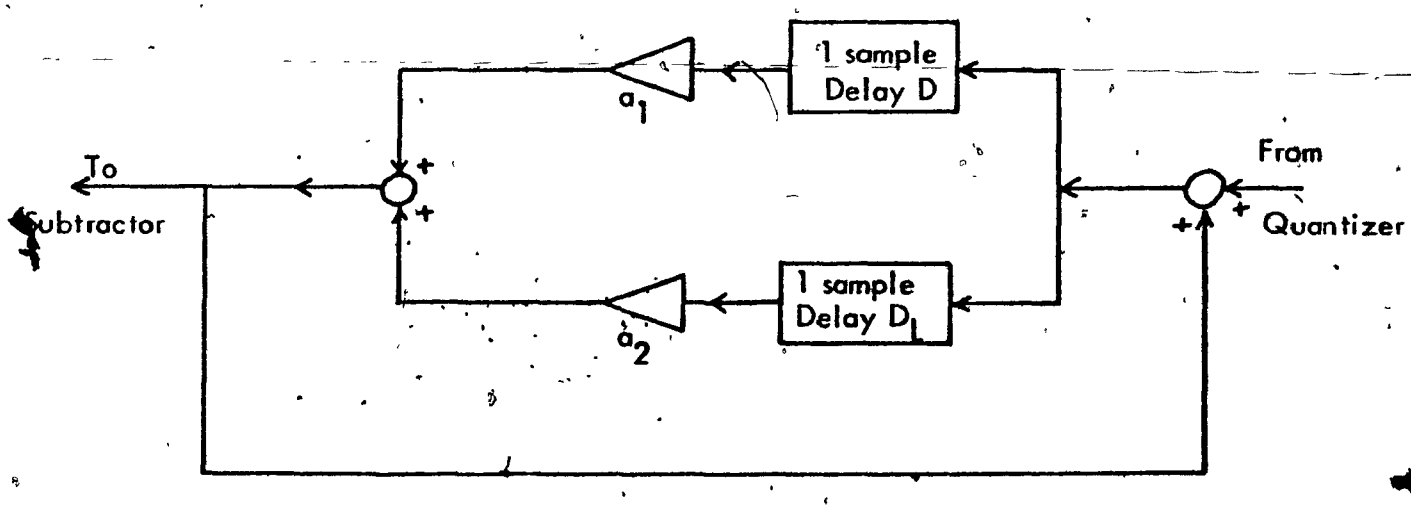

FIGURE 2.4.11 : PREVIOUS LINE-AND SAMPLE PREDICTOR

$$\hat{S}_o = a_1 S_1 + a_2 S_6 + a_3 S_f \tag{2.4.77}$$

where S_f is the sample value which is in the same location as S_o in the previous frame. Such a system is called a frame-line-and sample feedback system. However, the investigation of this system would be quite difficult due to the lack of information on frame-to-frame correlations. Fig. 2.4.12 shows a comparison of previous sample feedback DPCM with standard PCM and the delta modulation (DM) [60] for a particular picture with a fixed bit rate [61]. It can be seen that a well-defined DPCM holds a 12 db advantage over PCM for the same bit rate.

A lot of effort has also been spent on investigating frame-to-frame coding, intraframe coding and picture replenishment. Details of these techniques can be found in references given in [71].

Other modifications of the method include adaptive dual-mode coder-decoder [72], where a combination of delta-modulation and DPCM is used for TV signals. The switching between the two modes depends on the slope of the signal. It was found that further bit-rate reduction by a factor of two from DPCM is possible by making use of the statistical properties of video signals and by choosing a slightly different tradeoff between granular and slope overload noise.

2.5 Contour Coding

In the case of graphical images, the important information is the contour which are usually points of sharp brightness changes. From the statistical

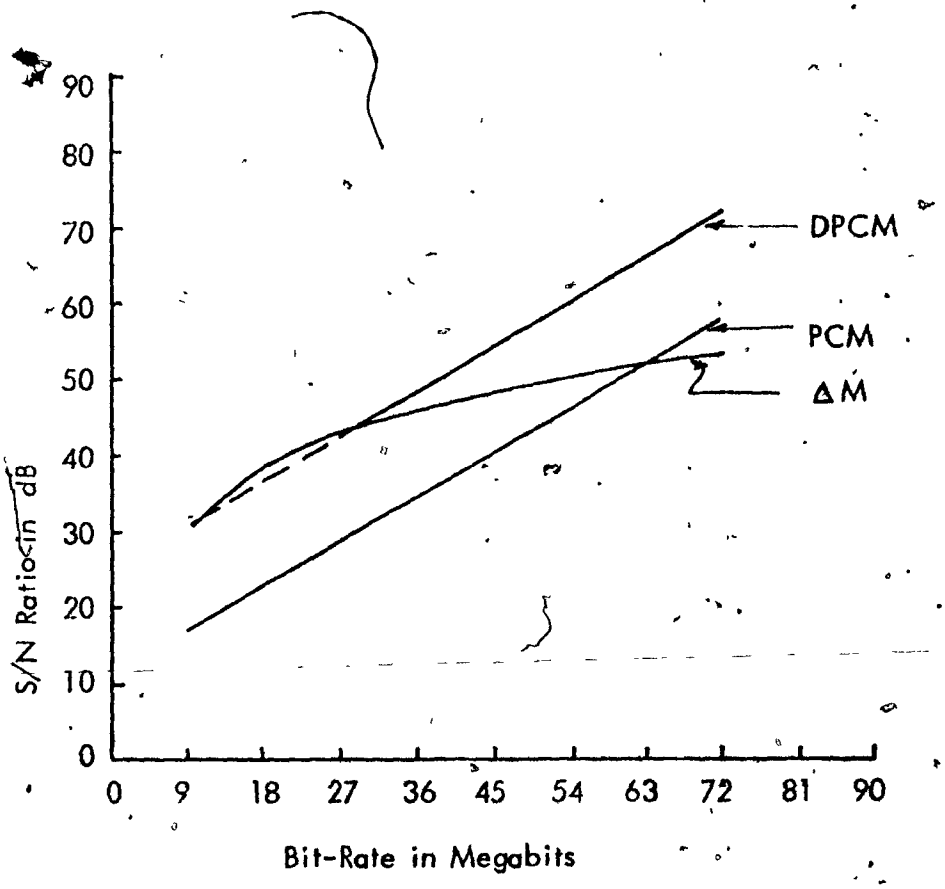

FIGURE 2.4.12 COMPARISON OF PREVIOUS-SAMPLE FEEDBACK DPCM [61] WITH STANDARD PCM AND ΔM FOR MONOCHROME 4.5 - Mc/s. TV. (SAMPLING RATE IS 9 Mc/s.) SINCE DPCM AND PCM ARE ASSUMED TO HAVE SAMPLING RATES TWICE THE BANDWIDTH OR 9 Mc/s., THESE CURVES ARE ONLY DEFINED AT MULTIPLES OF 9 MEGABITS.

point of view, these are the significant samples. By transmitting only the outline information, graphical images can be reconstructed exactly. The information which needs to be transmitted about the outline or contours in an image consists simply of the location of the contours. When continuous-tone images are considered, the location of the contours plus the gradient information of the area are both significant. Some of the contour coding techniques are described in [73] [74]. Their schemes make use of the fact that human observers are sensitive to abrupt changes in brightness over the edges. In areas of uniform brightness, the quantization noise is easily seen. This will create false contours. This subject is pursued in detail in Chapter IV.

The coding techniques described so far has but one property in common. They are more sensitive to channel errors. We shall analyse this effect in Chapter III. The transform method of coding picture has an advantage over most of the other data compression systems in that it is more immune to channel errors. The following presents a brief description of this technique.

2.6 Transform Image Coding [75]

Recent advancements in optical-processing techniques and computer software made possible the coding of pictures in the frequency domain. Transform coding is a method which accomplishes to some extent both statistical and psychovisual coding. A unitary transform operates on the set of statistically dependent picture elements resulting in a set of "more independent" coefficients. The unitary

transform operator has the orthogonal property. The coefficients are then quantized and coded before transmission. The number of bits assigned to each coefficient depends on the variance of that coefficient and the number of quantization levels which in turn is determined by the psychovisual property of the human eye. At the receiver, an inverse transform operation is done on the received data to derive the best replica of the original image.

We shall assume that an image array is represented by a square array of N x N intensity samples described by the function f (x,y) where (x,y) are spatial co-ordinates. The two dimensional forward transform of the image array F (u, v), (u, v) being spatial frequencies, is itself an N x N square array:

$$F(u,v) = \sum_{x=0}^{N-1} \sum_{y=0}^{N-1} f(x,y)\ a(x,y,u,v) \qquad (2.6.1)$$

where a (x, y, u, v) is the forward transformation kernel. The kernel is said to be separable symmetric if

$$a(x,y,u,v) = a_1(x,u)\, a_1(y,v) \qquad (2.6.2)$$

For most images, the statistical intensity variations are nearly equal in the vertical and horizontal directions. We will hence consider only separable symmetric kernels. Such cases are particularly easy to implement because the image can be first processed along each row, and then along each column. A reverse operation is done at the receiver to reconstruct the original image,

$$f(x,y) = \sum_{u=0}^{N-1} \sum_{v=0}^{N-1} F(u,v)\, b(x,y,u,v) \tag{2.6.3}$$

It can be shown that an equivalence in energy in the two domains exists [75]. We shall outline the proof below. Now,

$$F(u,v)F^*(u,v) = \left[\sum_{x=0}^{N-1} \sum_{y=0}^{N-1} f(x,y)\, a(x,y,u,v) \right] \times \sum_{\alpha=0}^{N-1} \sum_{\beta=0}^{N-1} f(\alpha,\beta)\, a^*(\alpha,\beta,u,v) \tag{2.6.4}$$

which on expansion, yields

$$F(u,v)F^*(u,v) = \sum_{x=0}^{N-1} \sum_{y=0}^{N-1} [f(x,y)]^2\, a(x,y,u,v)\, a^*(x,y,u,v)$$

$$+ \sum_{\substack{x=0 \\ x \neq \alpha}}^{N-1} \sum_{\substack{y=0 \\ y \neq \beta}}^{N-1} \sum_{\alpha=0}^{N-1} \sum_{\beta=0}^{N-1} f(x,y) f(\alpha,\beta)\, a(x,y,u,v)\, a^*(\alpha,\beta,u,v) \tag{2.6.5}$$

As a result of the orthonormal property of the transformation kernels, we get, by summing both sides over u, v,

$$\sum_{u=0}^{N-1} \sum_{v=0}^{N-1} |F(u,v)|^2 = \sum_{x=0}^{N-1} \sum_{y=0}^{N-1} [f(x,y)]^2 \tag{2.6.6}$$

which proves that there is an energy equivalence between the spatial and transform domains.

Transform image coding has two potential advantages: It provides good quality picture reproduction with the same number of bits as conventional PCM. Furthermore, it offers a certain immunity to channel errors and a possibility of bandwidth compression. Both of these issues will be discussed in greater detail in Chapter III.

Fig. 2.6.1 shows a block diagram of a generalized transform image coding system. In principle, the transforms can be implemented by optical, electrical or digital means.

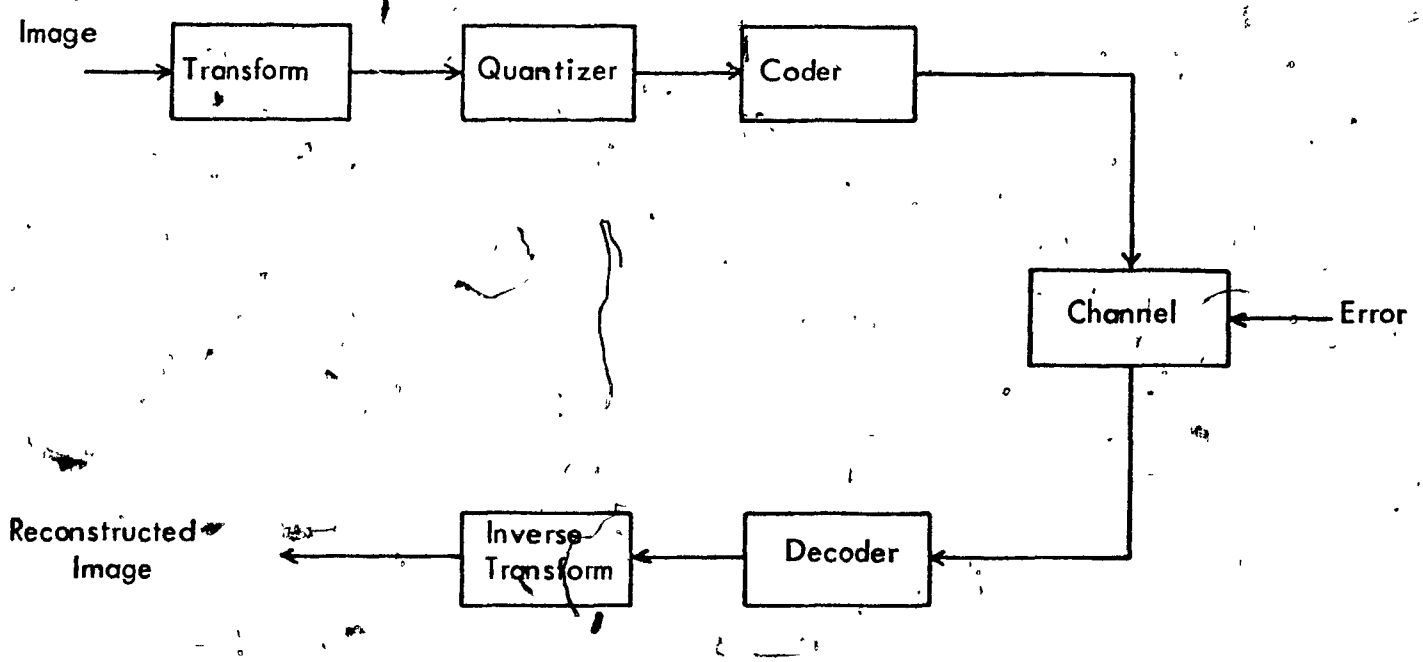

FIGURE 2.6.1 IMAGE TRANSFORM CODING SYSTEM

Note that in (2.6.1), although the variances of the picture elements $f(x,y)$ are the same, the variances of the transform samples $F(u,v)$ are not. This is one of the primary motivations for using transform coding techniques for redundancy reduction [66]. Since the information content in a sample is proportional to its variance, the samples with small variance can be discarded with a slight degradation. If we eliminate $N^2 - K^2$ samples, the m.s.e. becomes

$$\epsilon_S^2 = E\left\{\frac{1}{N^2}\sum_{y=0}^{N-1}\sum_{x=0}^{N-1}[f(x,y) - f^*(x,y)]^2\right\} \tag{2.6.7}$$

where $f^*(x,y)$ is the reconstructed image.

Substituting (2.6.1) into (2.6.7), it can be shown that

$$\epsilon_S^2 = R(0,0,0,0) - \frac{1}{N^2}\sum_{u=0}^{K-1}\sum_{v=0}^{K-1}\sigma_{uv}^2 \tag{2.6.8}$$

where σ_{uv}^2 is the variance of the (u,v) coefficient and $R(0,0,0,0)$ is the autocorrelation at the origin. This expression represents the error due to neglecting $N^2 - K^2$ samples and does not include the quantization error and channel error. The second source of error is the error due to quantization. If one assigns binary digits to each coefficient in proportion to $\log_2$(variance), then the quantization error in the (i,j) coefficient is

$$\overline{\epsilon_{qij}^2} = \frac{K_{ij}}{N^2}\frac{\sigma_{ij}^2}{2^{2n_{ij}}} \tag{2.6.9}$$

where

n_{ij} = number of binary digits used for the (i,j) th coefficient

K_{ij} = constant expressing the consequence of the scaling and companding associated with the quantization

σ_{ij}^2 = variance of the (i,j) th coefficient.

This topic together with channel noise will be presented in greater detail in Chapter III.

In the following, we shall describe three transform methods: the Karhunen-Loeve which is the optimal method, the Fourier and Hadamard transforms which possess fast computational algorithms.

2.6.1 Karhunen-Loeve Transform [75]-[77]

This transform consists of eigenvectors of the correlation matrix of the original image. Suppose that the $N \times N$ original picture is scanned and transformed into a N^2 vector. The correlation matrix of the image in an $N^2 \times N^2$ matrix of the form

$$[R] = E[z_i z_j] \qquad i = 1, 2, \ldots, N^2; \quad j = 1, 2, \ldots, N^2 \tag{2.6.10}$$

The forward Karhunen-Loeve transform is the orthogonal matrix such that

$$[A][R][A] = \begin{bmatrix} \lambda_1 & & & 0 \\ & \lambda_2 & & \\ & & \ddots & \\ 0 & & & \lambda_{N^2} \end{bmatrix} \tag{2.6.11}$$

where $\lambda_1 \geq \lambda_2 \geq \ldots \geq \lambda_{N^2}$ are the eigenvalues of $[R]$ arranged in decreasing order. Hence, the K-L transform $F(\omega)$ of the original image is

$$[F(\omega)] = [f(z)][A] \tag{2.6.12}$$

The inverse transform matrix is

$$[B] = [A]^T \tag{2.6.13}$$

Hence, if we truncate the sequence into K^2 terms, the m.s.e. is

$$\epsilon_s^2 = \sum_{i=K^2+1}^{N^2} \lambda_i \tag{2.6.14}$$

But, the sum of the eigenvalues is equal to the sum of the variances of the original random variable, i.e.

$$\sum_{i=1}^{K^2} \lambda_i + \sum_{i=K^2+1}^{N^2} \lambda_i = N^2 R(0,0,0,0) \tag{2.6.15}$$

Therefore,

$$\sum_{i=K^2+1}^{N^2} \lambda_i = N^2 R(0,0,0,0) - \sum_{i=1}^{K^2} \lambda_i \tag{2.6.16}$$

and the mean-square error is

$$\text{m.s.e.} = \epsilon_s^2 = \frac{1}{N^2} \sum_{i=K^2+1}^{N^2} \lambda_i$$

$$= R(0,0,0,0) - \frac{1}{N^2} \sum_{i=1}^{K^2} \lambda_i \qquad (2.6.17)$$

Since the λ_i's are monotonically decreasing in value, the resulting m.s.e. will be minimum for any K. This is to be expected because the transform samples are uncorrelated, hence all the redundancy has been removed.

However, there are two major problems associated with the K-L transform: Firstly, a great amount of computation has to be performed. Secondly, although the m.s.e. is a minimum for K-L transforms, it is not a valid error criterion for most pictorial data.

2.6.2 Fourier Transform Coding [75] [76], [78]

The two-dimensional Fourier transform of an image $f(x,y)$ is expressed as

$$F(u,v) = \frac{1}{N} \sum_{x=0}^{N-1} \sum_{y=0}^{N-1} f(x,y) \exp\left\{ - \frac{2\pi i}{N} (ux + vy) \right\} \qquad (2.6.18)$$

where $i = \sqrt{-1}$.

and the inverse Fourier transform is

$$f(x,y) = \frac{1}{N} \sum_{u=0}^{N-1} \sum_{v=0}^{N-1} F(u,v) \exp\left\{\frac{2\pi i}{N} (ux + vy)\right\} \tag{2.6.19}$$

Although $f(x,y)$ is a real function, the Fourier transform given by (2.6.18) is in general complex which may be rewritten as

$$F(u,v) = \frac{1}{N} \sum_{x=0}^{N-1} \sum_{y=0}^{N-1} f(x,y) \left\{\cos \frac{2\pi}{N} (ux + vy) - i \sin \frac{2\pi}{N} (ux + vy)\right\} \tag{2.6.20}$$

$$= F_R(u,v) - i F_I(u,v) \tag{2.6.21}$$

where

$$F_R(u,v) = \frac{1}{N} \sum_{x=0}^{N-1} \sum_{y=0}^{N-1} f(x,y) \cos \frac{2\pi}{N} (ux + vy) \tag{2.6.22}$$

$$F_I(u,v) = \frac{1}{N} \sum_{x=0}^{N-1} \sum_{y=0}^{N-1} f(x,y) \sin \frac{2\pi}{N} (ux + vy) \tag{2.6.23}$$

But, cosine is an even function and sine is odd in (u,v). Therefore,

$$F_R(u,v) = F_R(-u,v) \tag{2.6.24}$$

$$F_I(u,v) = -F_I(-u,-v) \tag{2.6.25}$$

and

$$F(u,v) = F^*(-u,-v) \tag{2.6.26}$$

so that only N^2 samples from one half of the transform plane have to be transmitted.

Fast computational algorithms exist for the Fourier transform [79] - [85]. Only $2N^2 \log_2 N$ computations are required as opposed to $2N^3$ operations required for K-L transforms. This becomes a considerable saving for large-size images.

2.6.3 Hadamard Transform Coding [75], [86]

The Fourier transform is a natural operator for most image coding because of its widespread use in other fields. But, there is another operator which possesses fast computation algorithms and the same properties of noise averaging and bit compression as offered by the Fourier transform method. The symmetric Hadamard matrix fulfills all these requirements and even has the advantage over Fourier transform coding in a saving of speed of an order of magnitude by storage of intermediate results [87].

The Hadamard matrix is a square array of plus and minus ones with rows and columns of the matrix orthogonal to each other. Thus

$$HH^T = NI \tag{2.6.27}$$

Since H is symmetric, then

$$HH = NI \tag{2.6.28}$$

The lowest-order Hadamard matrix is

$$H = \begin{bmatrix} 1 & 1 \\ 1 & -1 \end{bmatrix} \tag{2.6.29}$$

The Hadamard matrix G of order 2 N may be built up from the Nth order Hadamard matrix H by

$$G = \begin{bmatrix} H & H \\ H & -H \end{bmatrix} \tag{2.6.30}$$

Hence, the two dimensional Hadamard transform may be written as

$$F(u,v) = \sum_{x=0}^{N-1} \sum_{y=0}^{N-1} f(x,y)(-1)^{p(x,y,u,v)} \tag{2.6.31}$$

where

$$p(x,y,u,v) = \sum_{i=0}^{N-1} (u_i x_i + v_i y_i) \tag{2.6.32}$$

Fast computational algorithms also exist requiring only $2N^2 \log_2 N$ operations.

Fig. 2.6.2 is a graph showing the sample variances of the 256 coefficients arranged in order of magnitude, of the 256 subpicture of a specific picture [88]

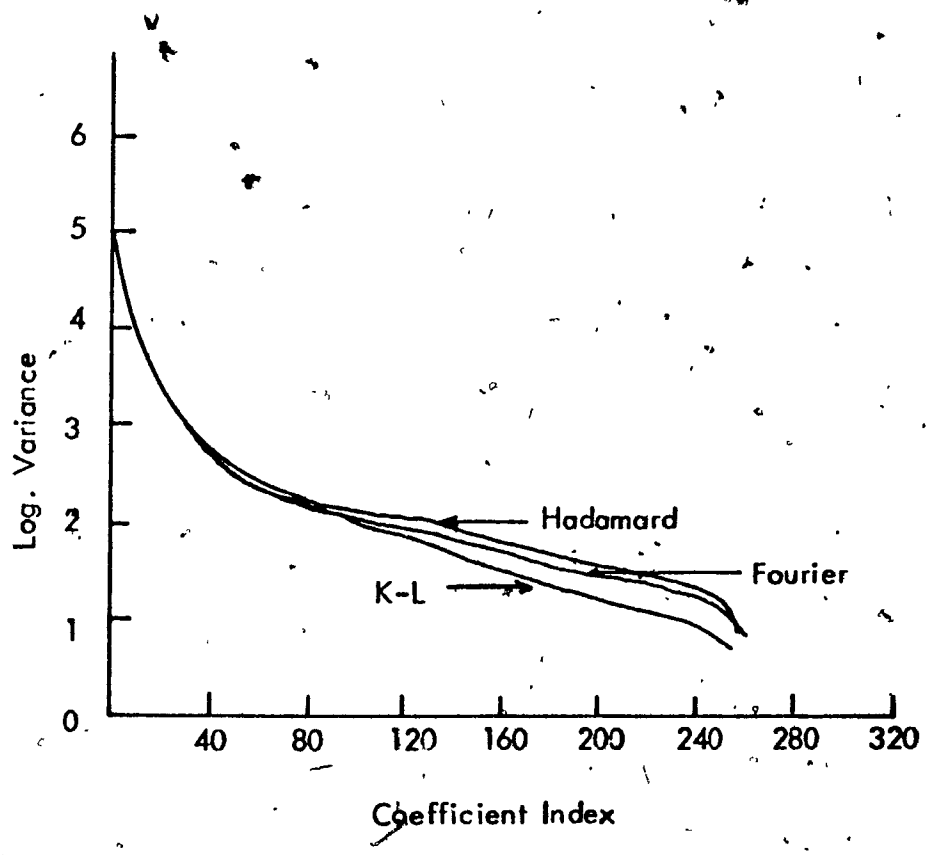

FIGURE 2.6.2 GRAPH SHOWING RELATIVE MAGNITUDES OF COEFFICIENT VARIANCES

CHAPTER III

EFFECTS OF CHANNEL NOISE ON SOME DATA COMPRESSION SYSTEMS

As we have pointed out before, data compression systems are usually more sensitive to the effect of channel errors than the corresponding uncompressed systems. This is due to the fact that redundancy has been reduced from the signal and thus all the samples transmitted are considered significant in the reconstruction of the original waveform at the receiver. In some cases, an error occurring in one of the codewords propagates beyond the time of occurrence of this error, until a sync pulse resets the system. For a fixed number of quantization levels, there are two ways to remedy the situation : either by increasing the transmitter power or by adding back some controlled redundancy. However, the two methods will reduce the energy compression ratio and the bit compression ratio, respectively. Transform coding method has the attractive feature that it is more immune to channel errors.

We shall use as a standard for comparing data compression techniques the fixed rate time-sampling PCM system. We assume that the channel noise is an additive white Gaussian process with zero mean and one sided spectral density of N_o.

3.1 Effect of Channel Noise on PCM Systems

In general, the total mean-square error in the reconstructed PCM signal can be expressed as a sum of three independent terms,

$$\epsilon^2 = \epsilon_q^2 + \epsilon_c^2 + \epsilon_m^2 \qquad (3.1.1)$$

where

ϵ_q^2 = mean square quantization error

ϵ_c^2 = mean square channel error

ϵ_m^2 = mean square mutual error

It can be shown that for a well-designed system [89], the last term in (3.1.1) is zero. The expression for ϵ_q^2 has been derived in Chapter II (2.3). Thus, we shall consider only ϵ_c^2 here.

Let P_B be the probability of bit error, and assume that each word has k bits. A k-bit word represents the number

$$X_1 2^{-1} + X_2 2^{-2} + \ldots + X_i 2^{-i} + \ldots + X_k 2^{-k} \tag{3.1.2}$$

where

$$X_i = 0 \text{ or } 1 \tag{3.1.3}$$

Suppose that P_B is small enough that we can restrict ourselves to one error per word. Assuming that the probability of a given bit in error is uniformly distributed over the length k of the word, we may write

$$\begin{aligned} &\Pr \text{ (one error in a word of length k)} \\ &= k P_B (1 - P_B)^{k-1} \end{aligned} \tag{3.1.4}$$

and

$$\begin{aligned} &\epsilon_c^2 \text{ (given that an error occurs in a word)} \\ &= \frac{1}{k} \sum_{i=1}^{k} (2^{-i})^2 \end{aligned} \tag{3.1.5}$$

Therefore the channel error ϵ_c^2 is given by

$$\epsilon_c^2 = \frac{kP_B(1-P_B)^{k-1}}{k} \sum_{i=1}^{k} 2^{-2i} \tag{3.1.6}$$

$$= \frac{P_B(1-P_B)^{k-1}}{3} \left(1 - \frac{1}{2^{2k}}\right) \tag{3.1.7}$$

Since P_B is usually small, we may approximate $P_B(1-P_B)^{k-1}$ as P_B.

Hence

$$\epsilon_c^2 = \frac{P_B}{3}\left(1 - \frac{1}{2^{2k}}\right) \tag{3.1.8}$$

Equation (3.1.8) represents the m.s. channel noise for straight binary encoded PCM. It may be shown that the same result holds for more than one bit error in the codeword [90].

The probability of bit error P_B depends on the modulation technique used, the channel and the detection technique. For matched filter, nonfading channel and coherent detection of antipodal signals,

$$P_B = \operatorname{erfc}\sqrt{\frac{2S}{N_0 R}} \tag{3.1.9}$$

where

$\frac{S}{N}$ = signal-to-noise ratio in the band

R = transmission bit-rate

and

$$\operatorname{erfc} x = \frac{1}{\sqrt{2\pi}} \int_x^{\infty} \exp(-y^2/2)\, dy \tag{3.1.10}$$

The bandwidth B is related to the sampling period τ by

$$B = \frac{1}{2\tau} \tag{3.1.11}$$

For a k-bit PCM word,

$$R = \frac{k}{\tau} = \frac{\log_2 q}{\tau} \tag{3.1.12}$$

where q is the number of levels equal to 2^k.

Hence,

$$P_B = \operatorname{erfc}\sqrt{\frac{2S}{N_o R}}$$

$$= \operatorname{erfc}\sqrt{\left(\frac{S}{N_o}\right) \cdot \frac{1}{B \log_2 q}} \tag{3.1.13}$$

Now, if we let $y = y - x$ in (3.1.10), we get

$$\operatorname{erfc} x = \frac{1}{\sqrt{2\pi}} \int_0^{\infty} e^{-\frac{(y-x)^2}{2}}\, dy$$

$$= \frac{1}{\sqrt{2\pi}} \int_0^{\infty} e^{-\frac{y^2}{2}}\, e^{-\frac{x^2}{2} + xy}\, dy \tag{3.1.14}$$

For $y > x$ and $x > 0$, then

$$xy > x^2$$

of

$$xy - \frac{x^2}{2} > \frac{x^2}{2}$$

Hence,

$$\operatorname{erfc} x < \frac{1}{\sqrt{2\pi}} e^{-\frac{x^2}{2}} \int_0^\infty e^{-\frac{y^2}{2}} dy$$

$$= \frac{e^{-\frac{x^2}{2}}}{2}$$

$$\sim e^{-x^2} \tag{3.1.15}$$

where $\sim$ means the same order of magnitude as. With the above approximations, (3.1.9) becomes

$$P_B = \operatorname{erfc}\sqrt{\frac{2S}{N_o R}} \sim \exp\left(-\frac{2S}{N_o R}\right) \tag{3.1.16}$$

From this equation, we can see that for fixed signal-to-noise ratio, the probability of bit error decreases with bit-rate. This is an important result which must not be neglected when data compression is considered.

3.2. Effect of Channel Noise on Run-length Encoded ZOP Systems

Usually, transmission errors cause both errors in the level information and the timing information in data compression systems. Hence, the m.s. channel error is given by

$$\epsilon_c^2 / \text{comp.} = \epsilon_{level}^2 + \epsilon_{time}^2 \qquad (3.2.1)$$

3.2.1. Errors in the Level Information

(1) For an asychronous system, only the level information is transmitted. But for this kind of system, one can only reduce the number of bits and no bandwidth reduction is possible. This is due to the fact that the highest frequency components still exist in the signal. Fig. 3.2.1 will clarify the situation.

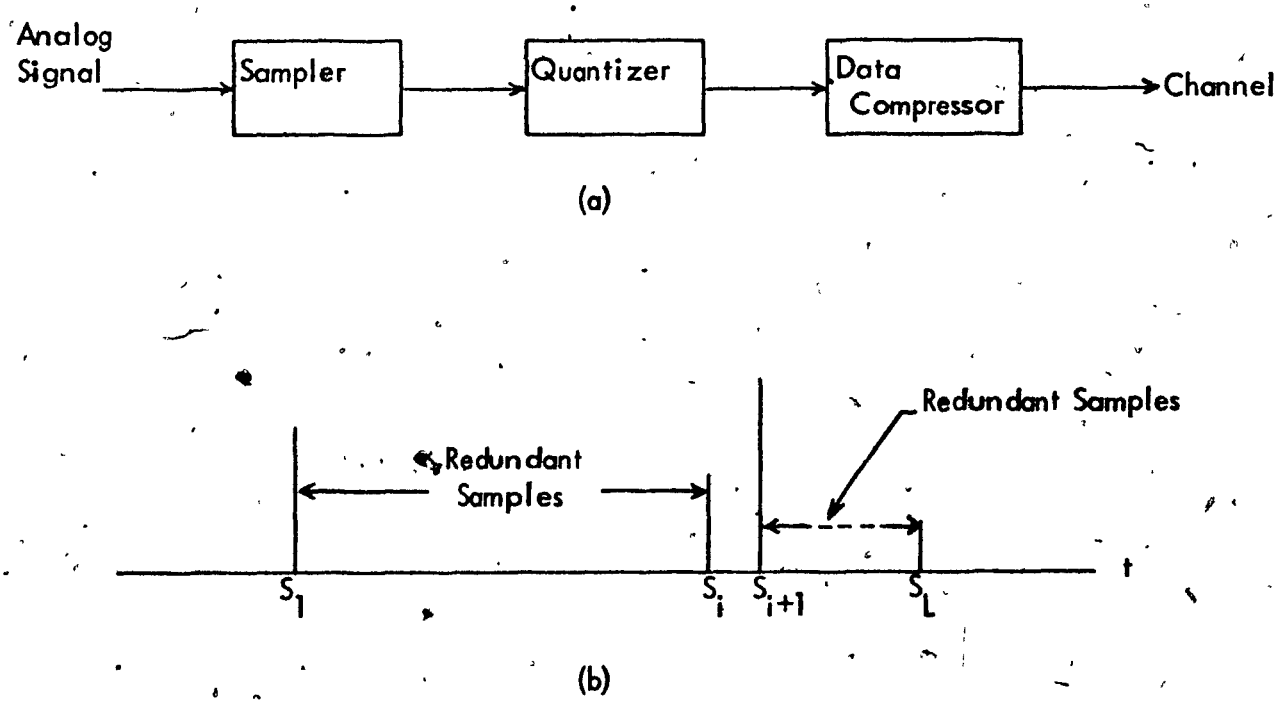

FIGURE 3.2.1 : (a) ASYNCHRONOUS SYSTEM
(b) SAMPLE PATTERN FROM DATA COMPRESSOR OF AN ASYNCHRONOUS SYSTEM

We have derived in Chapter II (2.4.1) the average value of the run-length and this is given by C_S which is the sample compression ratio. An error in the level information will thus affect an average of C_S words. Hence, for an asynchronous system

$$\epsilon_c^2 \,/\, \text{asyn.} = C_S \epsilon_c^2$$

$$= C_S \frac{P_B}{3} \left(1 - \frac{1}{2^{2k}}\right) \qquad (3.2.2)$$

Note that the maximum transmission rate is the same as in uncompressed system, hence the bit error probability is unchanged. The m.s. channel noise is simply C_S times that of the PCM system. Since no addressing scheme is used here, the bit compression ratio C_B is equal to the sample compression ratio C_S. One might, however, improve the performance of the compression system by increasing the quantization resolution, increasing the signal power and using coding techniques [2]. We shall not pursue this any further here.

(2) For a sychronous system, timing words are necessary and buffers are required to adjust the sample pattern from the compressor to achieve a bit rate reduction. This is shown in Fig. 3.2.2. The bit rate is reduced as a result of the buffering. Thus,

$$\text{transmission bit rate} = \frac{1}{C_B} \times \text{bit rate of PCM system} \qquad (3.2.3)$$

Therefore,

$$P_B' = \exp\left(-\frac{2S}{N_o R} C_B\right)$$

$$= \left[\exp\left(-\frac{2S}{N_o R}\right)\right]^{C_B}$$

$$= P_B^{C_B} \qquad (3.2.4)$$

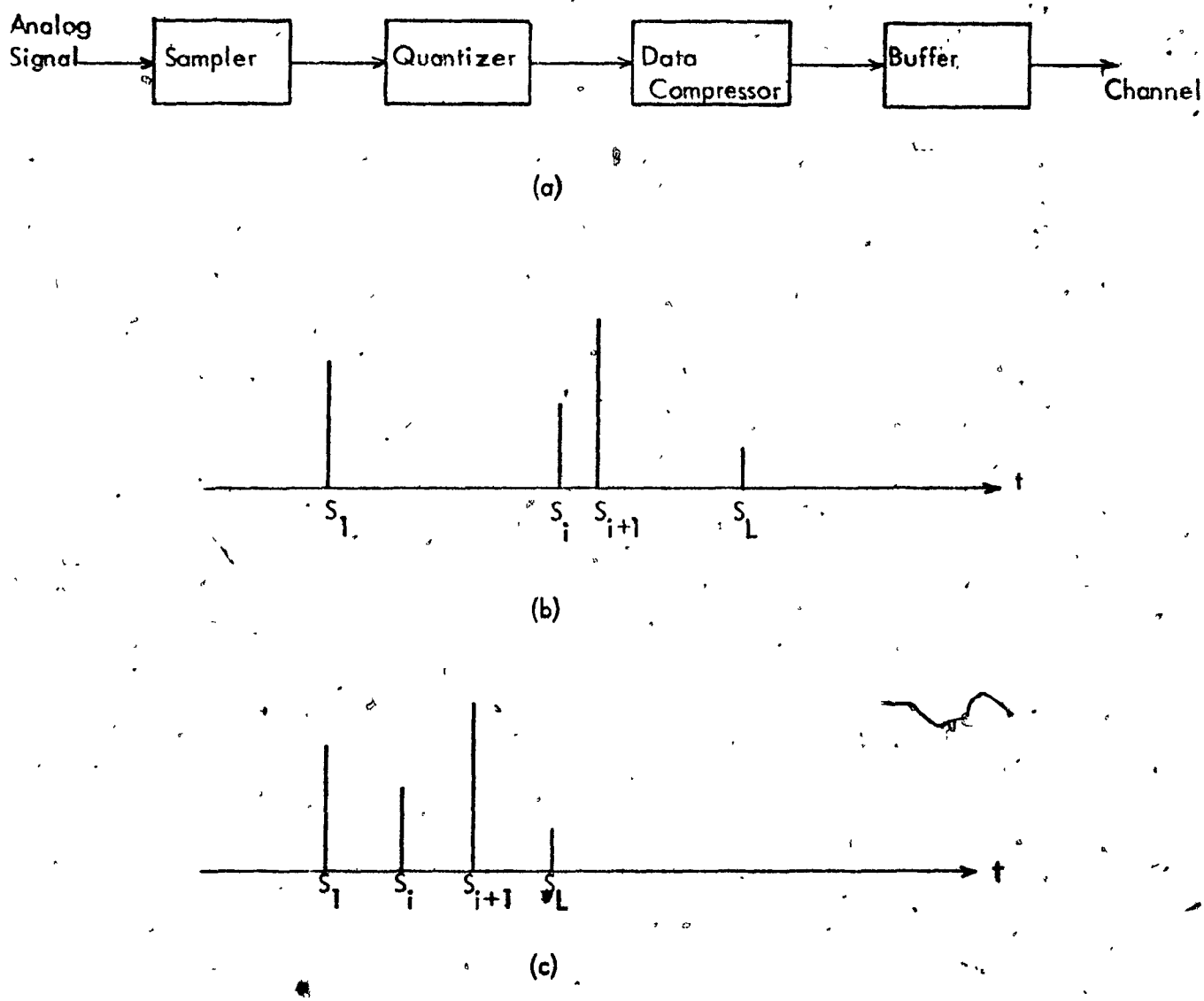

FIGURE 3.2.2 : (a) SYNCHRONOUS SYSTEM
(b) SAMPLE PATTERN AT OUTPUT OF DATA COMPRESSOR
(c) SAMPLE PATTERN AT OUTPUT OF BUFFER

Hence, the m.s. error due to an error in the level information is

$$\epsilon^2_{level} = \frac{C_S}{3} P'_B \left(1 - \frac{1}{2^{2k}}\right)$$

$$= \frac{C_S}{3} P_B C_B \left(1 - \frac{1}{2^{2k}}\right) \qquad (3.2.5)$$

3.2.2 Errors in the Timing Information

In this analysis, we shall assume the following :

(a) Probability of more than 1 run-length word per line in error is very small.

(b) Bit error is uniformly distributed in a word.

(c) The non-redundant samples are uncorrelated.

Let us define

n_1 = number of affected samples per erroneous non-redundant sample,

n_2 = number of erroneous non-redundant samples due to an error in a run-length word,

e_{RL} = error in the sample level due to an error in a run-length word,

r = number of bits in a run-length word,

N = actual number of non-redundant samples in a line,

L = number of samples in a line,

n = number of samples in a run.

Now, the squared error per sample given that a run-length word is in error is given by

$$e^2_{sample} = \frac{n_1 n_2 e^2_{RL}}{L} \tag{3.2.6}$$

Hence,

$$E\left[e^2_{sample}\right] = \frac{E[n_1]E[n_2]E[e^2_{RL}]}{L} \tag{3.2.7}$$

We may write the m.s. error in run-length encoding as

$$E\left[e^2\right] = \frac{E[n_1]E[n_2]E[e^2_{RL}]}{L} \Pr(1 \text{ run-length word in error}) \tag{3.2.8}$$

because of assumption (a). Our task is to find the four factors in (3.2.8). The number of non-redundant samples in a line is $\frac{L}{C_S}$, and total number of bits in the run-length words in a line is $\frac{rL}{C_S}$. Thus, the probability of a run-length in error is

$$\binom{\frac{rL}{C_S}}{1} P_B \quad (1 - P_B)^{\frac{rL}{C_S}-1} \tag{3.2.9}$$

where P_B is the probability of a bit error. This is equal to $\frac{rL}{C_S} P_B (1 - P_B)^{\frac{rL}{C_S}-1}$.

In practical channels, $P_B < 10^{-4}$ and also $\frac{rL}{C_S} \gg 1$. Therefore,

$$\Pr(1 \text{ run-length word in error}) \simeq \frac{rL}{C_S} P_B \tag{3.2.10}$$

Suppose that there is an error in the ith bit of the run-length word as represented below :

$$X_{r-1} 2^{r-1} + \ldots\ldots + X_i 2^i + \ldots\ldots + X_{i-1} 2^{i-1} + \ldots\ldots + X_o 2^o$$

$$X_i = 0 \text{ or } 1$$

The number of displaced samples is 2^{i-1}. Thus,

$$\text{if } 2^{i-1} \geq n, \text{ all samples in the run are affected}$$

$$\text{if } 2^{i-1} < n, \; 2^{i-1} \text{ samples are affected.}$$

Now,

$$p(n_1) = \text{probability that a certain bit is in error} = \frac{1}{r} \tag{3.2.11}$$

because of the uniform distribution.

Hence,

$$E\left[n_1 | n\right] = \text{expected number of affected samples per erroneous non-redundant sample for a run of } n \text{ samples}$$

$$= \sum_{n_1} n_1 \, p(n_1)$$

$$= \frac{1}{r} \sum_{n_1} n_1$$

$$= \frac{1}{r}\left(\sum_{i=1}^{w} 2^{i-1} + \sum_{i=w+1}^{i=r} n\right) \tag{3.2.12}$$

where

$$w = \text{the integral part of } 1 + \log_2 n \tag{3.2.13}$$

$$E[n_1] = \sum_{n=1}^{2^r-1} E[n_1 | n] p(n) \tag{3.2.14}$$

where $p(n)$ is the probability density of the run-length. From Chapter II, (2.4.1)

$$p(n) = p(1-p)^{n-1}$$

$$= \frac{1}{C_S}\left(1 - \frac{1}{C_S}\right)^{n-1} \tag{3.2.15}$$

Substituting (3.2.15) into (3.2.14), we get

$$E[n_1] = \sum_{n=1}^{2^r-1} \frac{1}{r} \left(\sum_{i=1}^{w} 2^{i-1} + \sum_{i=w+1}^{r} n \right) \frac{1}{C_S} \left(\frac{C_S - 1}{C_S} \right)^{n-1} \tag{3.2.16}$$

But,

$$\sum_{i=1}^{w} 2^{i-1} = 2^w - 1$$

and

$$\sum_{i=w+1}^{r} n = (r - w)n = nr - nw$$

Hence,

$$E[n_1] = \sum_{n=1}^{2^r-1} \frac{1}{r} (2^w - 1 + nr - nw) \frac{1}{C_S} \left(\frac{C_S - 1}{C_S} \right)^{n-1} \tag{3.2.17}$$

To find $E[n_2]$, note that the number of non-redundant samples per line N is $\frac{L}{C_S}$ for large L.

Suppose that an error occurs in a run-length word. The distribution for this error is uniform over the $\frac{L}{C_S}$ run-length words. The first non-redundant sample in a line is always unaffected but the last sample is always affected regardless of the location of the error in the run-length word. The probability that a non-redundant sample being affected increases linearly with its location on a line. Hence, on the average, the number of affected non-redundant samples on a line is

$$E[n_2] = \frac{\frac{L}{C_S} - 1}{2} \tag{3.2.18}$$

This result agrees with that derived in [2].

Now we shall find $E[e_{RL}^2]$. Let x_i and x_{i+1} be random variables denoting the levels of the two consecutive non-redundant samples.

$$E[e_{RL}^2] = E[(x_i - x_{i+1})^2]$$

$$= E[x_i^2] - 2E[x_i x_{i+1}] + E[x_{i+1}^2] \qquad (3.2.19)$$

We assume that x_i and x_{i+1} are uncorrelated (this is true in practice because adjacent non-redundant samples are very weakly correlated). Also x_i and x_{i+1} are random variables identically distributed, hence

$$E[x_i^2] = E[x_{i+1}^2] = E[x^2] \qquad (3.2.20)$$

and

$$E[x_i] = E[x_{i+1}] = E[x] \qquad (3.2.21)$$

Therefore,

$$E[e_{RL}^2] = 2[E(x^2) - E(x)^2] \qquad (3.2.22)$$

The random variable x can take on any discrete values $\frac{i}{2^k}$, $0 \le i \le 2^k - 1$, and assume that x is uniformly distributed over the 2^k levels, i.e. $p(x) = \frac{1}{2^k}$.

Then,

$$E^2[x] = \left(\sum_{i=0}^{2^k-1} p(x)\frac{i}{2^k}\right)^2$$

$$= \left(\frac{1}{2^{2k}}\sum_{i=0}^{2^k-1} i\right)^2$$

$$= \frac{(2^k-1)^2}{2^{2(k+1)}} \qquad (3.2.23)$$

$$E[x^2] = \sum_{i=0}^{2^k-1} p(x) \frac{i^2}{2^{2k}}$$

$$= \frac{1}{2^{3k}} \sum_{i=0}^{2^k-1} i^2$$

$$= \frac{1}{6} \frac{(2^k - 1)(2^{k+1} - 1)}{2^{2k}} \tag{3.2.24}$$

Substituting (3.2.23) and (3.2.24) into (3.2.22), we get

$$E[e_{RL}^2] = 2 \left[\frac{(2^k-1)(2^{k+1}-1)}{6 \cdot 2^{2k}} - \frac{(2^k-1)^2}{2^{2(k+1)}} \right]$$

$$= \frac{1}{6} \frac{(2^{2k} - 1)}{2^{2k}} \tag{3.2.25}$$

Combining (3.2.8), (3.2.10), (3.2.17), (3.2.18) and (3.2.25), we get the m.s. channel error for the run-length encoding

$$\epsilon_{time}^2 = \left\{ \left(\frac{rLP_B}{C_S}\right) \left(\frac{1}{L}\right) \left(\frac{1}{6}\right) \left(\frac{2^{2k}-1}{2^{2k}}\right) \left(\frac{\frac{L}{C_S} - 1}{2}\right) \sum_{n=1}^{2^r-1} \frac{1}{r} (2^w - 1 + nr - nw) \cdot \frac{1}{C_S} \left(\frac{C_S - 1}{C_S}\right)^{n-1} \right\}$$

$$= \frac{P_B}{12 C_S^2} \left(\frac{2^{2k}-1}{2^{2k}}\right) \left(\frac{L}{C_S} - 1\right) \sum_{n=1}^{2^r-1} (2^w - 1 + nr - nw) \left(\frac{C_S - 1}{C_S}\right)^{n-1} \tag{3.2.26}$$

Combining the m.s.e. in the level information and the timing information gives the m.s. channel error of a ZOP, run-length encoded system.

$$\epsilon_c^2 = \left\{ \frac{C_S}{3} P_B^{C_B} \left(1 - \frac{1}{2^{2k}}\right) \right.$$

$$+ \frac{P_B}{12\,C_S^2} \left(\frac{2^{2k}-1}{2^{2k}}\right) \left(\frac{L}{C_S} - 1\right) \sum_{n=1}^{2^r-1} (2^w - 1 + nr - nw) \left(\frac{C_S - 1}{C_S}\right)^{n-1} \Bigg\} \tag{3.2.27}$$

The total error in the system is

$$\epsilon^2 = \epsilon_q^2 + \epsilon_c^2 + \epsilon_{aperture}^2$$

Thus, the root mean square error is

$$\epsilon = \left\{ \frac{1}{12 \cdot 2^{2k}} + \frac{m(m+1)}{3(2^{2k})} + \frac{C_S}{3} P_B C_B \left(1 - \frac{1}{2^{2k}}\right) + \frac{P_B}{12\,C_S^2} \left(\frac{2^{2k}-1}{2^{2k}}\right) \left(\frac{L}{C_S} - 1\right) \sum_{n=1}^{2^r-1} (2^w - 1 + nr - nw) \left(\frac{C_S - 1}{C_S}\right)^{n-1} \right\}^{\frac{1}{2}} \tag{3.2.28}$$

We shall plot the r.m.s. error ϵ against P_B for some practical values of the parameters C_S, k, r and L. A similar curve is plotted for the PCM system, Fig. 3.2.3. It is apparent that for practical channels where P_B is of the order of 10^{-6}, bandwidth compression can be achieved with only a slight degradation in the signal quality compared to PCM trasmission.

3.3 DPCM System: Channel Noise and Bit Compression

We have seen in Chapter II (2.4.3) that the quantization error in a DPCM system is reduced from its corresponding value in PCM systems by a factor equal to the ratio of the variance of the difference signal to the variance of the input signal. But, the analysis thus far is restricted to noise free channels. Here,

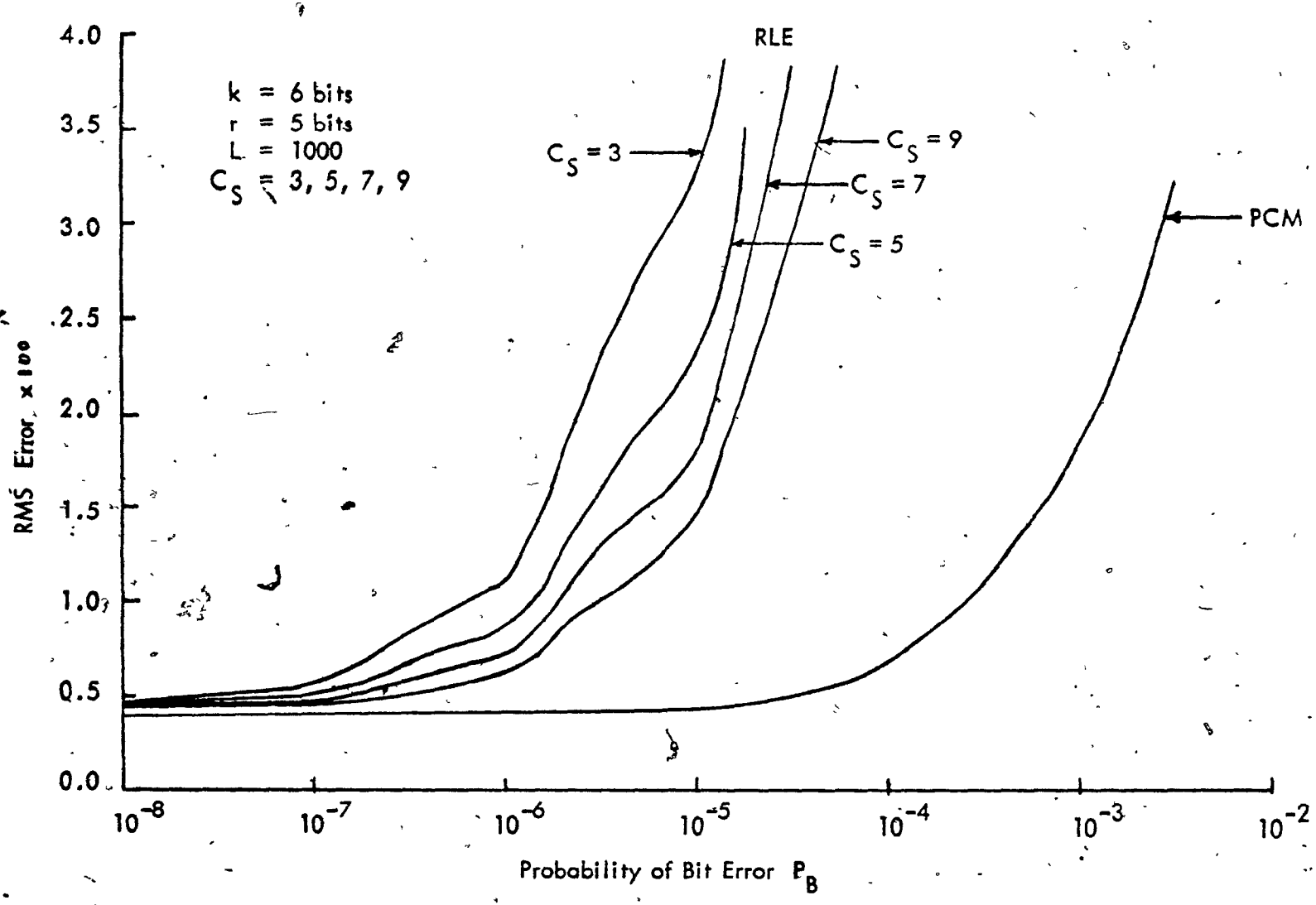
k = 6 bits
r = 5 bits
L = 1000
C_S = 3, 5, 7, 9
RLE
$C_S = 3$
$C_S = 9$
$C_S = 7$
$C_S = 5$
PCM
RMS Error, x 100
4.0
3.5
3.0
2.5
2.0
1.5
1.0
0.5
0.0
10^{-8}
10^{-7}
10^{-6}
10^{-5}
10^{-4}
10^{-3}
10^{-2}
Probability of Bit Error P_B

FIGURE 3.2.3

we shall analyse the DPCM system over noisy channels corrupted by additive white Gaussian noise of zero mean. Consider the model shown in Fig. 3.3.1.

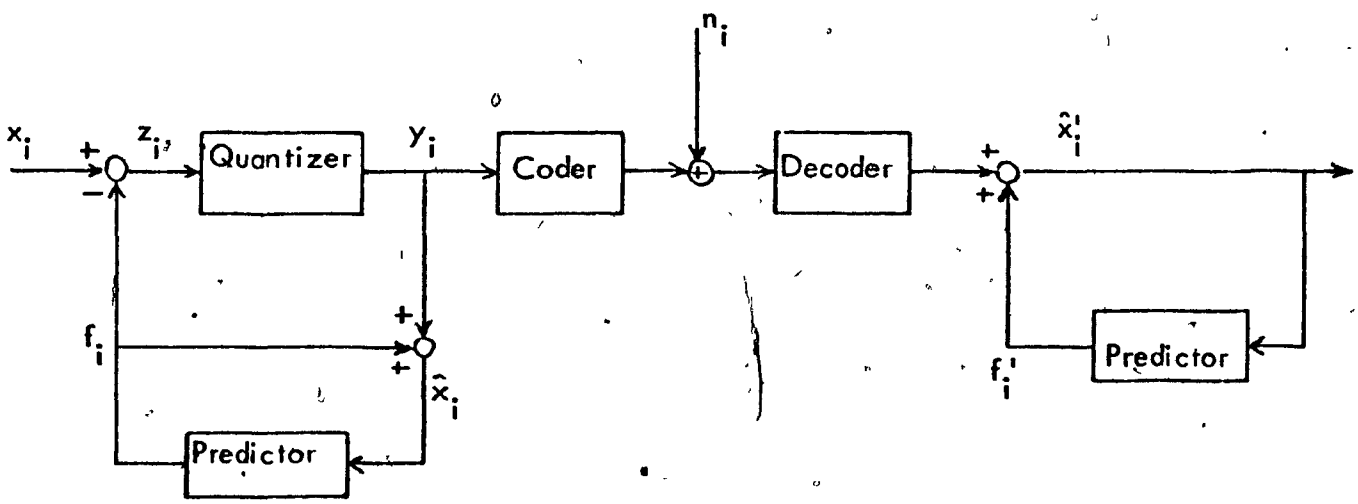

FIGURE 3.3.1 : DPCM WITH CHANNEL NOISE

With the notations in Fig. 3.3.1, the primed quantities differ from the unprimed ones only in the channel errors. Now,

$$\hat{x}_i = y_i + f_i = y_i + \sum_{j=1}^{\infty} h_j \hat{x}_{i-j} \tag{3.3.1}$$

where h_j's are the characteristics of the predictor. At the receiver,

$$\hat{x}_i' = y_i' + f_i'$$

$$= y_i + n_i + \sum_{j=1}^{\infty} h_j \hat{x}_{i-j} \tag{3.3.2}$$

Let

$$\hat{x}_i' = \hat{x}_i + \epsilon_i \tag{3.3.3}$$

Then,

$$\hat{x}_i + \epsilon_i = y_i + \sum_j h_j \hat{x}_{i-j} + \sum_j h_j \epsilon_{i-j} + n_i \tag{3.3.4}$$

Combining (3.3.1) and (3.3.4), we get

$$\hat{x}_i + \epsilon_i = \hat{x}_i + \sum_j h_j \epsilon_{i-j} + n_i \tag{3.3.5}$$

or

$$\epsilon_i = \sum_j h_j \epsilon_{i-j} + n_i \tag{3.3.6}$$

Therefore,

$$E[\epsilon_i^2] = \sum_{j,k} h_j h_k E[\epsilon_{i-j} \epsilon_{i-k}] + E[n_i^2] \tag{3.3.7}$$

3.3.1 One-sample Feedback Optimal Prediction

Suppose that we consider the one-sample feedback optical predictor which is simple in implementation. From our discussion in Chapter II (2.4.3), the parameters in the predictor are given by

$$h_1 = \rho_1 \tag{3.3.8}$$

$$h_j = 0 \quad \text{for } j \neq 1 \tag{3.3.9}$$

Hence,

$$E[\epsilon_i^2] = \rho_1^2 E[\epsilon_{i-1}^2] + E[n_i^2]$$

$$\doteq \rho_1^2 E[\epsilon_i^2] + E[n_i^2] \tag{3.3.10}$$

assuming stationarity of ϵ_i, or

$$E[\epsilon_i^2] = \frac{E[n_i^2]}{1 - \rho_1^2} \tag{3.3.11}$$

Assuming that $\hat{x}_i$ and ϵ_i are uncorrelated, then

$$E[\hat{x}_i'^2] = E[\hat{x}_i^2] + E[\epsilon_i^2] \tag{3.3.12}$$

or

$$\frac{E[\hat{x}_i'^2]}{E[x_i^2]} = \frac{E[\hat{x}_i^2]}{E[x_i^2]} + \frac{E[\epsilon_i^2]}{E[x_i^2]} \tag{3.3.13}$$

But,

$$\begin{aligned} \hat{x}_i &= y_i + f_i \\ &= z_i - e_i + f_i \\ &= (x_i - f_i) - e_i + f_i \\ &= x_i - e_i \end{aligned} \tag{3.3.14}$$

Where e_i is the quantization error. Therefore,

$$E[\hat{x}_i^2] = E[x_i^2] + E[e_i^2] \tag{3.3.15}$$

assuming that x_i and e_i are uncorrelated. Hence, (3.3.13) becomes

$$\frac{E[\hat{x}_i^2]}{E[x_i^2]} = \frac{E[x_i^2] + E[e_i^2]}{E[x_i^2]} + \frac{E[\epsilon_i^2]}{E[x_i^2]} \tag{3.3.16}$$

$$= 1 + \frac{E[e_i^2]}{E[x_i^2]} + \frac{E[\epsilon_i^2]}{E[x_i^2]}$$

$$= 1 + \frac{E[e_i^2]}{E[z_i^2]} \cdot \frac{E[z_i^2]}{E[x_i^2]} + \frac{E[n_i^2]}{E[x_i^2]} \cdot \frac{1}{1-\rho_1^2} \tag{3.3.17}$$

We have derived in Chapter II (2.4.3) that for DPCM with an optimal prediction, $\frac{E[z_i^2]}{E[x_i^2]} = 1 - \rho_1^2$. Then we may write

$$\frac{E[\hat{x}_i^2]}{E[x_i^2]} = 1 + \frac{E[e_i^2]}{E[z_i^2]}(1-\rho_1^2) + \frac{E[n_i^2]}{E[x_i^2]} \cdot \frac{1}{1-\rho_1^2} \tag{3.3.18}$$

Now,

$$\frac{E[e_i^2]}{E[z_i^2]} = \text{normalized quantization error}$$

and

$$\frac{E[n_i^2]}{E[x_i^2]} = \text{normalized channel error in a PCM system.}$$

We therefore conclude that the quantization noise is reduced by a factor of $(1-\rho_1^2)$, but the channel noise is amplified by a factor of $\frac{1}{1-\rho_1^2}$. If the quantization noise is reduced by k db, then the channel noise is increased also by k db. This result agrees with the conclusion drawn by O'Neal [61], [62], but differs from that claimed in [59] where the authors concluded that the effect of channel noise on DPCM is no more severe than on PCM. It is worth pointing out that the mathematical results in [59] are basically the same as that derived here although the conclusions differ due to different interpretations. If one, however, increases the output power of the transmitter such that the power of the difference signal is the same as that of the input signal, then the conclusion drawn in [59] holds.

3.3.2 Two-sample Feedback

Suppose the parameters of the predictor network are such that

$$h_i = 0 \quad \text{if} \quad i \neq 1, 2 \tag{3.3.19}$$

From (3.3.7), we get

$$E[\epsilon_i^2] = \sum_{j,k} h_j h_k E[e_{i-j} e_{i-k}] + E[n_i^2]$$

$$= \sum_j h_j^2 E[\epsilon_{i-j}^2] + \sum_{j \neq k} h_j h_k E[e_{i-j} e_{i-k}] + E[n_i^2] \tag{3.3.20}$$

Using (3.3.19) and the stationary property of ϵ_i, we get

$$E[\epsilon_i^2] = (h_1^2 + h_2^2)\, E[\epsilon_i^2] + 2h_1h_2\, E[\epsilon_{i-1}\,\epsilon_{i-2}] + E[n_i^2] \tag{3.3.21}$$

Now, using (3.3.6),

$$\begin{aligned} E[\epsilon_{i-1}\,\epsilon_{i-2}] &= E[\epsilon_{i-2}(\sum_j h_j\,\epsilon_{i-1-j} + n_{i-1})] \\ &= E[\sum_j h_j\,\epsilon_{i-2}\epsilon_{i-1-j}] \\ &= \sum_j h_j\, E[\epsilon_{i-2}\,\epsilon_{i-1-j}] \\ &= h_1\, E[\epsilon_{i-2}^2] + h_2\, E[\epsilon_{i-2}\,\epsilon_{i-3}] \end{aligned} \tag{3.3.22}$$

assuming that ϵ_i and n_i are uncorrelated.

Invoking the stationary property of the ϵ_i's again, (3.3.22) becomes

$$E[\epsilon_{i-1}\,\epsilon_{i-2}] = h_1\, E[\epsilon_{i-2}^2] + h_2\, E[\epsilon_{i-1}\,\epsilon_{i-2}]$$

or

$$\begin{aligned} (1 - h_2)\, E[\epsilon_{i-1}\,\epsilon_{i-2}] &= h_1\, E[\epsilon_{i-2}^2] \\ &= h_1\, E[\epsilon_i^2] \end{aligned} \tag{3.3.23}$$

Then, (3.3.21) may be written as

$$E[\epsilon_i^2] = (h_1^2 + h_2^2)\, E[\epsilon_i^2] + \frac{2h_1^2h_2}{1 - h_2}\, E[\epsilon_i^2] + E[n_i^2] \tag{3.3.24}$$

or,

$$E[\epsilon_i^2] = \frac{E[n_i^2]}{1 - (h_1^2 + h_2^2) - \frac{2h_1^2 h_2}{1 - h_2}} \tag{3.3.25}$$

Suppose that we shall use the optimal predictor. Using (2.4.52) in Chapter II and assuming that $\bar{R} >> 1$,

$$\rho_1 = h_1 + h_2 \rho_1 \tag{3.3.26}$$

$$\rho_2 = h_1 \rho_1 + \rho_2 \tag{3.3.27}$$

Thus, h_1 and h_2 can be solved to give

$$h_1 = \frac{\rho_1 (1 - \rho_2)}{1 - \rho_1^2} \tag{3.3.28}$$

and

$$h_2 = \frac{\rho_2 - \rho_1^2}{1 - \rho_1^2} \tag{3.3.29}$$

Substitutting in (3.3.25), it simplifies to

$$E[\epsilon_i^2] = \frac{(1 - \rho_1^2)}{1 - 2\rho_1^2 - \rho_2^2 + 2\rho_1^2 \rho_2} E[n_i^2] \tag{3.3.30}$$

Again the channel noise is greater than that in PCM. This agrees also with the mathematical result derived in [59].

The above conclusion, however, does not imply that DPCM provides no advantage. Since channel noise in digital systems can easily be made extremely small and the degradation is usually due primarily from quantization, it is desirable

to decrease the quantization noise by k db even though the channel noise is increased by the same amount. We would like to stress again at this point that the superior performance of DPCM over PCM depends on the design being matched to the signal statistics. For the non-optimal case $(h_1 = 1)$, the digital channel errors introduce a permanent change in the d.c. level of $\hat{x}_i'$ which will then execute an unrestricted random walk until the output saturates. Whereas for the optimal system, the prediction is essentially a delay in series with an attenuator. Hence, the effect of transmission error decays exponentially and no random walk is executed.

We may write the total r.m.s. error in the one-sample optimal system as

$$\text{r.m.s. error} = \left[\frac{1}{12 \cdot 2^{2k}} (1 - \rho_1^2) + \frac{P_B}{3} \left(1 - \frac{1}{2^{2k}}\right) \frac{1}{1 - \rho_1^2}\right]^{\frac{1}{2}} \tag{3.3.31}$$

This is plotted for typical values of ρ_1 and k in Figs. 3.3.2 and 3.3.3 together with that for PCM for a comparison.

3.3.3 Bit Compression

It can be seen from the plot in Fig. 3.3.2 that at low probability of bit error, the r.m.s. error is reduced significantly from that of PCM. Thus, we can redesign the DPCM system, neglecting channel noise, so that the number of bits required to represent each sample is reduced while maintaining the same r.m.s. error as that in PCM.

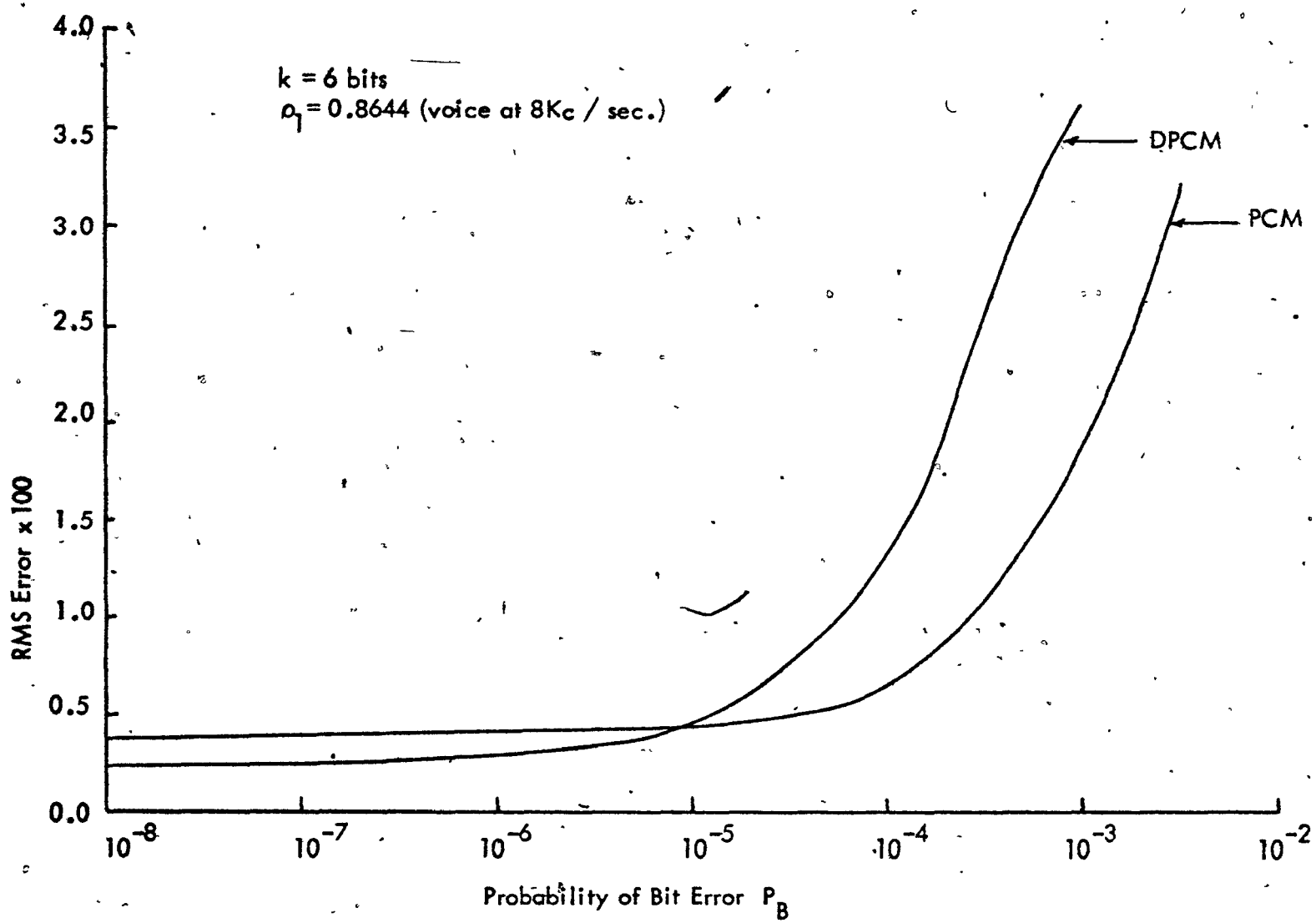
k = 6 bits
ρ_1 = 0.8644 (voice at 8Kc / sec.)
DPCM
PCM
RMS Error x 100
4.0
3.5
3.0
2.5
2.0
1.5
1.0
0.5
0.0
10^{-8}
10^{-7}
10^{-6}
10^{-5}
10^{-4}
10^{-3}
10^{-2}
Probability of Bit Error P_B

FIGURE 3.3,2

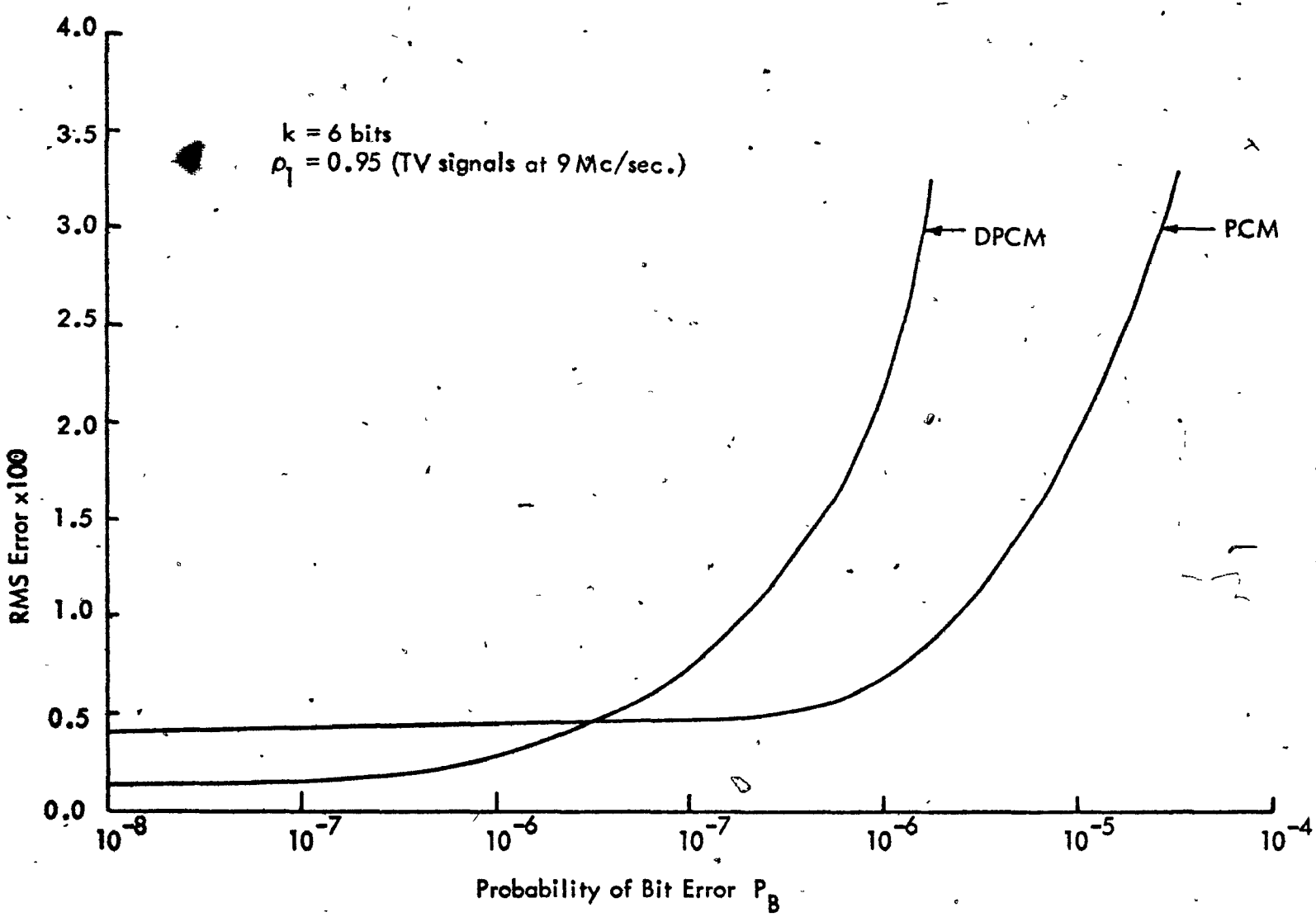
k = 6 bits
ρ_1 = 0.95 (TV signals at 9 Mc/sec.)
DPCM
PCM
RMS Error x100
4.0
3.5
3.0
2.5
2.0
1.5
1.0
0.5
0.0
10^{-8}
10^{-7}
10^{-6}
10^{-7}
10^{-6}
10^{-5}
10^{-4}
Probability of Bit Error P_B

FIGURE 3.3.3

Suppose we limit ourselves only to quantization noise.

$$\text{S/N ratio improvement} \Big|_{1\ \text{sample}} = \frac{1}{1-\rho_1^2}$$

$$= 10 \log_{10} \frac{1}{1-\rho_1^2} \quad \text{db} \tag{3.3.32}$$

For $\rho_1 = 0.8644$ (particular example given for voice in [57]), then

$$\text{S/N ratio improvement} = 3.95 \quad \text{, or}$$

$$\simeq 6 \text{ db.}$$

If we wish to reduce the bit rate instead, we let the quantization noise of the DPCM system equal to that in PCM system. Define M to be number of bits per sample for PCM system and M' to be number of bits per sample for DPCM system. We may write

$$K_{PCM} \frac{\sigma^2}{2^{2M}} = K_{DPCM} \frac{\sigma'^2}{2^{2M'}} \tag{3.3.33}$$

where σ^2 and σ'^2 are the variance of the input signal to the quantizer for PCM and DPCM, respectively, and K_{PCM} and K_{DPCM} are constants denoting the consequence of scaling.

Let $K_{DPCM} = K_{PCM}$, then

$$M' = M + \frac{1}{2} \log_2 \left(\frac{\sigma'}{\sigma}\right)^2 \tag{3.3.34}$$

where $\left(\frac{\sigma'}{\sigma}\right)^2 = \frac{E(z_i^2)}{E(x_i^2)} = 1 - \rho_1^2$ as derived before for a one-sample feedback case.

For $\rho_1 = 0.8644$, $M = 7$ bits,

$$M' \simeq 6 \text{ bits}$$

Thus approximately 1 bit per sample is saved for this system.

For TV signals sampled at 9 Mc/sec, ρ_1 is typically 0.95. [61] In that case S/N ratio improvement is approximately 12 db, and about 2 bits per sample can be saved by used DPCM. Fig. 3.3.4 shows the r.m.s. error for different quantizer levels.

The performance could be improved by using variable length coding schemes to encode the signal before transmission. Since the probability density of the signal levels is uniform, the average number of bits required for their representation can be reduced by using variable-length coders such as the Huffman Coder [91]. It was shown [66], that 3 bit DPCM can be reduced to 2.28 bits per picture element for a particular example. The drawback in using variable length coding is that of buffer requirment and the delay in transmission introduced from buffering.

The bit compression ratio can be derived as follows :

$$M' = M + \frac{1}{2}\log_2\left(\frac{\sigma'}{\sigma}\right)^2$$

The bit compression ratio is

$$C_B = \frac{M}{M'} = \frac{M}{M + \frac{1}{2}\log_2\left(\frac{\sigma'}{\sigma}\right)^2}$$

$$= \frac{1}{1 + \frac{1}{2M}\log_2\left(\frac{\sigma'}{\sigma}\right)^2} \qquad (3.3.35)$$

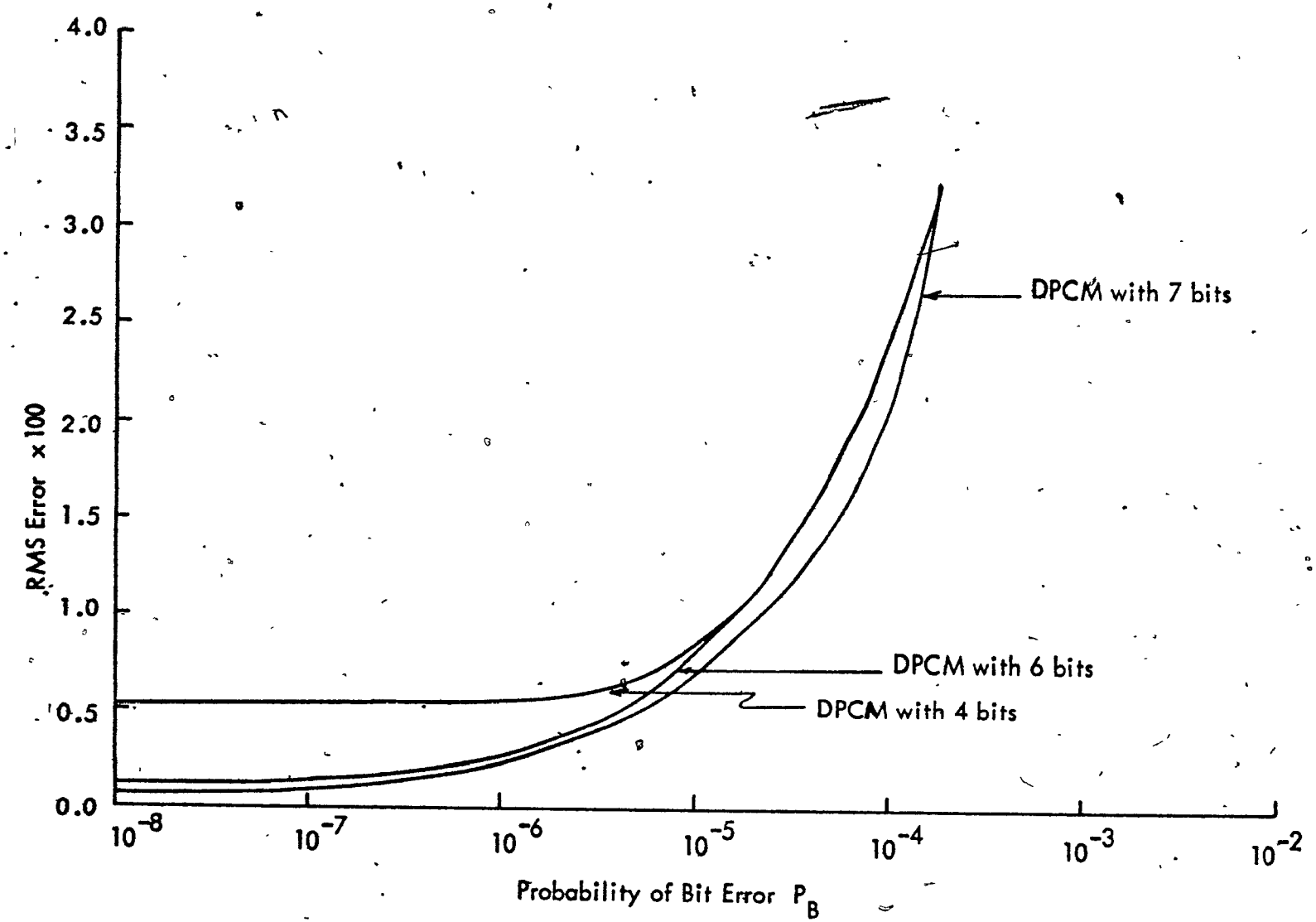
4.0
3.5
3.0
2.5
2.0
1.5
1.0
0.5
0.0
RMS Error x 100
DPCM with 7 bits
DPCM with 6 bits
DPCM with 4 bits
10^{-8}
10^{-7}
10^{-6}
10^{-5}
10^{-4}
10^{-3}
10^{-2}
Probability of Bit Error P_B

FIGURE 3.3.4

3.4 Fourier Transform Coding : Effect of Errors and Bit Compression

We have mentioned before that an attractive feature of transform coding method is its immunity to channel errors. Each of the reconstructed samples is a weighted sum of all points in the spatial frequency domain. Thus, an error in a particular sample affects all the reconstructed samples slightly instead of a big error in one sample. The human eye is sensitive to the large errors instead of small averaged-out errors, resulting in a noise immunity property. We shall consider the one-dimensional Fourier transform to illustrate the situation. Fig. 3.4.1 is a block diagram representation of a Fast Fourier Transform (FFT) coding system [92]. One-dimensional transform consists of scanning the picture and blocks of N samples are coded each time.

Let us denote $\underline{s}$ and $\underline{f}$ as the sample vector and the transform vector, respectively, and F_N be an Nth order Fourier transform matrix. We can write

$$\underline{f} = F_N \underline{s} \tag{3.4.1}$$

s_i and f_i $(i = 0, \ldots, N-1)$ are the elements of the two vectors. The discrete Fourier transform and its inverse are expressed as

$$f_i = \sum_{k=0}^{N-1} s_k W^{ik} \qquad (i = 0, 1, \ldots, N-1) \tag{3.4.2}$$

$$s_k = \frac{1}{N} \sum_{i=0}^{N-1} f_i W^{-ik} \qquad (k = 0, 1, \ldots, N-1) \tag{3.4.3}$$

where

$$W = e^{i\frac{2\pi}{N}} \quad , \; i = \sqrt{-1} \tag{3.4.4}$$

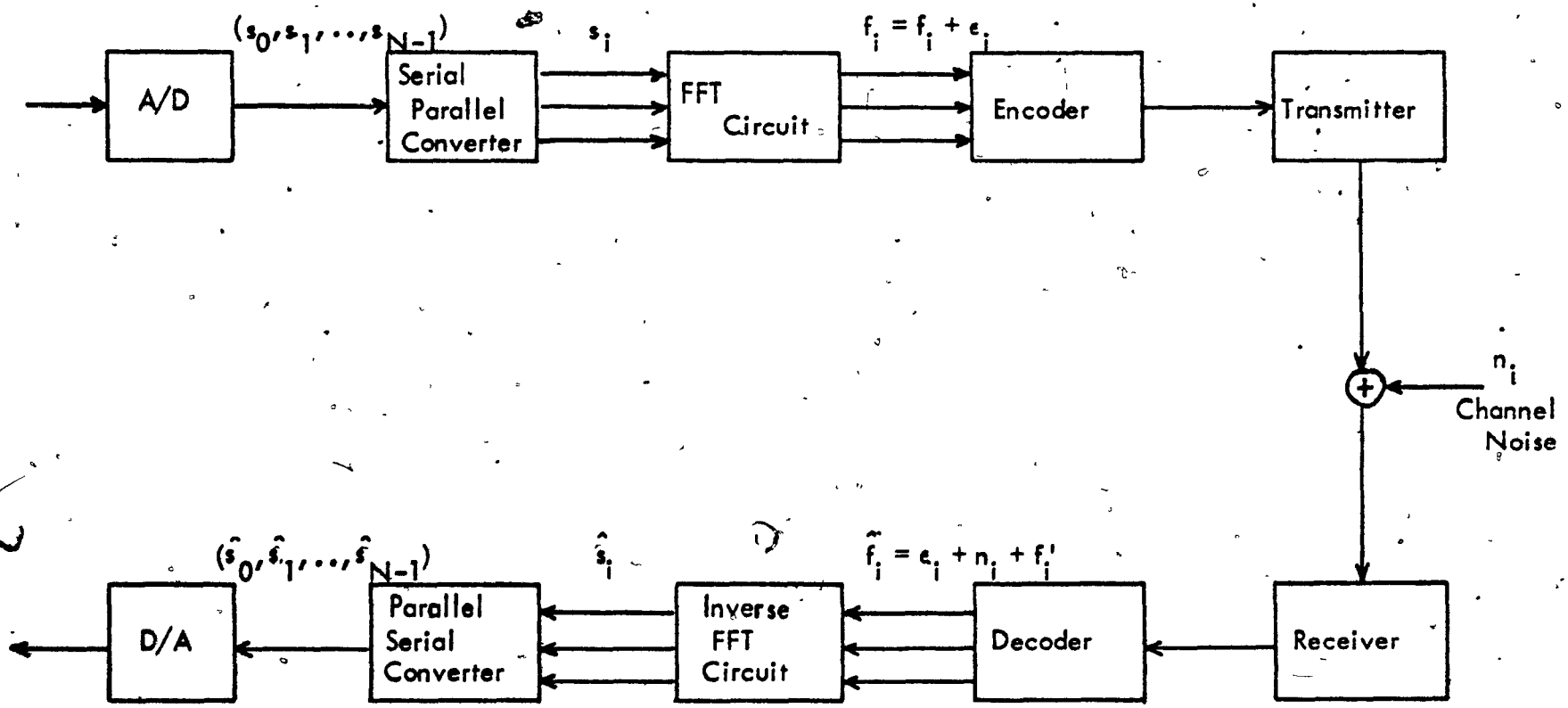

FIGURE 3.4.1 ; BLOCK DIAGRAM OF A FFT CODING SYSTEM

In general, $\{f\}$ is a complex-valued sequence although $\{s\}$ is real. We shall express $\{f\}$ as a real sequence $\{f'\}$ as follows :

$$f_0 = \sum_{k=0}^{N-1} s_k \tag{3.4.5}$$

is pure real because s_k's are real.

$$f_{\frac{N}{2}} = \sum_{k=0}^{N-1} s_k e^{ik\pi}$$

$$= \sum_{k=0}^{N-1} s_k (-1)^k \tag{3.4.6}$$

is also real.

$$f_{N-i} = \sum_{k=0}^{N-1} s_k e^{i\left[(Nk - jk)\frac{2\pi}{N}\right]}$$

$$= \sum_{k=0}^{N-1} s_k e^{i2\pi k} e^{-i(jk\frac{2\pi}{N})}$$

$$= \left\{\sum_{k=0}^{N-1} s_k e^{i(jk\frac{2\pi}{N})}\right\}^*$$

$$= f_i^* \qquad (j = 1, 2, \ldots, \frac{N}{2} - 1) \tag{3.4.7}$$

where $\{*\}$ denotes the complex conjugate. Therefore,

$$s_k = \frac{1}{N}\left[f_0 + f_{\frac{N}{2}} e^{-i(k\pi)} + \sum_{j=1}^{\frac{N}{2}-1} f_j e^{-i(jk\frac{2\pi}{N})}\right]$$

$$+ \sum_{j=1}^{\frac{N}{2}-1} f_j^* \, e^{-i(N-j)k\frac{2\pi}{N}} \Bigg]$$

But,

$$f_{N-j} \, e^{-i(N-j)k\frac{2\pi}{N}} = f_j^* \, e^{-i(N-j)k\frac{2\pi}{N}}$$

$$= f_j^* \, e^{ijk\frac{2\pi}{N}} = \left[f_j \, e^{-ikj\frac{2\pi}{N}} \right]^* \tag{3.4.8}$$

Hence,

$$s_k = \frac{1}{N} \left\{ f_0 + f_{\frac{N}{2}} (-1)^k + 2 \sum_{j=1}^{\frac{N}{2}-1} \mathrm{Re}\, [f_j \, e^{ijk\frac{2\pi}{N}}] \right\} \tag{3.4.9}$$

Where Re [ ] means the real part of. Let us define the following elements of the vector $\underline{f}'$ by

$$\begin{aligned} f_0' &= f_0 \\ f_{2j-1}' &= \mathrm{Re}\,[f_j] \\ f_{2j}' &= \mathrm{Im}\,[f_j] \\ f_{N-1}' &= f_{\frac{N}{2}} \qquad (j = 1, 2, \ldots, \tfrac{N}{2}-1) \end{aligned} \tag{3.4.10}$$

Then,

$$s_k = \frac{1}{N} \left\{ f_0' + (-1)^k f_{N-1}' + 2 \sum_{j=1}^{\frac{N}{2}-1} [f_{2j-1}' \cos(jk\tfrac{2\pi}{N}) + f_{2j}' \sin(jk\tfrac{2\pi}{N})] \right\} \tag{3.4.11}$$

Therefore, one can transmit the real-valued sequence $\{f'\}$ over the channel and get the reconstructed signal at the receiver by using the operation (3.4.11). The reconstructed signal differs from the original one due to quantization noise and channel noise.

Let $\underline{\epsilon}$ be the quantization noise vector, $\underline{n}$ be the channel noise vector, $\underline{f'}$ be the exact tranform vector. The received sequence $\underline{\hat{f}}$ is given by

$$\underline{\hat{f}} = \underline{f'} + \underline{\epsilon} + \underline{n}$$

and

$$\begin{aligned} \underline{\hat{s}} &= \text{reconstructed signal} \\ &= F^{-1}\{\hat{f}\} \\ &= F^{-1}\{\underline{f'} + \underline{\epsilon} + \underline{n}\} \end{aligned} \tag{3.4.12}$$

Where F^{-1} is the inverse FFT operator. Since FT operation is linear,

$$\begin{aligned} \underline{\hat{s}} &= F^{-1}\{f'\} + F^{-1}\{\underline{\epsilon}\} + F^{-1}\{\underline{n}\} \\ &= \underline{s} + F^{-1}\{\underline{\epsilon}\} + F^{-1}\{\underline{n}\} \end{aligned} \tag{3.4.13}$$

Therefore, the error in the reconstucted signal is

$$\underline{e} = \underline{\hat{s}} - \underline{s} = F^{-1}\{\underline{\epsilon}\} + F^{-1}\{\underline{n}\} \tag{3.4.14}$$

We shall consider quantization noise first. The same development applies to channel noise.

3.4.1 Quantization Noise [92]

Consider the kth term in the quantization error sequence. From 3.4.11),

$$e_k = \frac{1}{N}\left\{\epsilon_0 + (-1)^k \epsilon_{N-1} + 2\sum_{i=0}^{\frac{N}{2}-1}\left[\epsilon_{2i-1}\cos(ik\frac{2\pi}{N}) + \epsilon_{2i}\sin(ik\frac{2\pi}{N})\right]\right\} \tag{3.4.15}$$

Since each e_k is equally likely, the mean square quantization error in the reconstructed signal is

$$\overline{e^2} = \frac{1}{N}\sum_{k=0}^{N-1}\overline{e_k^2} \tag{3.4.16}$$

$\overline{e_k^2}$ can be written as

$$\overline{e_k^2} = \frac{1}{N^2}\left\{\overline{\epsilon_0^2} + \overline{\epsilon_{N-1}^2} + 4\sum_{i=1}^{\frac{N}{2}-1}\left[\overline{\epsilon_{2i-1}^2\cos^2(ik\frac{2\pi}{N})} + \overline{\epsilon_{2i}^2\sin^2(ik\frac{2\pi}{N})}\right]\right\} \tag{3.4.17}$$

where we have assumed that the error samples are uncorrelated. Therefore,

$$\overline{\epsilon^2} = \frac{1}{N^2}\left\{\overline{\epsilon_0^2} + \overline{\epsilon_{N-1}^2} + \frac{4}{N}\sum_{k=0}^{N-1}\sum_{i=1}^{\frac{N}{2}-1}\left[\overline{\epsilon_{2i-1}^2\cos^2(ik\frac{2\pi}{N})} + \overline{\epsilon_{2i}^2\sin^2(ik\frac{2\pi}{N})}\right]\right\}$$

$$= \frac{1}{N^2}\left\{\overline{\epsilon_0^2} + \overline{\epsilon_{N-1}^2} + \frac{4}{N}\left[\sum_{i=1}^{\frac{N}{2}-1}\overline{\epsilon_{2i-1}^2}\sum_{k=0}^{N-1}\cos^2(ik\frac{2\pi}{N}) + \sum_{i=1}^{\frac{N}{2}-1}\overline{\epsilon_{2i}^2}\sum_{k=0}^{N-1}\sin^2(ik\frac{2\pi}{N})\right]\right\} \tag{3.4.18}$$

It can be shown that [93], after some manipulation,

$$\sum_{k=0}^{N-1} \cos^2 (jk \frac{2\pi}{N}) = \sum_{k=0}^{N-1} \sin^2 (jk \frac{2\pi}{N}) = \frac{N}{2} \tag{3.4.19}$$

Equation (3.4.18) becomes

$$\overline{e^2} = \frac{1}{N^2} \left\{ \overline{\epsilon_0^2} + \overline{\epsilon_{N-1}^2} + 2 \sum_{i=1}^{\frac{N}{2}-1} \left[\overline{\epsilon_{2i-1}^2} + \overline{\epsilon_{2i}^2} \right] \right\} \tag{3.4.20}$$

If the jth sample is coded with k_i bits, the quantization error in the jth sample is given by

$$\overline{\epsilon_i^2} = K_i \frac{\sigma_i'^2}{2^{2k_i}} \tag{3.4.21}$$

where $\sigma_i'^2$ is the variance of the jth coefficient f_i', and K_i is a constant expressing the effect of scaling and companding. Hence, by assuming all K_i equal to K

$$\overline{e^2} = \frac{K}{N^2} \left\{ \frac{\sigma_0'^2}{2^{2k_0}} + \frac{\sigma_{N-1}'^2}{2^{2k_{N-1}}} + 2 \sum_{i=0}^{\frac{N}{2}-1} \left[\frac{\sigma_{2i-1}'^2}{2^{2k_{2i-1}}} + \frac{\sigma_{2i}'^2}{2^{2k_{2i}}} \right] \right\} \tag{3.4.22}$$

This expression gives the quantization error in the system. It has been shown [94] that this quantity is a minimum when the contributions of all the terms in (3.4.22) are equal while keeping the bit rate equal to that of PCM transmission.

3.4.2 Channel Noise

Suppose that each of the coefficients are encoded with the same number of bits as in PCM system and denote this number by M. Then each of the

coefficients are equally likely to make an error. We can apply (3.4.20) to evaluate the channel noise. Let σ_N^2 denote the channel noise power. Then the m.s. channel noise in a FFT system is

$$\begin{aligned} \overline{e_n^2} &= \frac{1}{N^2}\left\{\overline{n_0^2} + \overline{n_{N-1}^2} + 2\sum_{i=1}^{\frac{N}{2}-1}\left[\overline{n_{2i-1}^2} + \overline{n_{2i}^2}\right]\right\} \\ &= \frac{1}{N^2}\left\{\sigma_N^2 + \sigma_N^2 + 2(N-2)\,\sigma_N^2\right\} \\ &= \frac{2(N-1)\,\sigma_N^2}{N^2} \end{aligned} \tag{3.4.23}$$

where

$$\sigma_N^2 = \frac{P_B}{3}\left(1 - \frac{1}{2^{2M}}\right) \tag{3.4.24}$$

Thus if the same bit rate as PCM is used, the m.s. channel error in a Fourier transform encoding is reduced from the corresponding value in PCM by a factor of $2(N-1)/N^2$. However, the quantization error in this case is given by

$$\overline{\epsilon_i^2} = K_i \frac{\sigma_i'^2}{2^{2M}} \tag{3.4.25}$$

and (3.4.20), and it would not be a minimum since now the contribution from each term may be different.

If the coefficients are encoded according to the following rule [95] by equating the quantization noise to that of PCM system,

$$k_i = M + \frac{1}{2} \log_2 \left(\frac{\sigma_i'^2}{N\sigma^2} \right) \tag{3.4.26}$$

where σ^2 is the signal power, then we can achieve reduction in bit rate. The m.s. channel error in this case is different from (3.4.23) and is not easy to compute. However, the inherent property of Fourier transform distributes the error evenly over all samples rather than localized on one particular sample. This makes the noise behave like a low frequency noise structure which is not as annoying to the human eye as the high frequency "salt and pepper" pattern caused by the localised errors. This aspect has been discussed and demonstrated by experimental evidence [75]. For high error channels, error-correcting codes have been found to improve the performance significantly.

3.3.3 Bit Compression

Suppose that the jth coefficient is coded with k_i bits. The total m.s. quantization error is given by

$$\sum_{i=0}^{N-1} K_i \frac{\sigma_i'^2}{2^{2k_i}} \tag{3.4.27}$$

If each term has the same contribution, the quantization error is a minimum. If we constraint this to equal the quantization noise for the PCM case, then each must equal ϵ^2_{PCM}/N. We may write

$$\overline{\epsilon_i^2} = \frac{1}{N} \overline{\epsilon^2_{PCM}} \tag{3.4.28}$$

and,

$$k_i = M + \frac{1}{2} \log_2 \left(N \frac{K_i}{K_{PCM}}\right) + \log_2 \left(\frac{\sigma_i'}{N\sigma}\right) \tag{3.4.29}$$

Assume that the scaling factor $K_i' = K_{PCM}$, then

$$k_i = M + \frac{1}{2} \log_2 \left(\frac{\sigma_i'^2}{N\sigma^2}\right) \tag{3.4.30}$$

The nearest integer of k_i is the number of bits used to code the jth coefficient. If this method is to reduce the bit-rate, it is necessary that the average bit assignment be less than M, i.e.

$$\frac{1}{N} \sum_{i=0}^{N-1} k_i < M \tag{3.4.31}$$

Due to the lack of data for video signals, an example for 56 Kbits/sec. (voice) PCM is used for illustration [95]. $N = 16$ and $\sigma = 1024$. This is shown in Table I. A comparison of the PCM, DPCM and transform methods are given in Table II.

FOURIER TRANSFORM (N = 16) $\sigma = 1024$.

$R_{PCM} = 56$ k bits/sec.

i	$\frac{\sigma_i}{N}$	$\frac{\sigma_i}{N\sigma}$	k_i
0	336	0.328	7
1	544	0.530	8
2	548	0.540	8
3	306	0.298	7
4	352	0.343	7
5	162	0.158	6
6	181	0.176	6
7	118	0.115	6
8	119	0.116	6
9	106	0.103	5
10	90	0.088	5
11	81	0.079	5
12	46	0.045	4
13	76	0.074	4
14	23	0.023	4
15	51	0.050	4

Total bits	92
R_o k bits/sec.	46.0
Bit rate reduction =	10 k bits/sec.

TABLE I : EXAMPLE OF BIT-RATE REDUCTION [95]

	PCM	DPCM	2 - d TRANSFORM (N^{th} order)			1 - d TRANSFORM (N)		
			K.L.	H.T.	F.T.	K.L.	H.T.	F.T.
No. of bits/pel to obtain approximately the same quantity of a particular picture	8	3	2	2	2	2.3	2.3	2.3
Sensitivity to picture-to-picture variation	none	large	moderate	small	small	moderate	small	small
Delay	none	1 sample on 1 line	N lines			1 line		
Complexity	very simple	simple	complicated	moderate	moderate	complicated	moderate	moderate
Cost of coding	small	small	large	moderate	large	large	moderate	large

TABLE II : COMPARISON OF PCM, DPCM AND TRANSFORM CODING

CHAPTER IV

IMAGE RECONSTRUCTION BY INTERPOLATION

4.1 Contouring Effect

The transmission of digital signals through PCM has been used for more than one decade. The extension to TV signals has also been investigated. One of the difficulties encountered is in the choice of the number of quantization levels. Experiments have shown that a seven-bit encoder is good enough for all black and white pictures. A six-bit encoder is just sufficient to produced fair pictures. A five-bit encoder allows proper reproduction of half-tone pictures but introduces false contours [96]. This effect is due to the small number of quantization levels used and the sensitivity of the eye to sharp variations in the brightness. The encoder has to make a decision as to where to switch between the two successive levels when the brightness of the image is progressively changing. The decision line appears as a contour on the reconstructed image.

The zero-order-predictor which we have considered in Chapter II (2.4.1) operates by looking for those parts of the images where the brightness is constant and transmitting only the location of the transition. Hence, it transmits the position of the contours.

Previous experiments have shown that most observers are unable to distinguish more than eight to ten half-tones between full black and full white. Therefore, a four-bit encoder should be more than sufficient if one could neglect the contouring effect. However, even for a five-bit quantizer, this effect is still

very significant. It becomes imperceptible for a seven-bit encoder. It is obvious, however, that the number of contours increases and the distance between them decreases with the number of bits. Hence, the ZOP renders a higher compression ratio if the number of bits used is small.

4.2 Reduction of Contouring Effect

Basically there are two methods which can combat the effect of contours.

(1) Pseudo-Random Noise

This technique has been suggested by Roberts [40]. A "noise" is superimposed to the analog signal before encoding. The noise has a uniform distribution over the range between two successive levels and has the effect of breaking up the contours. Experiments have been performed and are found to be successful [55], [56]. The only disadvantage of this technique is slight degradation of the picture quality due to the increase in background noise. Well-designed dither patterns improve the result.

(2) Interpolation

In most images, the brightness varies progressively between levels. Hence, a linear interpolation should resemble the original signal quite well. In

essence, the method replaces a step jump by a ramp function which has a low and unnoticeable slope. This has the effect of replacing the contour by a low frequency structure which is less objectionable to the eye.

The interpolation starts before the transition and depends on the value of the transition before triggering the interpolator. A transmission delay results and memorizing of at least one line is necessary.

The above technique is suggested in [96] and no published analysis or experimental work has been done at this time although some people in the Bell Northern Research Institute are considering a simulation. We shall present an error analysis of the interpolation process for three algorithms in the next section.

The transmitting part of the system contains only the zero-order-predictor followed by a run length encoder, while at the receiver, an interpolating equipment is implemented together with the decoder. The operation of the system is as follows: The image is encoded with five-bits per sample (thus without the interpolation the contouring effect is still quite significant). At the receiver, the interpolator reconstructs the signal by drawing a straight line according to the predesigned algorithms, which aim at suppressing the contouring effect. We assume that with the present day technology, generation of points at very fine quantized values are possible. Thus the operation is equivalent to creating additional bits per sample to those portions of the signal. These operations must be performed at the sampling rate (10 Mc/sec. for conventional TV).

If the interpolation succeeds in reducing contouring effect, bit rate reduction is possible. A bit compression ratio of about five comparing with conventional PCM TV transmission is predicted [96]

4.3 Analysis of the Interpolation Process

It is obvious that some error is introduced by interpolating across the contour. The amount of this error in the root mean square sense depends on the particular algorithm chosen to implement the process.

Suppose that x is the original signal, $\hat{x}$ is the quantized version of the signal (the same signal is obtained after decoding if we assume error-free transmission), and x_i is the interpolated signal. Let e_i be the error introduced by the interpolation process. The m.s. error is

$$E[(x-x_i)^2] = E\{[x-(\hat{x}+e_i)]^2\}$$

$$= E[(x-\hat{x})^2] + E[e_i^2] \qquad (4.3.1)$$

where we have assumed that e_i and $(x-\hat{x})$ are uncorrelated. But $E[(x-\hat{x})^2]$ is the quantization error present in the system even if there is no interpolation. Thus $E[e_i^2]$ is the m.s. error introduced by the interpolation process.

We shall make the following assumptions (1). The signal process $\hat{x}$ is Markov, hence the increments are independent; (2) The difference in levels is a random variable of a stationary process and is independent of the run-length distribution;

(3) The process is bounded; (4) The random step function model as described in Chapter II is assumed.

The interpolation detects the contours whose transition is unity (for higher transitions, no interpolation is performed since in most cases they are real contours). It evaluates the size of the transition and selects the up or down mode for the interplator and follows the algorithm selected.

For our analysis, we shall assume that interpolation is only triggered if two consecutive runs are at least three with a unity transition in between. Such a choice is intuitively reasonable. We shall derive the probability that the interpolation is being triggered.

According the the above description,

$$\Pr(\text{interpolation}) = \Pr(\text{run-length} \geq 3;\ \text{transition} = 1 \text{ unit},\ \text{run length} \geq 3) \tag{4.3.2}$$

Fig. 4.3.1 shows such a situation.

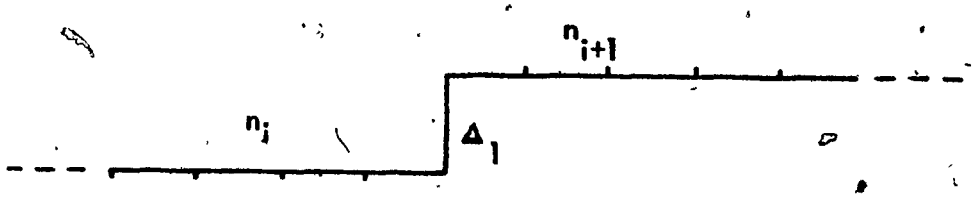

FIGURE 4.3.1 SITUATION WHEN INTERPOLATION IS BEING TRIGGERED

With the notations shown in Fig. 4.3.1, the probability of interpolation is $Pr\,(n_i \geq 3,\ \Delta_1 = 1 \text{ unit}, n_{i+1} \geq 3)$. Since the jump in level is independent of the run lengths,

$$Pr\,(n_i \geq 3,\ \Delta_1 = 1 \text{ unit},\ n_{i+1} \geq 3) = Pr\,(n_i \geq 3,\ n_{i+1} \geq 3)\ Pr\,(\Delta_1 = 1 \text{ unit}) \tag{4.3.3}$$

Also the run-lengths are independent. Therefore, we have probability of interpolation $= [Pr\,(n_i \geq 3)]^2\ Pr\,(\Delta_1 = 1 \text{ unit})$ (4.3.4)

Let p denote the probability of a jump in level. Thus the probability that level remains the same as the previous one is $(1-p)$. Hence, the probability of obtaining a run of three is $p\,(1-p)^2$, where we have assumed the stationary property of the incremental process.

Thus, the probability of run of at least three is

$$p\,(1-p)^2 + p\,(1-p)^3 + \ldots + p\,(1-p)^{T-1} \tag{4.3.5}$$

where T is the maximum run length. Hence,

$$\begin{aligned}
[\,Pr\,(n_i \geq 3)\,]^2 &= [p\,(1-p)^2 + p\,(1-p)^3 + \ldots + p\,(1-p)^{T-1}\,]^2 \\
&= p^2\,[(1-p)^2 + (1-p)^3 + \ldots + (1-p)^{T-1}\,]^2 \\
&= p^2\,(1-p)^4\,\left[\frac{1-(1-p)^{T-2}}{1-(1-p)}\right]^2 \\
&= (1-p)^4\,[1-(1-p)^{T-2}\,]^2
\end{aligned} \tag{4.3.6}$$

Thus the probability that interpolation is performed is given by

$$(1-p)^4 [1-(1-p)^{T-2}]^2 \times Pr(\Delta_1 = 1 \text{ unit}) \tag{4.3.7}$$

Typical values are $p = 0.2$, $T = 32$ and $Pr(\Delta_1 = 1 \text{ unit}) = 0.15$. Hence, $Pr(\text{interpolation}) \simeq 0.06144$.

We shall next derive the m.s. error introduced by three different algorithms.

(1) Suppose we interpolate by constructing a straight line between 1 sample before and 1 sample after the contour as shown in Fig. 4.3.2, independent of the size of the run lengths.

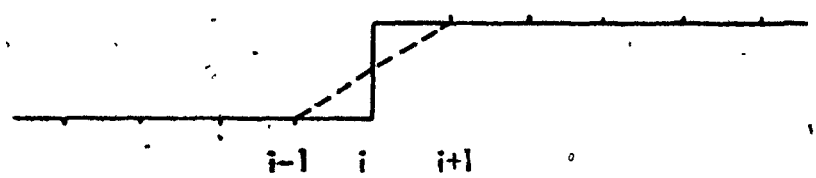

FIGURE 4.3.2 . ALGORITHM 1

Let Δ denote the size of 1 unit jump. Then, error in the ith sample is $\frac{\Delta}{2}$. The m.s. error is

$$\text{m.s.e.} = E[e_i^2] = \sum_{l=3}^{T} e_i^2 [Pr(n_i = l)]^2 Pr(\Delta) \tag{4.3.8}$$

Since the present algorithm constructs the straight line independently of the run-lengths, e_i^2 is a constant equal to $(\frac{\Delta}{2})^2$. Thus,

$$\text{m.s.e.} = \frac{\Delta^2}{4} \cdot \sum_{l=3}^{T} [\Pr(n_i = l)]^2 \Pr(\Delta)$$

$$= \frac{\Delta^2}{4} \cdot \Pr(\text{interpolation})$$

$$= (1-p)^4 [1-(1-p)^{T-2}]^2 \frac{\Delta^2}{4} \times \Pr(\Delta) \qquad (4.3.9)$$

If we assume that there is no aperature error in the zero order predictor, then Δ has the size of 1 quantum step equal to $\frac{1}{2^k}$ where 2^k is the number of quantizer levels.

For $p = 0.2$; $T = 32$, $k = 5$ and $\Pr(\Delta) = 0.15$,

$$\text{m.s.e.} \simeq \frac{0.06144}{4} \times \frac{1}{2^{10}} \simeq 0.01536 \times \frac{1}{2^{10}}$$

$$\text{r.m.s. error} \simeq 0.00388$$

The quantization error is the system is $\frac{1}{12^{2k}}$ and the

$$\text{r.m.s. value} \simeq \underline{0.00902}$$

Interplation error is about 40% of the quantization error, which is acceptable if it succeeds in suppressing the contouring effect.

(2) Suppose that we now change our interpolation algorithm such that the reconstructed line is dependent on the run-lengths n_i and n_2 as denoted in Fig. 4.3.3.

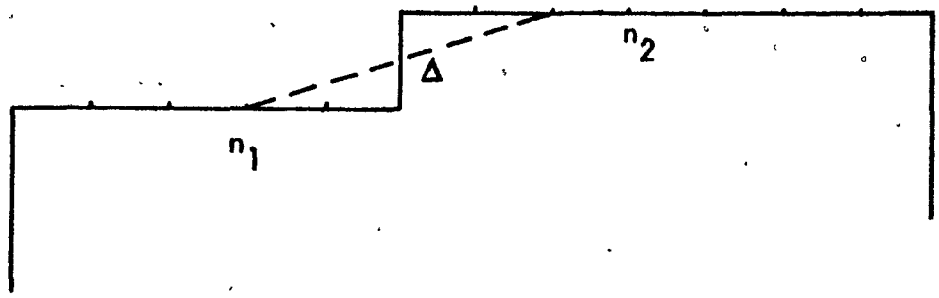

FIGURE 4.3.3 ALGORITHM 2

The shorter of the two runs is determined. Suppose that n_1 is smaller than n_2. Let $\bar{n}$ equal to $[\frac{n_1}{2}]$ where $[x]$ denotes the integral part of x. Start interpolation from $[\frac{n_1}{2}]$ back from contour to $[\frac{n_1}{2}]$ after the contour using linear interpolation. It is obvious that for all cases the interpolation cuts the contour at the half point. As an example, suppose $n_1 = 5$, $n_2 = 7$. Then n_1 is chosen and $\bar{n} = [\frac{5}{2}] = 2$. Thus the interpolator would start at 2 samples back from the contour and end at 2 samples after the contour.

Let

$$\bar{n} = [\frac{n_1}{2}] \text{ or } [\frac{n_2}{2}] \tag{4.3.10}$$

The probability of a run of n_1 followed by a run of n_2 with one unit jump in between is

$$[p(1-p)^{n_1-1}][p(1-p)^{n_2-1}] \times Pr(\Delta) \tag{4.3.11}$$

The square error made in this case is

$$\{ [(\frac{1}{2\bar{n}})^2 + (\frac{2}{2\bar{n}})^2 + \ldots + \frac{(\bar{n}-1)^2}{(2\bar{n})^2}] + (\frac{1}{2})^2 \} \Delta^2 \tag{4.3.12}$$

$$= \frac{\Delta^2}{4} + \frac{2}{(2\bar{n})^2} [1^2 + 2^2 + \ldots + (\bar{n}-1)^2] \Delta^2 \tag{4.3.13}$$

$$= \frac{\Delta^2}{4} + \frac{\Delta^2}{3(2\bar{n})^2} [\bar{n}(\bar{n}-1)(2\bar{n}-1)] \tag{4.3.14}$$

Hence,

$$\text{m.s.e.} = \sum_{n_2=3}^{T} \sum_{n_1=3}^{T} p^2 (1-p)^{n_1+n_2-2} \Pr(\Delta) [\frac{1}{4} + \frac{1}{3(2\bar{n})^2} (\bar{n})(\bar{n}-1)(2\bar{n}-1)] \Delta^2 \tag{4.3.15}$$

The computer has been used to generate the result for $p = 0.2$, $\Pr(\Delta) = 0.15$, $T = 32$. The result is

$$\text{m.s.e.} = 0.0244 \times \frac{1}{2^{2k}}$$

$$\text{r.m.s.} = 0.156 \times \frac{1}{2^k}$$

For $k = 5$,

$$\text{r.m.s. error} = 0.00488$$

This algorithm offers more flexibility than the first algorithm and yet maintaining an acceptable level of the r.m.s. error

(3) Suppose that we use the following algorithm:

Let n_1 and n_2 be the run-lengths. Let $[\frac{n_1}{2}]$ and $[\frac{n_2}{2}]$ be the integral parts of $\frac{n_1}{2}$ and $\frac{n_2}{2}$, respectively. Start from $[\frac{n_1}{2}]$ samples back and interpolate till $[\frac{n_2}{2}]$ samples after the contour. As an example, $n_1 = 5$, $n_2 = 9$. Hence $[\frac{n_1}{2}] = 2$ and $[\frac{n_2}{2}] = 4$. Thus the interpolation starts from two samples back and ends at 4 samples after the contour, as shown in Fig. 4.3.4.

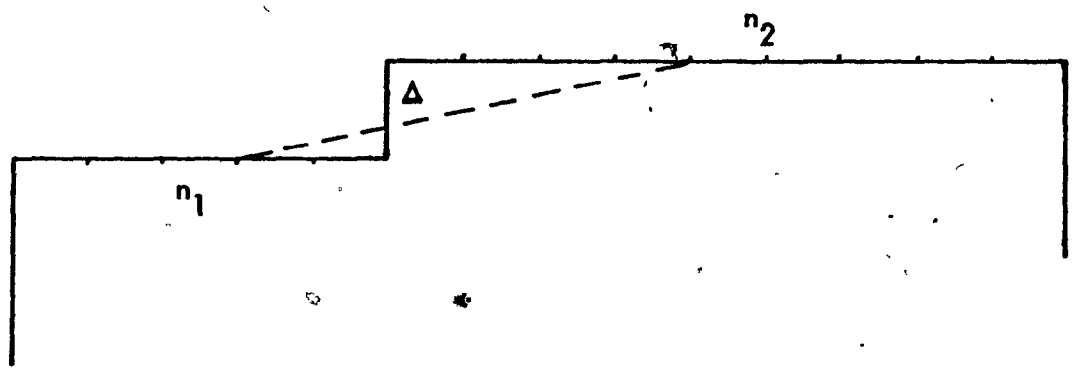

FIGURE 4.3.4 ALGORITHM 3

Let

$$n' = [\frac{n_1}{2}] + [\frac{n_2}{2}] \tag{4.3.16}$$

The square error one makes in this case is

$$e^2 = \{[(\frac{1}{n'})^2 + (\frac{2}{n'})^2 + \ldots + \frac{([\frac{n_1}{2}]-1)^2}{(n')^2}] + [(\frac{1}{n'})^2 + (\frac{2}{n'})^2 + \ldots + \frac{[\frac{n_2}{2}]^2}{(n')^2}]\}\Delta^2 \tag{4.3.17}$$

Thus the m.s.e. is

$$\sum_{n_2=3}^{T} \sum_{n_1=3}^{T} (1-p)^{n_1+n_2-2} \, p^2 \, Pr(\Delta) \, e^2 \tag{4.3.18}$$

A computer program has been written to generate the result for $p = 0.2$, $Pr(\Delta) = 0.15$, $T = 32$.

$$\text{m.s.e.} = 0.4075 \times \frac{1}{2^{2k}}$$

For $k = 5$,

$$\text{r.m.s error} = 0.638 \times \frac{1}{2^5}$$

$$= \underline{0.0199}$$

Thus the increase in r.m.s. error is quite significant. From the standpoint of r.m.s error, the second algorithm is more acceptable than this one. But, one must not forget that the sink in the system is the human observer. Hence, even though a large r.m.s. error is introduced in the third algorithm, its ability to combat contouring effect might be superior. No definite conclusion can be drawn at this point unless a subjective test is done to test the different methods.

The effect of channel errors on the zero-order predictor has been discussed in Chapter III. It is more sensitive to transmission errors like most data compression systems. But, it is possible to improve the situation by taking advantage of the line-to-line correlation. If an error is detected in a line, we simply have to repeat the previous line.

The total m.s.e. of the system can be obtained by adding the interpolation error to the system error of a run-length encoded system obtained in Chapter III, equation 3.2.28. The resulting r.m.s. error is plotted as a function of the bit error probability in Fig. 4.3.5.

4.4 Sensitivity Weighted Error

As has been pointed out before, the root-mean-square error is not the correct fidelity criterion for pictures. It has been shown that pictures which are subjectively optimal are quite different from pictures optimized in the mean square error sense. Thus one may conclude that the sensitivity function of the human eye has to be taken into consideration, resulting in the definition of the "weighted system error". It is calculated for any system by averaging the product of the power spectral density of the system error and a non-negative weighting function over a certain frequency band. The weighting function scales the power spectral density of the error so that at each frequency the contribution of the error power to the fidelity criterion depends on the sensitivity of the human observer to the picture noise at that frequency.

Suppose that the frequency response of the human visual system is $S(f)$ and the power spectral density of the noise is $G(f)$, then the weighted power is given by

$$E = \int_{-\infty}^{\infty} S(f)\, G(f)\, df \tag{4.4.1}$$

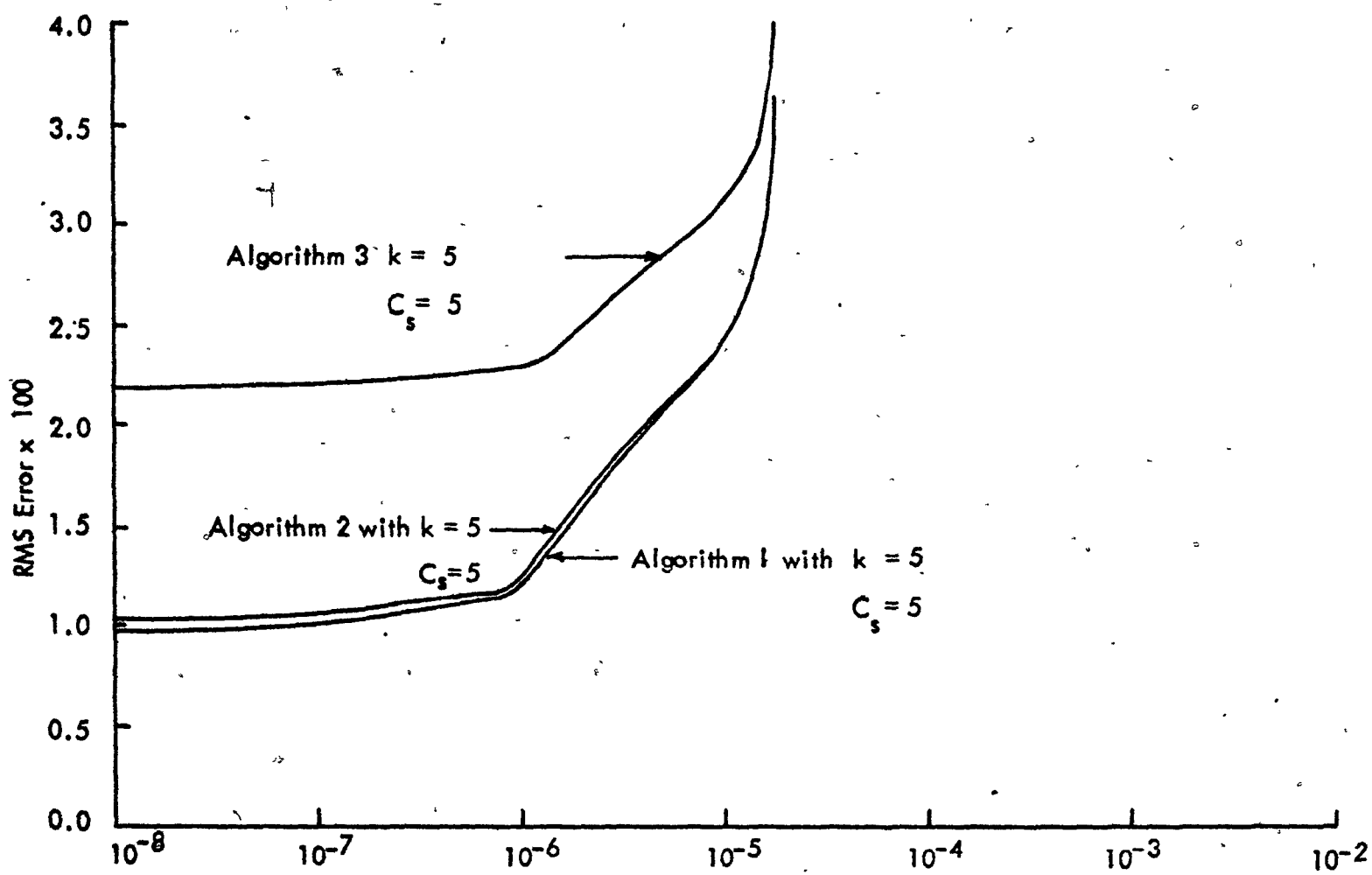

PROBABILITY OF BIT ERROR.

FIGURE 4.3.5

It may be seen that the use of interpolation replaces the contour by a a lower frequency structure. Since the sensitivity function has an attenuation effect at low frequencies, the actual weighted error power at the eye is expected to be less than the weighted error power. This corresponds to the reduction of the contouring effect in a subjective test.

CHAPTER V

CONCLUSION

Certain techniques which achieve data compression have been considered in this thesis. Chapter I introduced the significance of data compression. Three compression ratios which have been most commonly used as figures of merit for compression systems were defined. Classifications of data compression systems according to technique and their effect on the signals were given. Picture coding was discussed in Chapter II in the light of bit-rate and bandwidth reduction. Particular emphasis has been placed on zero-order prediction-run length encoded systems, DPCM systems and transform coding.

The effect of transmission errors on these systems were analysed in Chapter III. Most data compression schemes were found to be more vulnerable to transmission errors. Although well-designed DPCM systems will reduce quantization noise from the corresponding PCM system, they suffer more from channel errors than PCM. For bit error probabilities of 10^{-6} or more, the r.m.s. error of the compressed systems starts to increase almost exponentially, and is therefore unacceptable. For practical channels where $P_B < 10^{-6}$, it is possible to achieve bandwidth reduction with only a small signal degradation as compared to the uncompressed system. Transform picture coding, however, offers a certain immunity to channel errors by averaging out each error over the whole ensemble of picture elements, thus producing a less annoying effect on the eye than the "salt-and-pepper" pattern present in conventional PCM transmission. The use of transform methods in conjunction with block coding also reduces the bit rate to a level comparable to that of DPCM systems.

One could, in principle, reduce the bit rate by quantizing the signal with fewer levels. Quantization with fewer than 64 levels will introduce a contouring effect which is particularly noticeable in large areas of uniform brightness. A reconstruction algorithm using linear interpolation at the contours has been introduced in Chapter IV. Although this technique might suppress the contouring effect, it would also introduce a new source of error. Statistical analysis of this error source is presented. For certain algorithms, the r.m.s. error does not significantly differ from that of uninterpolated cases.

It was also noted that although r.m.s. error gives indications of system performance in some cases, it is not a proper criterion for most pictorial data. Because the human observer is the sink in the system, subjective evaluation of the technique is indispensable for further investigation.

REFERENCES

1. D.R. Weber, "A Synopsis on Data Compression", Proc. Nat. Tel. Conf., 1965.

2. G. Husson, "Data Compression Systems", M.Eng. Thesis, McGill U., 1970.

3. G.L. Rega, "A Unified Approach to Digital TV Compression", Proc. Nat. Tel. Conf., 1965.

4. L.D. Davisson, "The Concept of Energy Compression Ratio and Its Application to Run-length Coding", Final Report, 1966, Session of the Goddard Summer Workshop.

5. L.D. Davisson, "Information Systems", Goddard Summer Workshop Report, 1966.

6. C.M. Kortman, "Redundancy Reduction - A Practical Method of Data Compression", Proc. IEEE, vol. 55, no. 3, pp. 253-263; March 1967.

7. T.J. Lynch, "Data Compression with Error-control Coding for Space Telemetry", NASA Tech. Report, NASA TR: R-261, June 1967.

8. H. Blasbalg and R. Van Blerkom, "Message Compression", IRE Trans. on Space Electronics and Telemetry, pp. 228-238, Sept. 1962.

9. C.A. Andrews, J.M. Davies and G.R. Schwarz, "Adaptive Data Compression", Proc. IEEE, vol. 55, no. 3, pp. 267-277, March 1967.

10. H.N. Massey, "An Experimental Telemetry Data Compressor", Proc. of Nat. Tel. Conf., pp. 25-28, 1965.

11. L.W. Gardenhire, "Redundancy Reduction : the Key to Adaptive Techniques", Proc. Nat. Tel. Conf., June 1964.

12. A.V. Balakrishnan, "An Adaptive Nonlinear Data Predictor", Proc. Nat. Tel. Conf., 1962.

13. R.L. Kutz, J.A. Sciulli and R.A. Stampfl, "Adaptive Data Compression for Video Signals", Advances in Communication Systems, Academic Press, vol. 3, 1968.

14. P. Elias, "Predictive Coding - Part I", IRE Trans. on Inf. Theory, vol. IT - 1, pp. 16-33, March 1955.

15. M. Kanefsky, "Data Compression Using Bit-plane Encoding", Conference on Adaptive Telemetry, Goddard Space Flight Centre, 1967.

16. G.R. Schwarz, "Buffer Design for Data Compression Systems", IEEE Trans. on Com. Tech., vol. COM-16, August 1968.

17. J.E. Medlin, "The Prevention of Transmission Buffer Overflow in Telemetry Data Compressors", IEEE Trans. on Com. Tech., vol. COM-16, Feb. 1968.

18. L.D. Davisson, "The Theoretical Analysis of Data Compression Systems", Proc. IEEE, Feb. 1968.

19. T.S. Huang, W.F. Schreiber and O.J. Tretiak, "Image Processing", Proc. IEEE, vol. 59, no. 11, Nov. 1971.

20. W.F. Schreiber, "The Measurement of Third Order Probability Distribution of Television Signals", IRE Trans. on Inf. Theory, vol. IT-2, pp. 94-105, Sept. 1956.

21. E.R. Kretzmer, "Statistics of TV Signals", BSTJ, vol. 31, p. 763, July 1952.

22. P. Elias, "A Note on Autocorrelation and Entropy", Proc. IRE (Correspondence), vol. 39, p. 839, July 1951.

23. L.E. Franks, "A Model for the Random Video Process", BSTJ, vol. 45, no. 5, pp. 609-629, April 1966.

24. D. Estoumet, "Etude Statistique d'un Signal d'image", l'Onde Electrique, Sept. 1969.

25. D. Estoumet, "Compression d'information de Signaux d'images par les Systems Differentials Codes", l'Onde Electrique, Sept. 1969.

26. A.J. Seyler and Z.L. Budrikis, "Detail Perception after Scene Changes in Television Image Presentations", IEEE Trans. on Inf. Theory, Vol. IT-11, Jan. 1965.

27. N.G. Deriugin, "The Power Spectrum and the Autocorrelation of the Television Signal", Telecommunications, Vol. 7, 1957.

28. J.H. Lanning and R.H. Battin, "Random Processes in Automatic Control", McGraw Hill Book Co., N.Y., 1965.

29. S. Narayanan and L.E. Franks, "The Spectra of Digitally Encoded Video Signals", Int. Conf. Com., Denver, June 1969.

30. J.J. De Palma and E.M. Lowry, "Sine-wave Response of the Visual System, II Sine-wave and Square-wave Contrast Sensitivity", J. Opt. Soc. Am., Vol. 52, pp. 328-335, March 1962.

31. A.D. Jowler, "Observer Reaction to Low-frequency Interference in Television Pictures", Proc. IRE, Vol. 39, pp 1332-1336, Oct. 1951.

32. D.H. Kelly, "Visual Responses to Time-dependent Stimuli", J. Opt. Soc. Am., Vol. 51, pp. 422-429, 1961.

33. R.B. Marimont, "Linearity and the Mach Phenomenon", J. Opt. Soc. Am., Vol. 53, pp. 400-401, March 1963.

34. S.S. Stevens, "Handbook of Experimental Psychology", N.Y. Wiley, 1951.

35. G.Biernson, "A Feedback-control Model of Human Vision", Proc. IEEE, Vol. 54, pp. 858-872, June 1966.

36. D.W. Hamlyn, "The Psychology of Perception", N.Y., The Humanities Press, Inc., 1957.

37. G.C. Higgins and L.A. Jones, "The Nature and Evaluation of the Sharpness of Photographic Images", J. Soc. Motion Pictures and TV Engineers, Vol. 58, pp. 277-290, April 1952.

38. R.P. Kruger, "Computer Processing of Radiographic Images", Ph.D. Dessertation, U. of Missouri, 1971.

39. W.F. Schreiber, "Picture Coding", Proc. IEEE, March 1967.

40. L.G. Roberts, "Picture Coding Using Pseudo-random Noise", IRE Trans. Inf. Theory, Vol. IT-8, Feb. 1962.

41. R.E. Graham, "Subjective Experiments in Visual Communication", IRE Nat. Conv. Record, Vol. 6, pt. 4, pp. 100-106, 1958.

42. D.P. Peterson and D. Middleton, "Sampling and Reconstruction of Wave-number-limited Functions in n-dimensional Euclidean Spaces", Inf. Control, Vol. 5, pp. 279-323, 1962.

43. T.S. Huang and O.J. Tretiak, "Research in Picture Processing", Opt. and Electro-optical Inf. Processing Tech., Cambridge, Mass.: MIT Press, Chapter 3, 1965.

44. D.N. Graham, "Optimum Filtering to Reduce Quantization Noise", M.S. Thesis, MIT, Jan. 1962.

45. B. Lippel and M. Kurland, "The Effect of Dither on Luminance Quantization of Pictures", IEEE Trans. Com. Tech., Vol. COM-19, No. 6, Dec. 1971.

46. J.O. Limb, "Design of Dither Waveforms for Quantized Visual Signals", BSTJ, Sept. 1969.

47. J.E. Thompson, "A 36 M bits/s. Television Codec Employing Pseudorandom Quantization", IEEE Trans. on Com Tech., Vol. COM-19, No. 6, Dec. 1971.

48. J.J. Stiffler, "Space Technology Vol. 5, Telecommunications", NASA SP-69.

49. C. Cherry et al., "An Experimental Study of the Possible Bandwidth Compression of Visual Image Signals", Proc. IEEE, Vol. 51, Nov. 1963.

50. J. Capon, "A Probabilistic Model for Run-Length Coding of Pictures", IRE Trans. Inf. Theory, Dec. 1959.

51. P.C. Goldmark and J.M. Hollywood, "A New Technique for Improving the Sharpness of Television Pictures", Proc. IRE, Vol. 39, pp. 1314-1322, Oct. 1951.

52. A.J. Seyler, "Statistics of Television Frame Differences", Proc. IEEE, Dec. 1965.

53. N.V. Philips, Gloeilampenfabrieken of Holland, French Patent No. 987, 238. Applied for May 23, 1949, Issued August 10, 1951.

54. C.C. Cutler, "Differential Quantization of Communication Signals", U.S. Patent No. 2,605,361, July 29, 1952.

55. M.R. Aaron, J.S. Fleischmer, R.A. McDonald and E.N. Protonotarios, "Response of Delta Modulation to Gaussian Signals", BSTJ, Vol. 48, pp. 1167-1195, May-June 1969.

56. R.A. McDonald, "Signal-to-Noise Performance and Idle Channel Performance of Differential Pulse-Code-Modulation Systems with Particular Applications to Voice Signals", BSTJ, Vol. 45, Sept. 1966.

57. R.W. Donaldson and R.J. Douville, "Analysis, Subjective Evaluation, Optimization, and Comparison of the Performance Capabilities of PCM, DPCM, ΔM, AM, PM Voice Communication Systems", IEEE Trans. Com Tech., Vol. COM-17, No. 4, pp. 421-431, Aug. 1969.

58. J. Yan and R.W. Donaldson, "Subjective Effects of Channel Transmission Errors on PCM and DPCM Voice Communication Systems", IEEE Trans. on Com. Vol. COM-20, No. 3, June 1972.

59. K.Y. Chang and R.W. Donaldson, "Analysis, Optimization and Sensitivity Study of Differential PCM Systems Operating on Noisy Communication Channels", IEEE Trans. on Com., Vol. COM-20, No. 3, June 1972.

60. J.B. O'Neal, "Delta Modulation Quantizing Noise Analytical and Computer Simulation Results for Gaussian and TV Input Signals", BSTJ, Vol. 45, pp. 117-142, Jan 1966.

61. J.B. O'Neal, "Predictive Quantizing Systems (Differential PCM) for the Transmission of Television Signals", BSTJ, Vol. 45, May-June 1966.

62. J.B. O'Neal, "A Bound on Signal-to-Quantizing Noise Ratios for Digital Encoding Systems", Proc. IEEE, Vol. 55, pp. 287-292, March 1967.

63. K. Nitadori, "Statistical Analysis of ΔPCM", Electronics and Communications in Japan, 48, No. 2, Feb. 1965.

64. A. Papoulis, "Probability, Random Variables, and Stochastic Processes", McGraw Hill Book Company, Inc. 1965. See Chapter 11, p. 385 ff.

65. P.F. Panter and W. Dite, "Quantization Distortion in Pulse-count-modulation with Non-uniform Spacing of Levels", Proc. IRE, 39, pp. 44-48, Jan. 1951.

66. A Habibi, "Comparison of nth order DPCM Encoder with Linear Transformations and Block Quantization Techniques", IEEE Trans. Com Tech., Vol. COM-19, No. 6, Dec. 1971.

67. E.G. Kimme and FF. Kuo, "Synthesis of Optimal Filters for a Feedback Quantization System", IEEE Trans. on Circuit Theory, CT-10, No. 3, pp. 405-413, Sept. 1963.

68 H.A. Spang and P.M. Schultheiss, "Reduction of Quantizing Noise by the Use of Feedback", IRE Trans. Com. Systems, p. 373, Dec. 1962.

69. M. Fukada, "Private Notes on DPCM Systems", McGill University.

70. B. Smith, "Instantaneous Companding of Quantized Signals", BSTJ, Vol. 36, pp. 44-48, Jan. 1951.

71. L.C. Wilkins and P.A. Wintz, "Bibliography on Data Compression, Picture Properties, and Picture Coding", IEEE Trans. on Inf. Theory, Vol. IT-17, No. 2, March 1971.

72. A.H. Frei, H.R. Schindler and P. Vettiger, "An Adaptive Dual-mode Coder/Decoder for TV Signals", IEEE Trans. Com. Tech., Vol. COM-19, No. 6, Dec. 1971.

73. W.F. Schreiber, T.S. Huang and O.J. Tretiak, "Contour Coding of Images", WESCON Conv. Record, Aug. 1968.

74. D.N. Graham, "Image Transmission by Two-dimensional Contour Coding", Proc. IEEE, Vol. 55, pp. 336-346, March 1967.

75. H.C. Andrews, "Techniques in Image Processing", Academic Press 1970, N.Y. London.

76. H.P. Kremer and M.V. Mathews, "A Linear Coding for Transmitting a Set of Correlated Signals", IRE Trans. on Inf. Theory, IT-2, pp. 41-46, Sept. 1956.

77. H.L. Van Trees, "Detection, Estimation, and Modulation Theory, Part I", John Wiley and Sons Inc., N.Y., London, Sydney.

78. G.B. Anderson and T.S. Huang, "Piecewise Fourier Transformation for Picture Bandwidth Compression", IEEE Trans. Com. Tech., Vol. COM-19, No. 2, April 1971.

79. G.D. Bergland, "A FFT Algorithm for Real-valued Series", Communications of the ACM, Vol. 11, No. 10, pp. 703-710, Oct. 1968.

80. G.D. Bergland, "A Guided Tour of the FFT", IEEE Spectrum, pp. 41-52, July 1969.

81. C. Bingham, M.D. Godfrey and J.W. Tukey, "Modern Techniques of Power Spectrum Estimation", IEEE Trans. on Audio and Electroacoustic, Vol. AV-15, No. 2, pp. 56-69, June 1967.

82. E.O. Brigham and R.E. Morrow, "The FFT", IEEE Spectrum, pp. 63-70, Dec. 1967.

83. W.T. Cochran, J.W. Cooley et. al., "What is the FFT?", IEEE Trans. on Audio and Electroacoustics, Vol. AV-15, No. 2, pp. 45-55, June 1967.

84. J.W. Cooley and J.W. Tukey, "An Algorithm for the Machine Calculation of Complex Fourier Series", Math. of Comput., Vol. 19, pp. 297-301, April 1965.

85. R.C. Singleton, "A Method for Computing the FFT with Auxiliary Memory and Limited High-speed Storage", IEEE Trans. on Audio Electroacoustics, Vol. AV-15, No. 2, pp. 91-97, June 1967.

86. W.K. Pratt, J. Kane and H.C. Andrews, "Hadamard Transform Image Coding", Proc. IEEE, Vol. 57, No. 1, Jan. 1969.

87. H.C. Andrews,"A High Speed Algorithm for the Computer Generation of Fourier Transforms", IEEE Trans. Computers (short notes), Vol. C-17, pp. 373-375, April 1968.

88. P.A. Wintz, "Transform Picture Coding", Proc. IEEE, Vol. 60, pp. 809-820, July 1972.

89. R.E. Totty and G.C. Clark, "Reconstruction Error in Waveform Transmission", IEEE Trans. Inf. Theory (Corresp.), Vol. IT-13, pp. 336-338, April 1967.

90. S. Karp, "Noise in Digital-to-analog Conversion due to Bit Errors", IEEE Trans. Vol. SET-10, No. 3, Sept. 1964.

91. R.G. Gallager, "Information Theory and Reliable Communication", John Wiley and Sons Inc., 1968, pp. 52-55.

92. G.S. Robinson and R.L. Granger, "Fast Fourier Transform Speech Compression", Proc. 1970 IEEE Int. Conf. Communications paper 26-5, June 1970.

93. H.B. Dwight, "Tables of Integrals and Other Mathematical Data", The MacMillian Co., N.Y. 1961.

94. J.J.Y. Huang and P.M. Schultheiss, "Block quantization of correlated Gaussian Random Variables", IEEE Trans. Com. Syst., Vol. CS-11, pp. 289-296, Sept. 1963.

95. S.J. Companella and G.S. Robinson, "A Comparison of Orthogonal Transformations for Digital Speech Processing", IEEE Trans. Com. Tech., Vol. COM-19, No. 6, pp. 1045-1050, Dec. 1971.

96. J. Deregnaucourt and G. Husson, "Reconstruction Des Images Codes Par Interpolation Anticipee", IEEE Int. Conf. on Conf. on Communications, June 1971.